Remote Sensing - Multispectral Applications

Lectures in Bertinoro
23 Aug – 2 Sep 2004

Paul Menzel
NOAA/NESDIS/ORA

Satellite remote sensing of the Earth-atmosphere

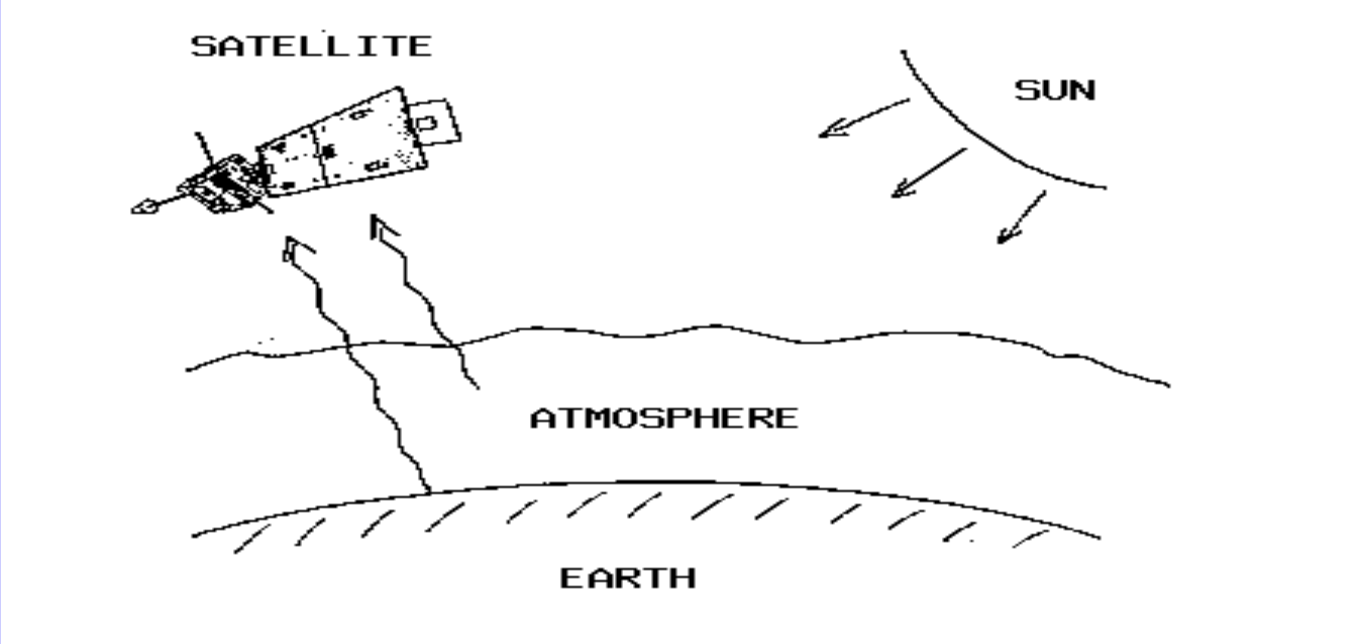

Observations depend on

telescope characteristics (resolving power, diffraction)
detector characteristics (signal to noise)
communications bandwidth (bit depth)
spectral intervals (window, absorption band)
time of day (daylight visible)
atmospheric state (T, Q, clouds)
earth surface (Ts, vegetation cover)

Remote Sensing Advantages

* provides a regional view

* enables one to observe & measure the causes & effects of climate & environmental changes (both natural & human-induced)

* provides repetitive geo-referenced looks at the same area

* covers a broader portion of the spectrum than the human eye

* can focus in on a very specific bandwidth in an image

* can also look at a number of bandwidths simultaneously

* operates in all seasons, at night, and in bad weather

Solar (visible) and Earth emitted (infrared) energy

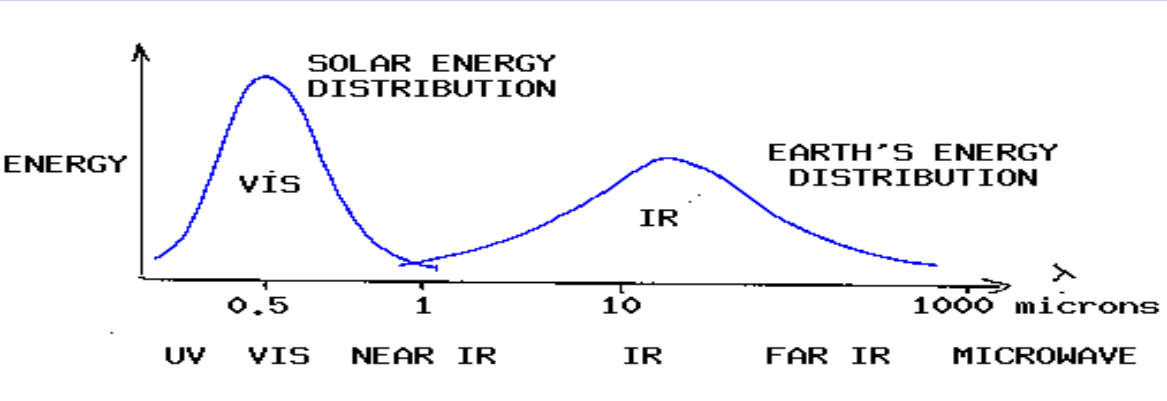

Incoming solar radiation (mostly visible) drives the earth-atmosphere (which emits infrared).

Over the annual cycle, the incoming solar energy that makes it to the earth surface (about 50 %) is balanced by the outgoing thermal infrared energy emitted through the atmosphere.

The atmosphere transmits, absorbs (by H2O, O2, O3, dust) reflects (by clouds), and scatters (by aerosols) incoming visible; the earth surface absorbs and reflects the transmitted visible. Atmospheric H2O, CO2, and O3 selectively transmit or absorb the outgoing infrared radiation. The outgoing microwave is primarily affected by H2O and O2.

Key Areas of Uncertainty in Understanding Climate & Global Change

* Earth's radiation balance and the influence of clouds on radiation and the hydrologic cycle

* Oceanic productivity, circulation and air-sea exchange

* Transformation of greenhouse gases in the lower atmosphere, with emphasis on the carbon cycle

* Changes in land use, land cover and primary productivity, including deforestation

* Sea level variability and impacts of ice sheet volume

* Chemistry of the middle and upper stratosphere, including sources and sinks of stratospheric ozone

* Volcanic eruptions and their role in climate change

Radiative Energy Balance

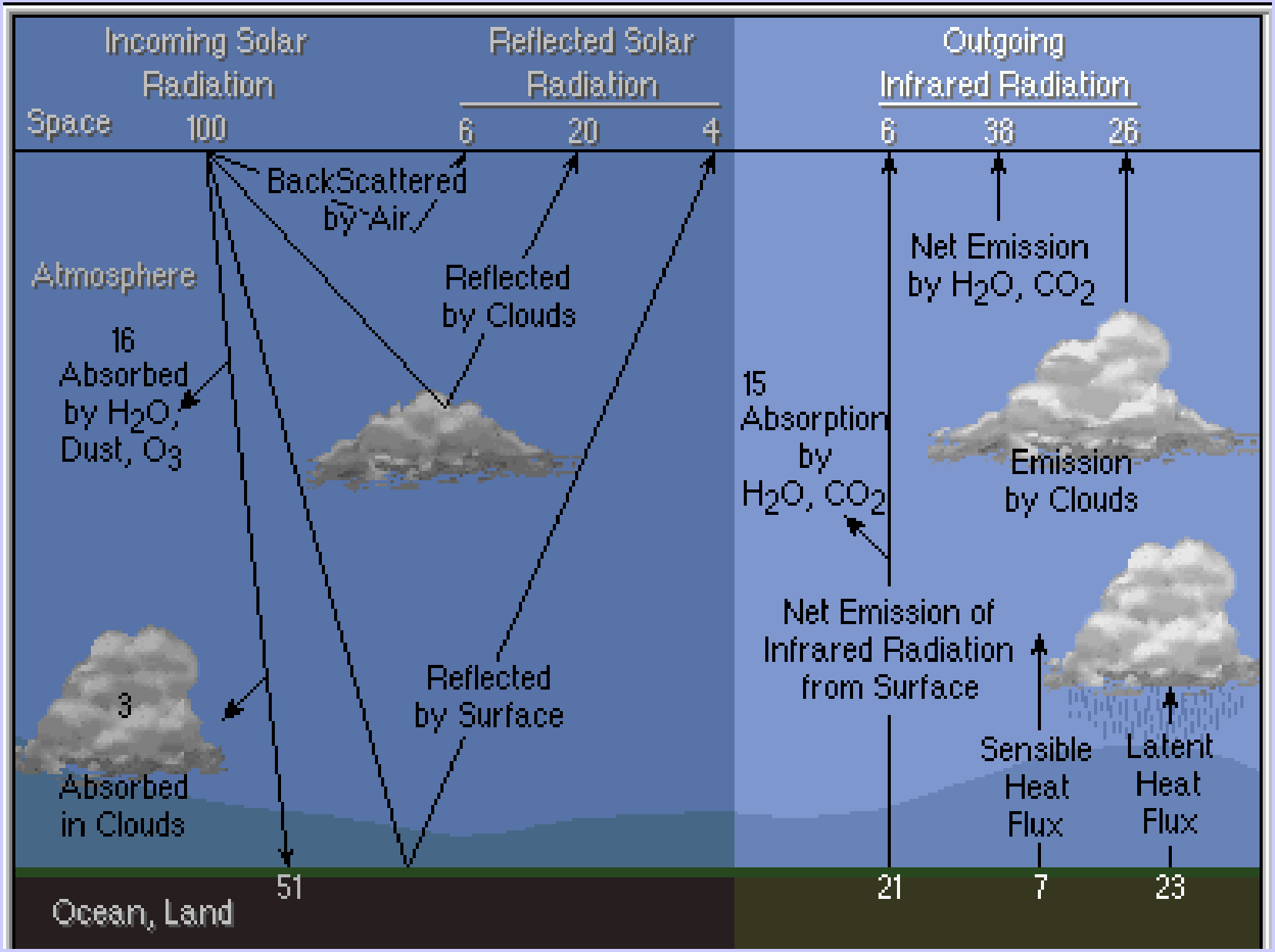

Solar Spectrum

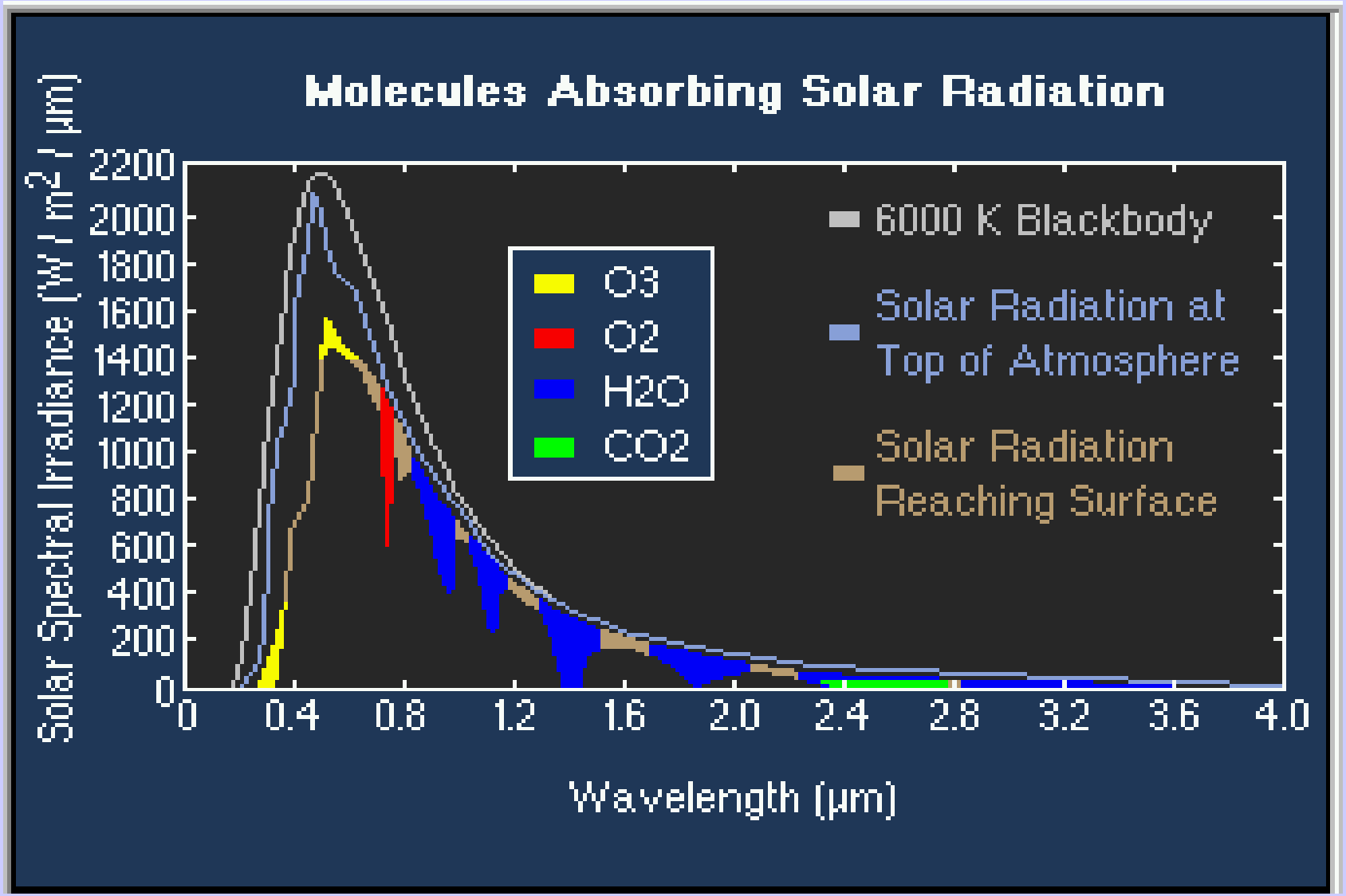

Earth emitted spectra overlaid on Planck function envelopes

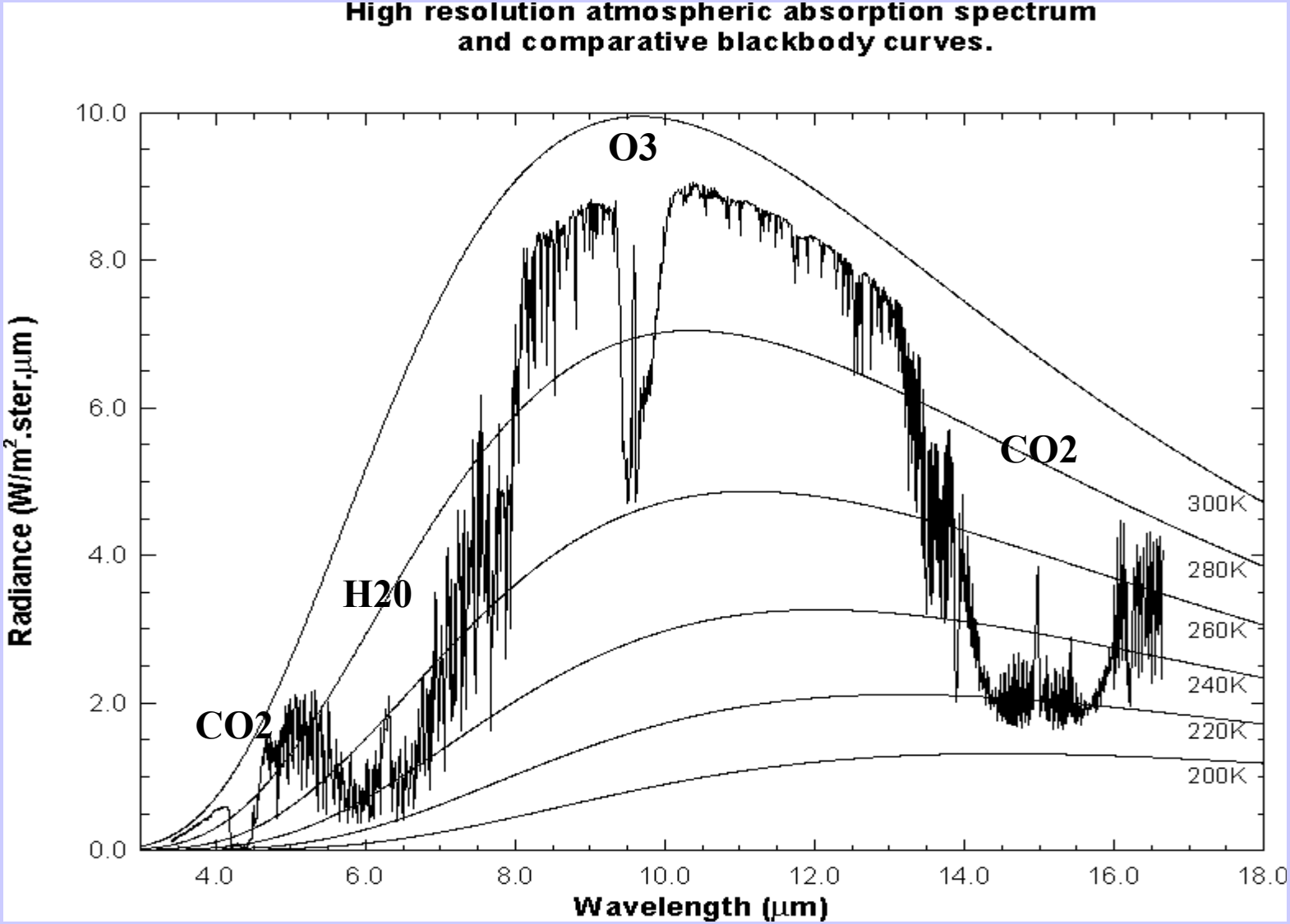

Radiative Transfer through the Atmosphere

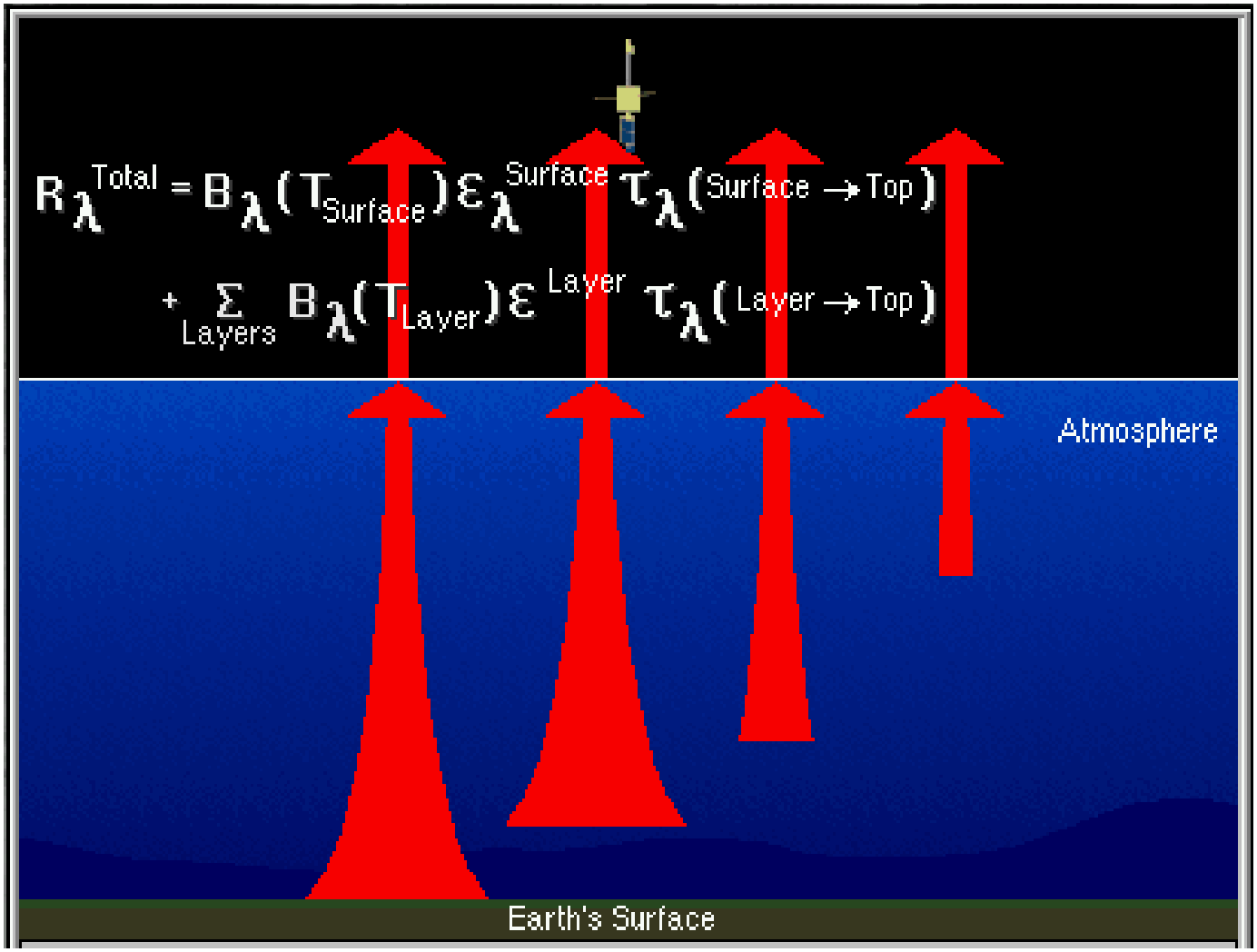

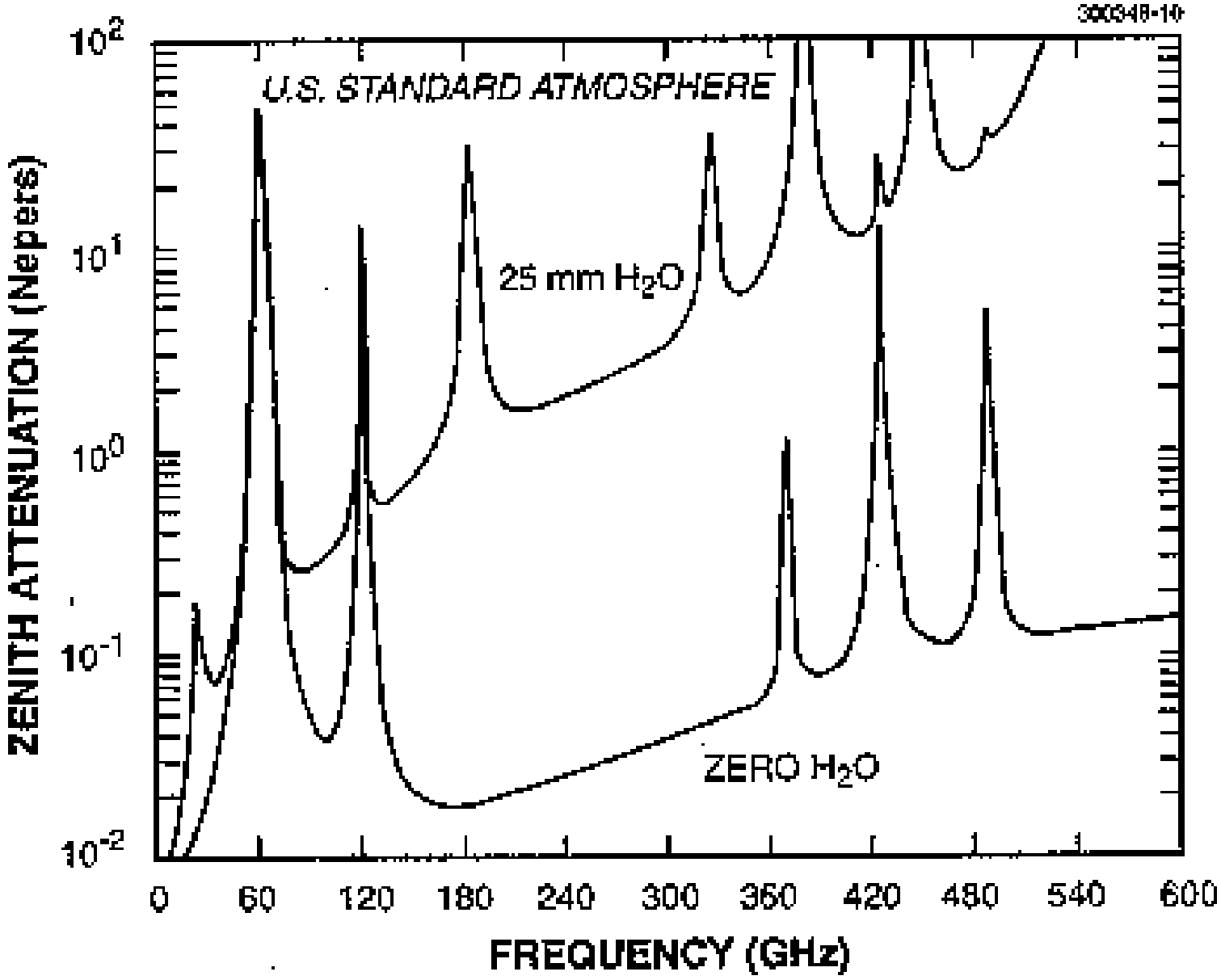
U.S. STANDARD ATMOSPHERE
25 mm H_2O
ZERO H_2O
ZENITH ATTENUATION (Nepers)
10^2
10^1
10^0
10^{-1}
10^{-2}
0
60
120
180
240
300
360
420
480
540
600
FREQUENCY (GHz)

Clouds viewed from polar orbiting TIROS launched 1 Apr 1960

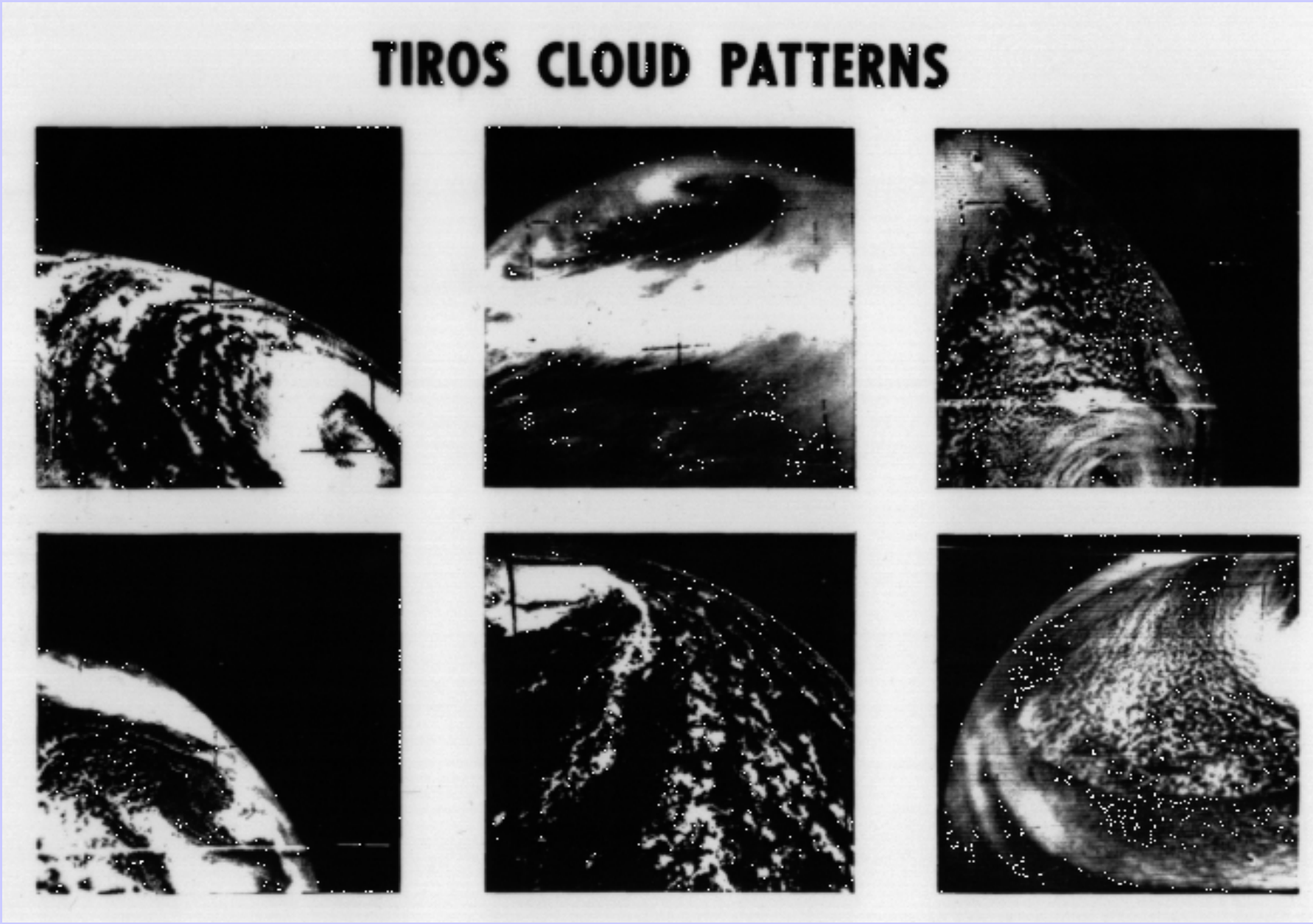

Evolution of Leo Obs

Terra was launched in 1999 and the EOS Era began

MODIS, CERES, MOPITT, ASTER, and MISR reach polar orbit

Aqua and ENVISAT followed in 2002

MODIS and MERIS leading to VIIRS
AIRS leading to IASI and CrIS
AMSU leading to ATMS

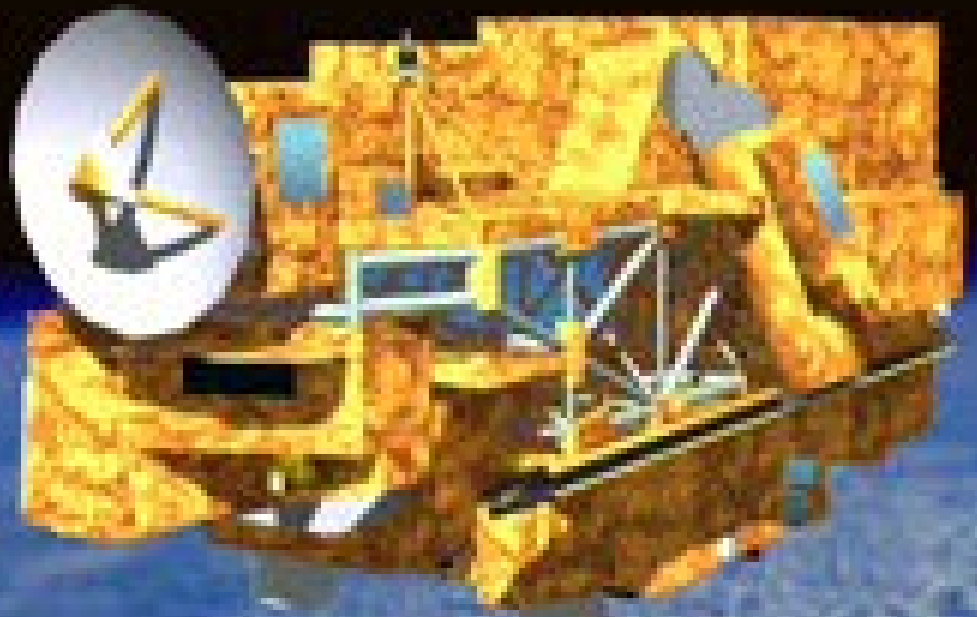

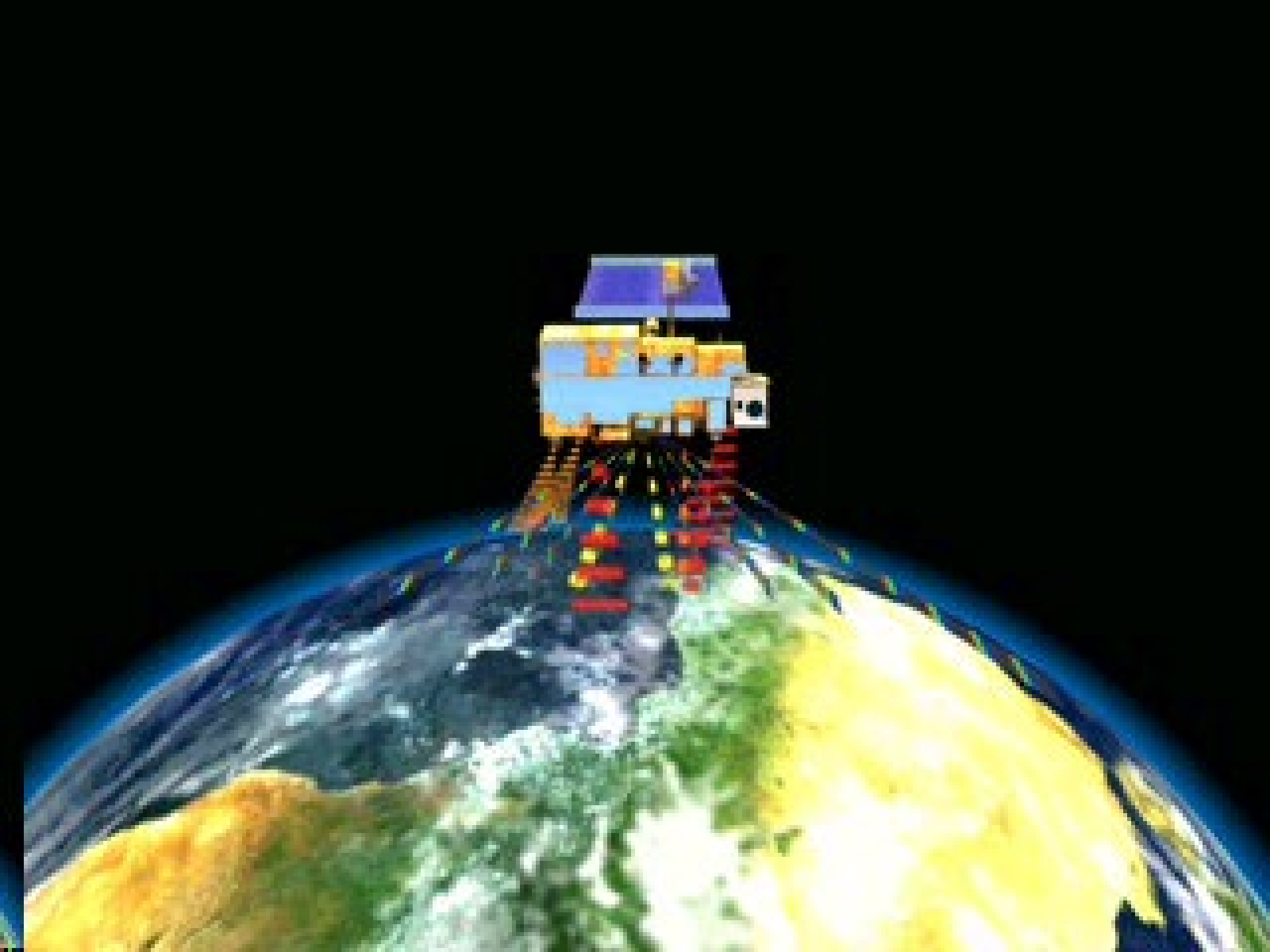

VIIRS, MODIS, FY-1C, AVHRR

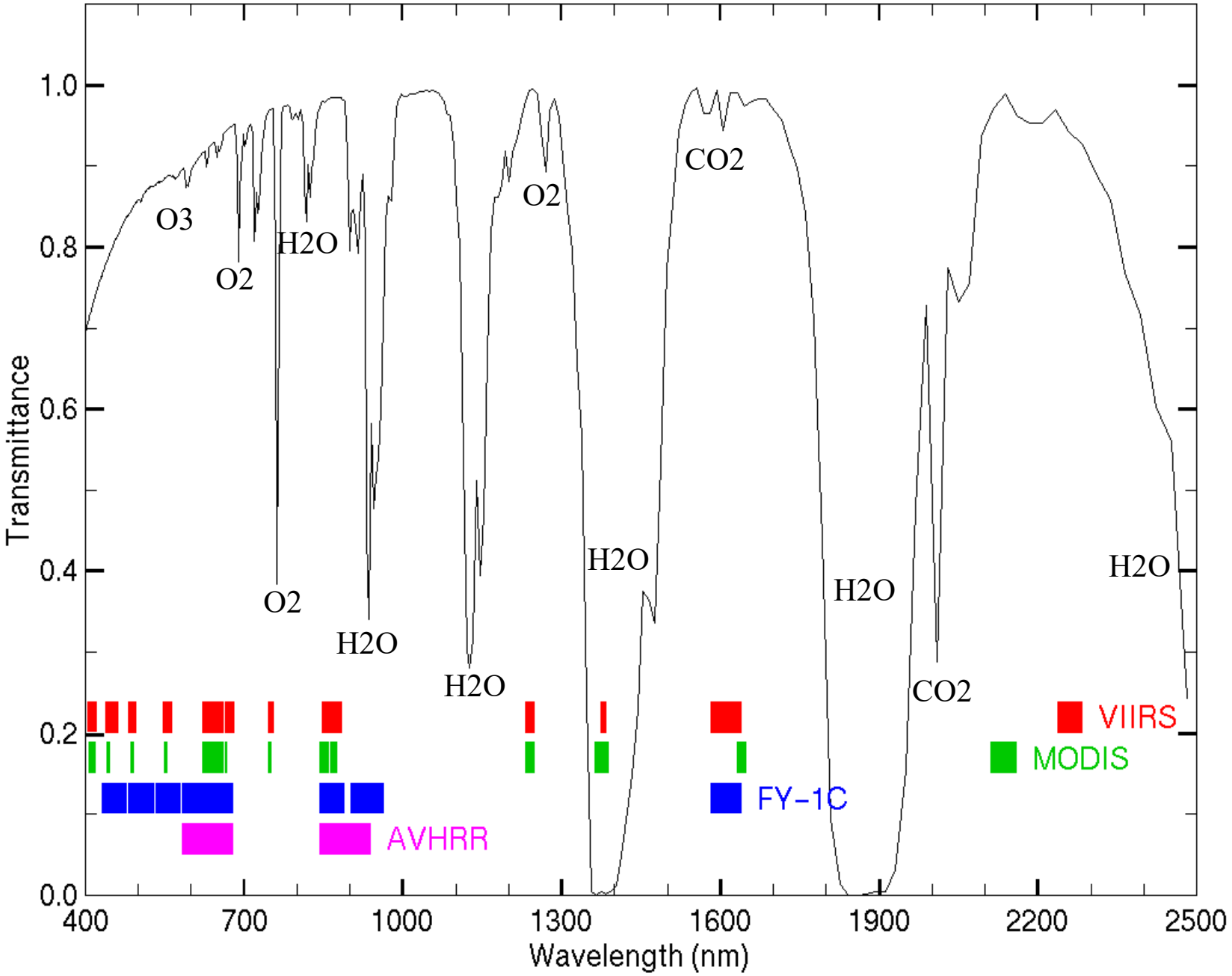

MODIS IR Spectral Bands

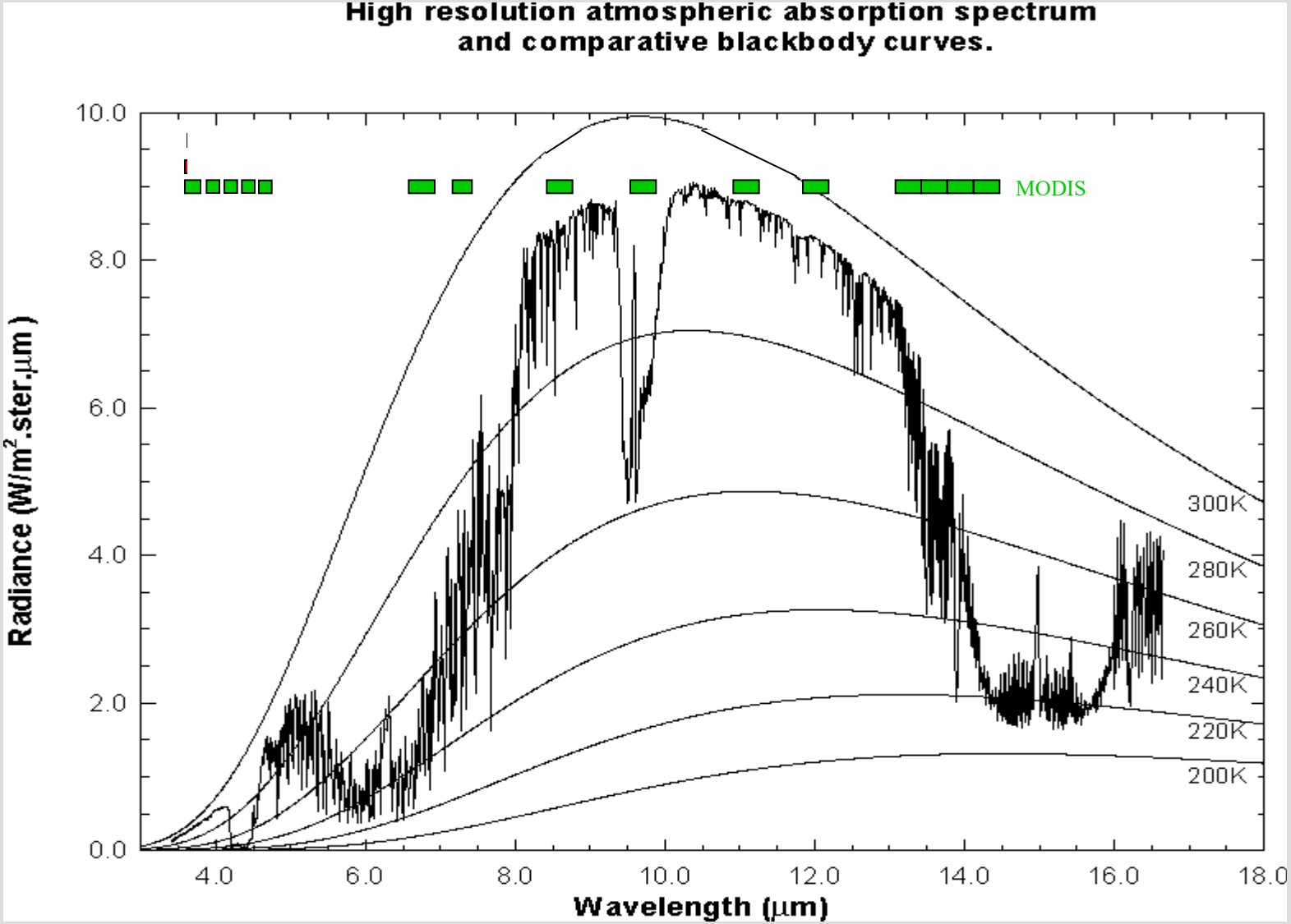

OCEAN-SOLAR RADIATION

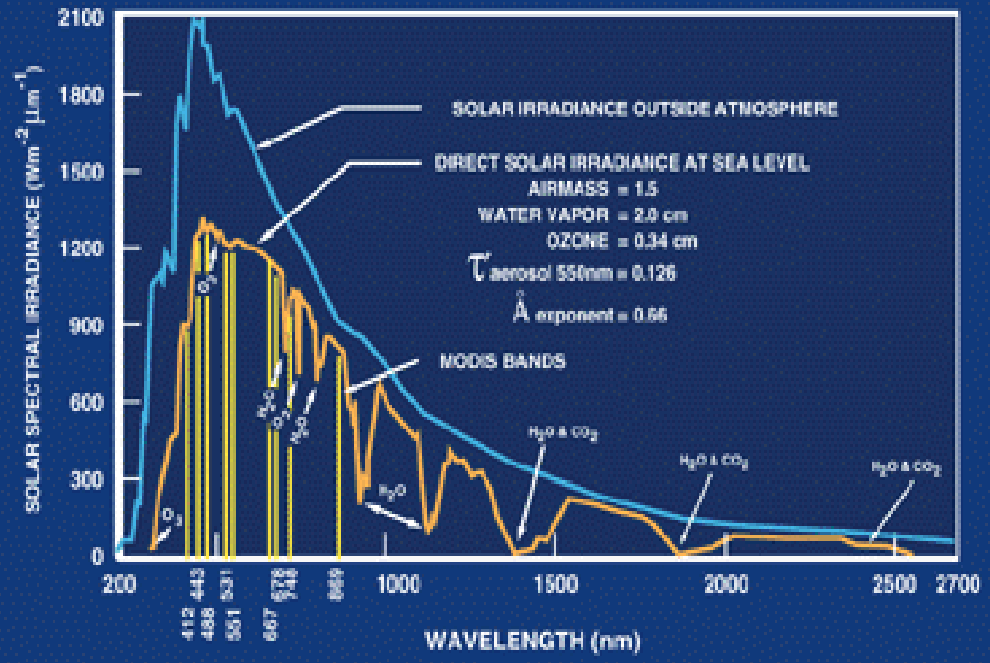

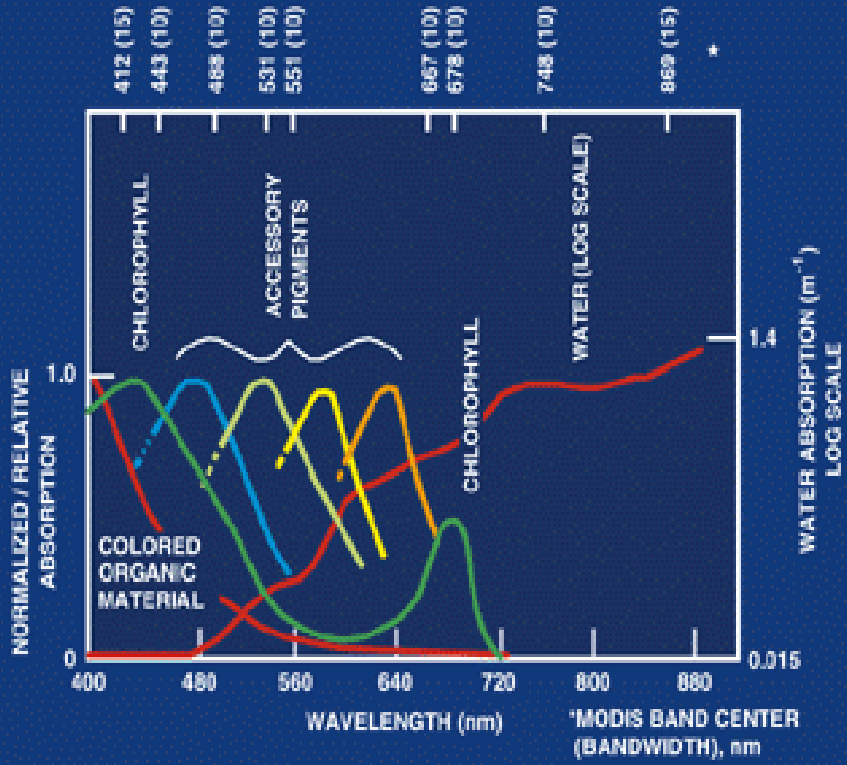

MODIS SEA SURFACE TEMPERATURE

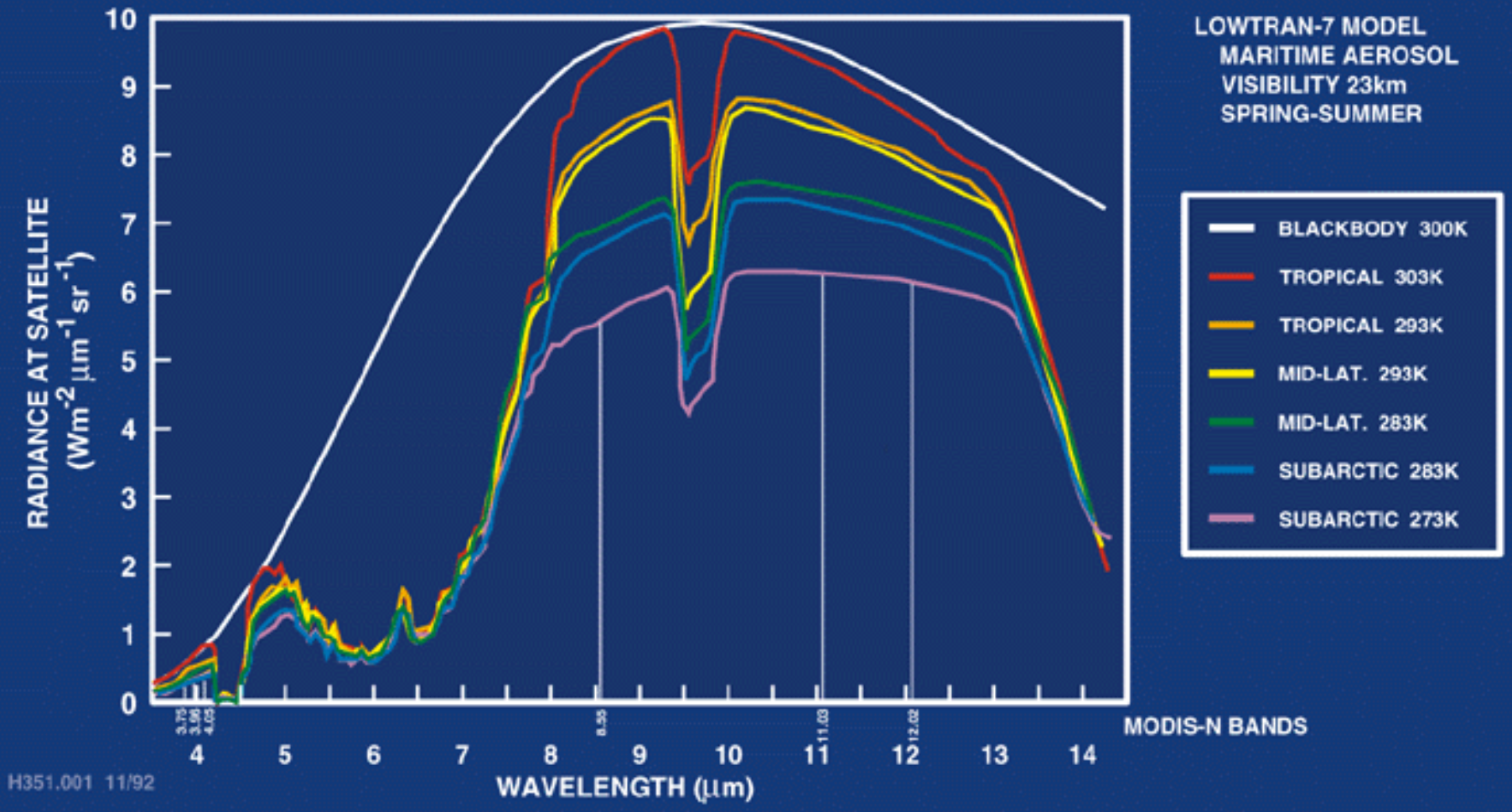

H351.001 11/92

Chlorophyll - MODIS and SeaWiFS

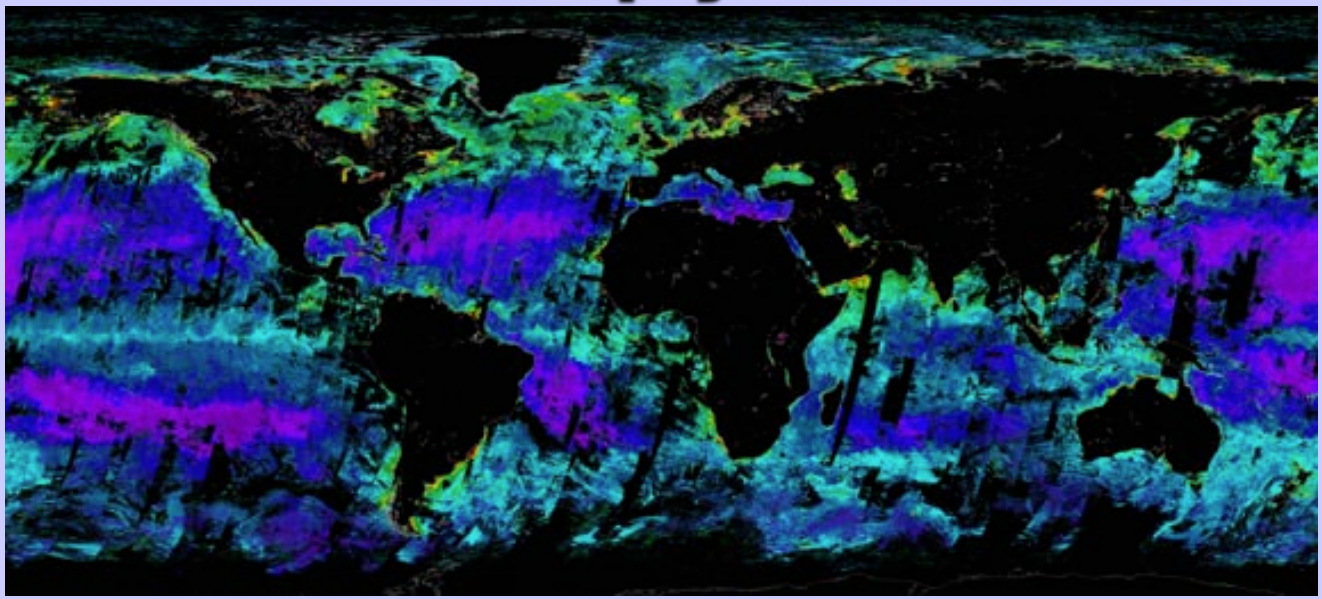

MODIS Chlor
243-250, 2000
U. Miami

MODIS tropics coverage is greater (time of day + no tilt loss). MODIS reveals global fine structure. Color scales not identical, cal not final.

SeaWiFS Chlor
241-248, 2000
SeaWIFS Project

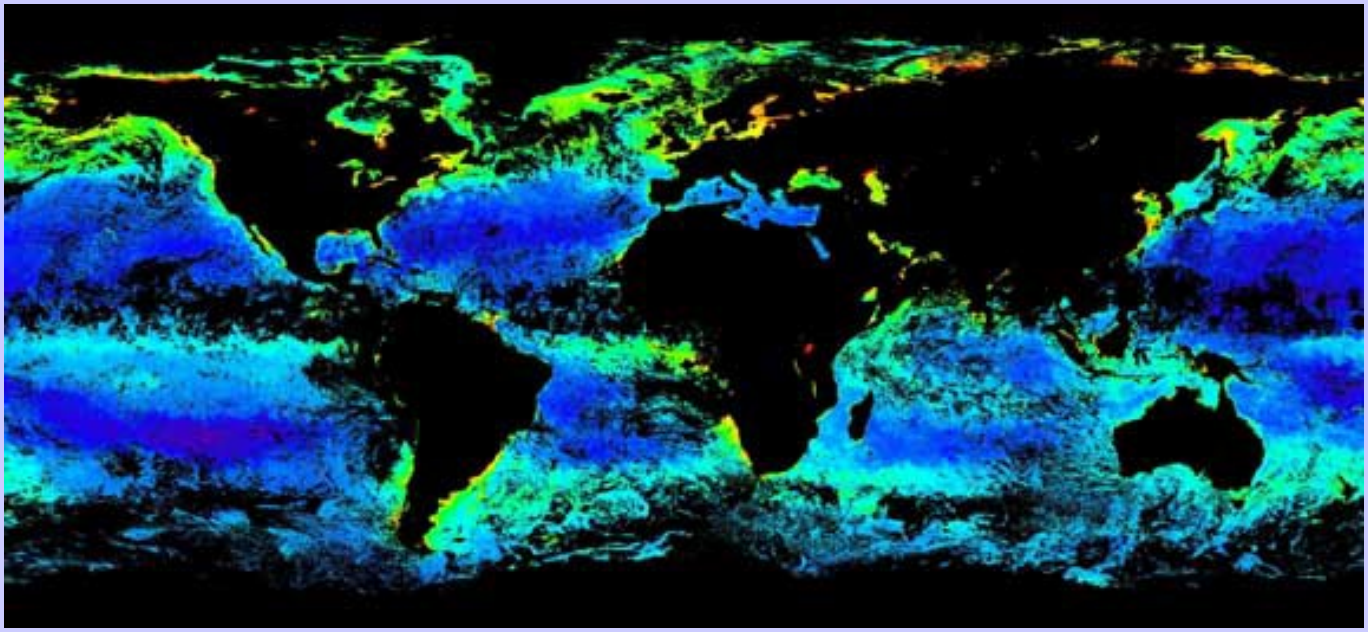

SST - MODIS and AVHRR

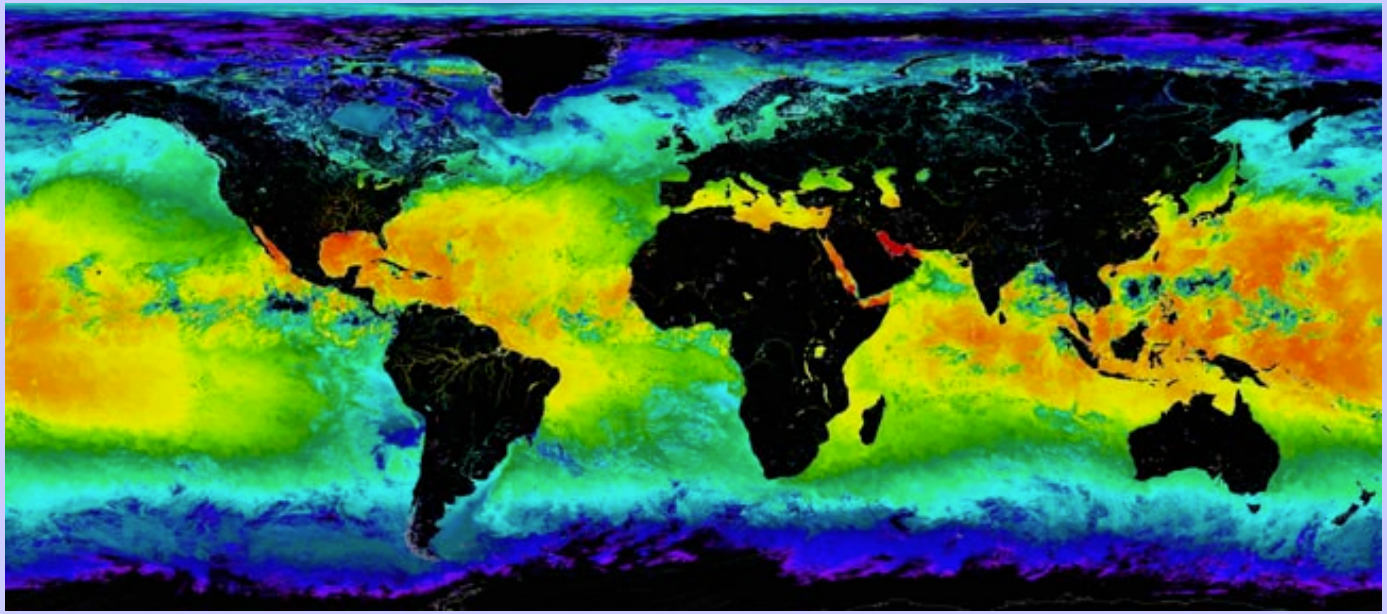

MODIS 4 micron Night SST

Improved coverage in tropical regions. Color scales are not identical, cloud mask is not applied.

AVHRR Night SST

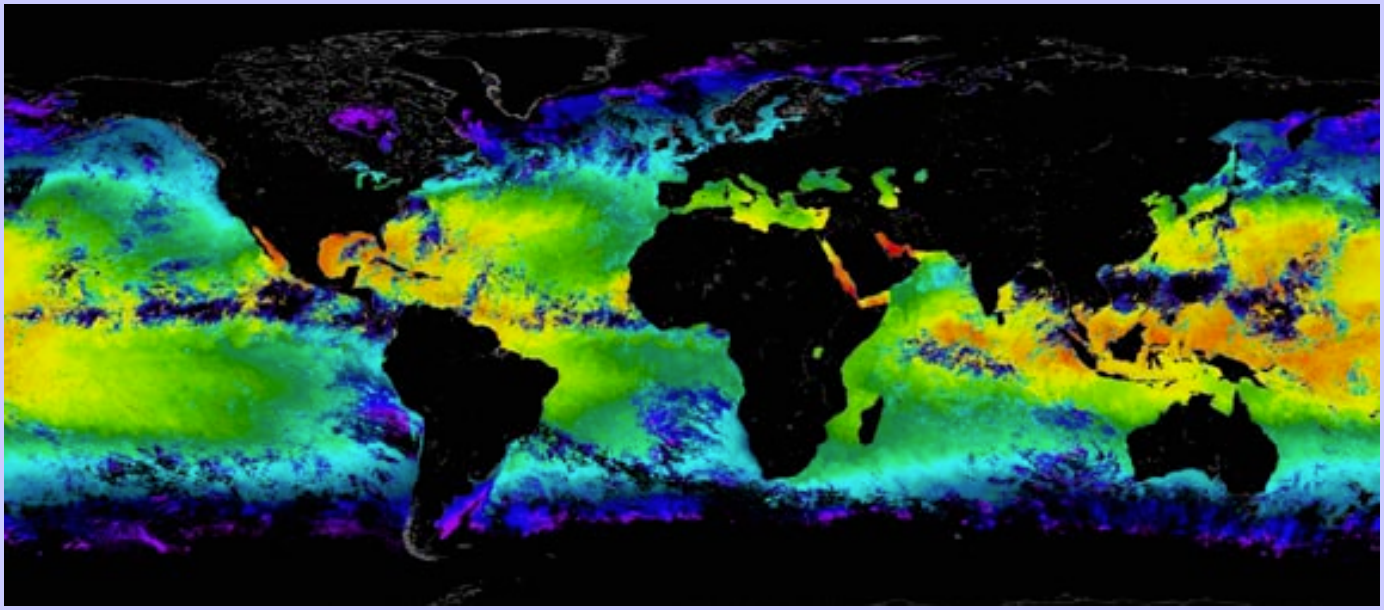


MODIS views the Mississippi

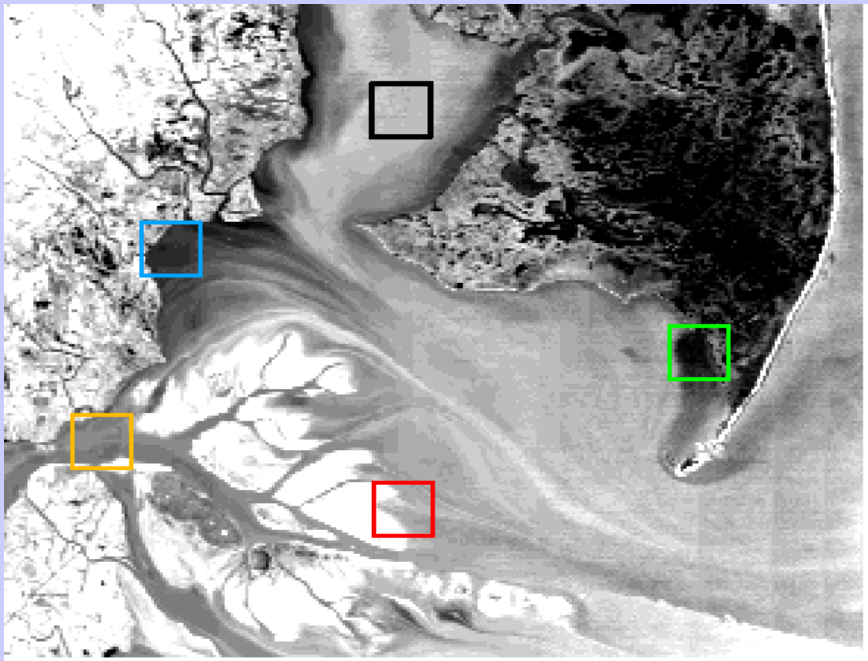

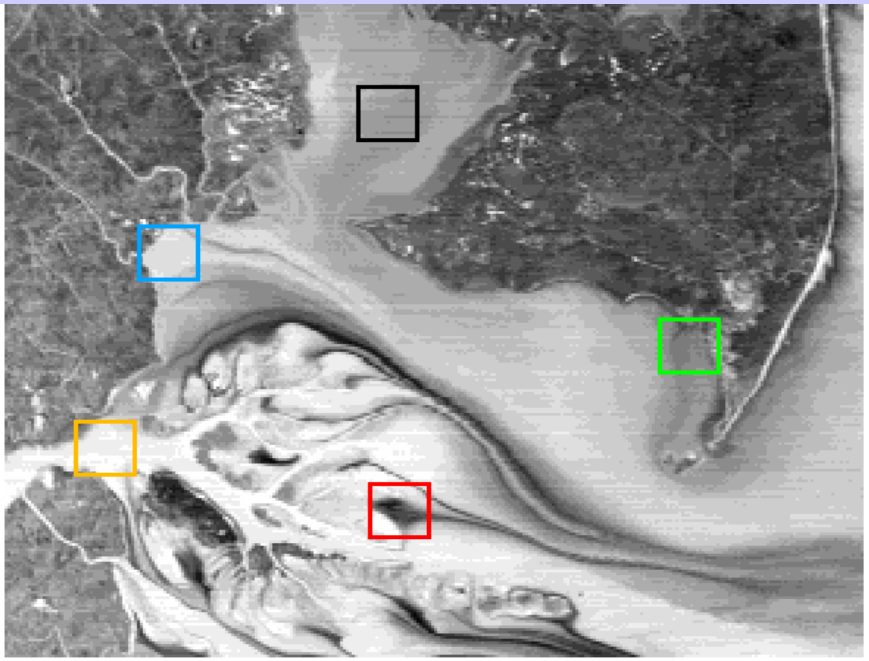

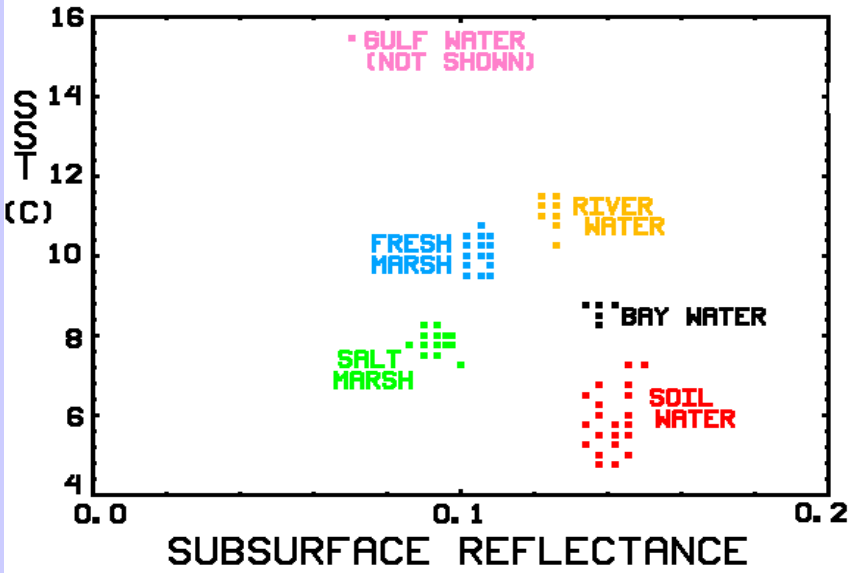

MAMS WATER TYPE ANALYSIS
DEC 4 1990

SHOWN:

* .66um REFLECTANCE (LEFT)
* SPLIT WINDOW SST (RIGHT)

LAND-SOLAR RADIATION

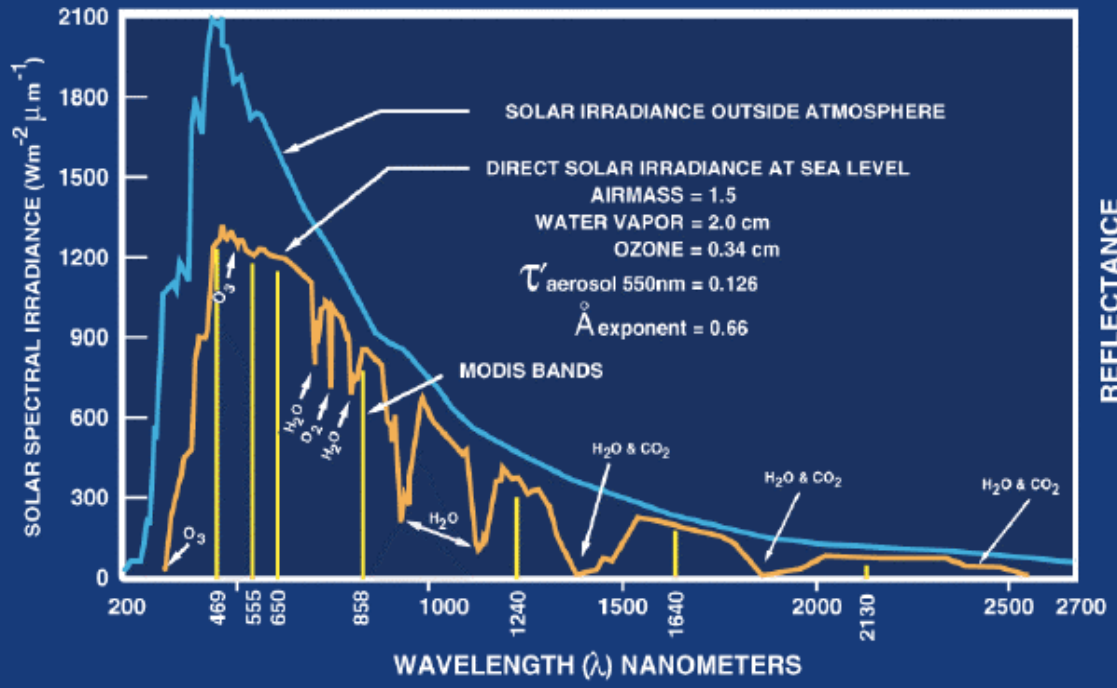

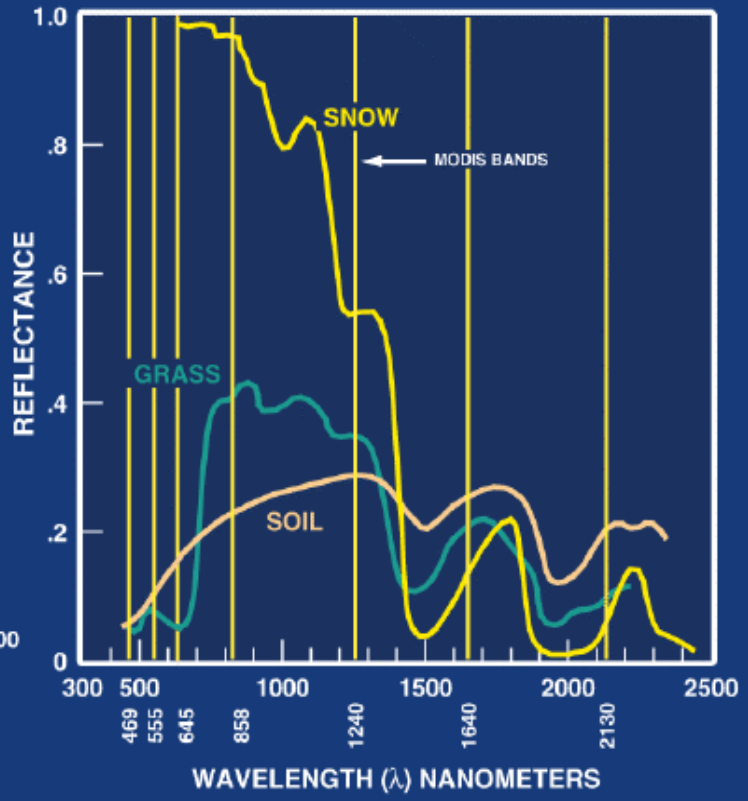

LAND - THERMAL RADIATION

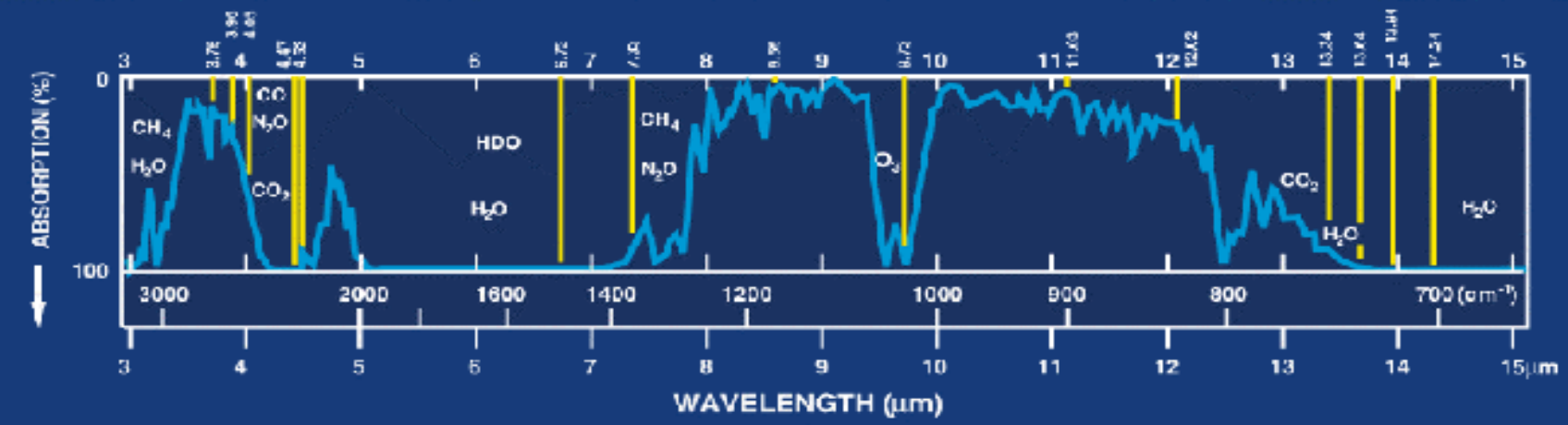

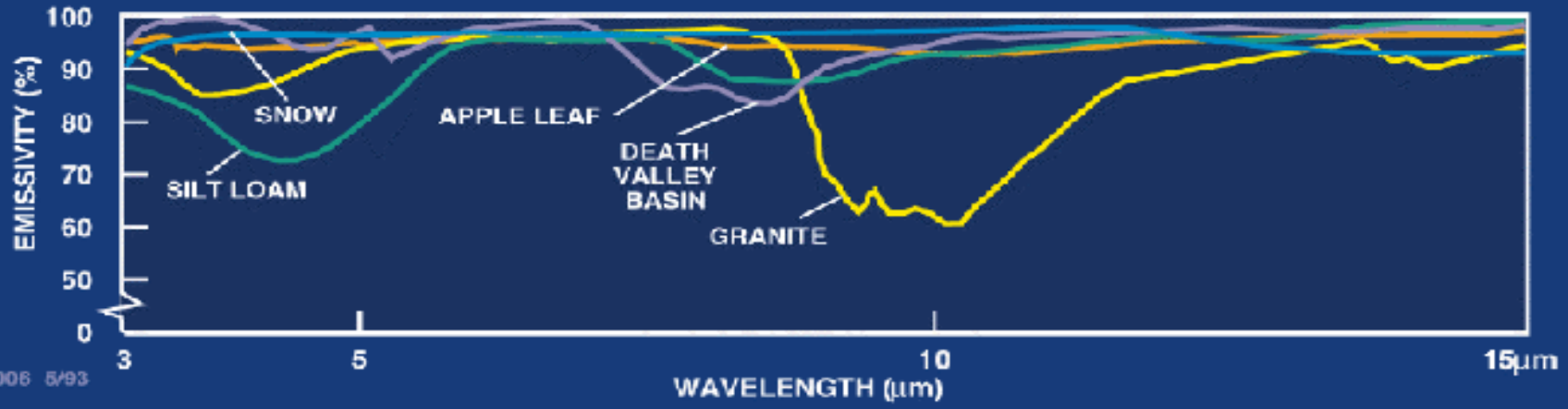

C351.006 5/93

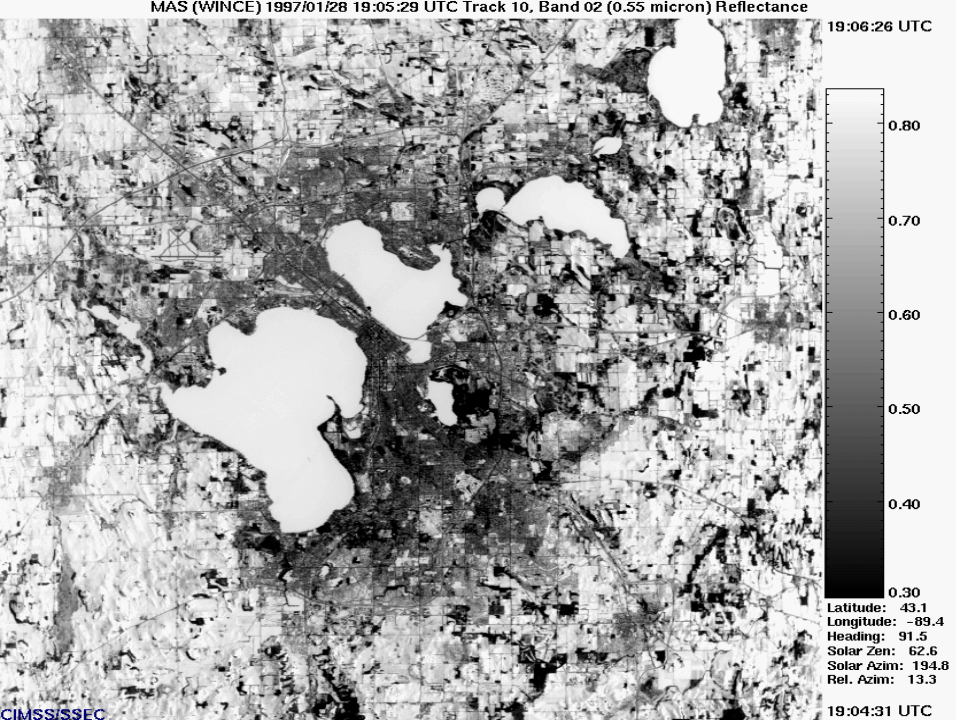

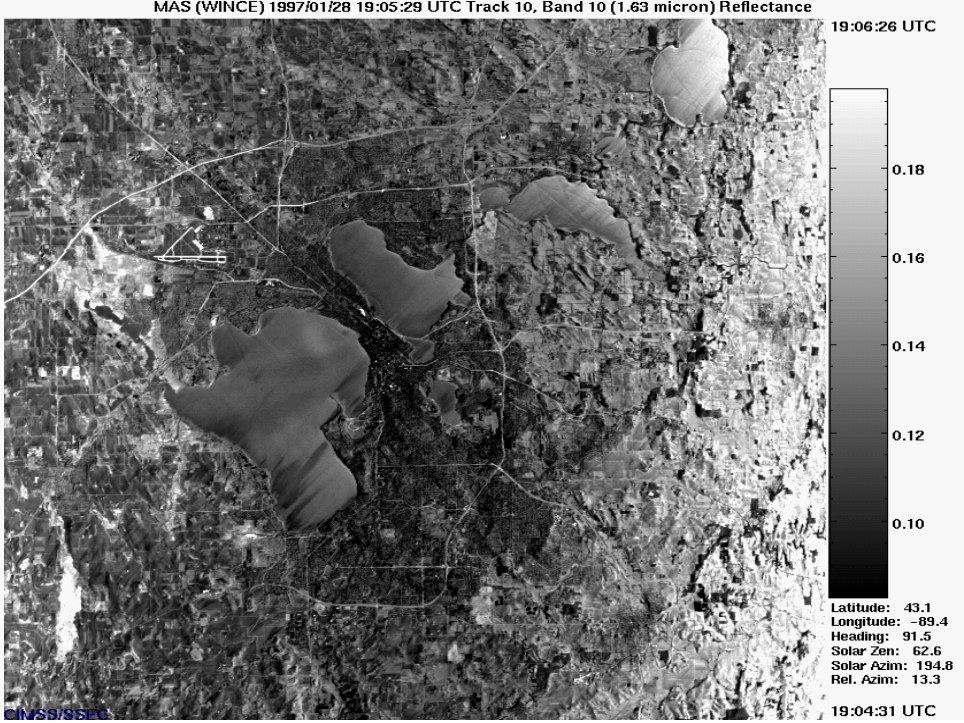

MODIS Airborne Simulator (MAS)
0.6, 1.6, & 11.0 um data over Madison in Jan 97

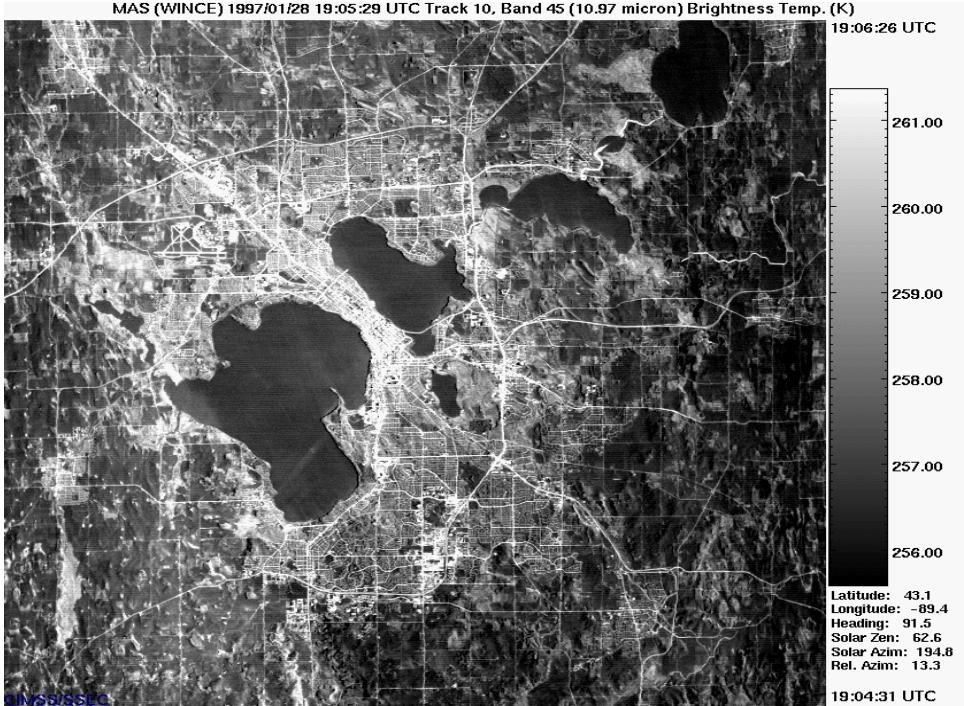

Observing Sea Ice Leads With MODIS

MODIS Band 1 Image of Western Arctic, 1 km (subsampled)

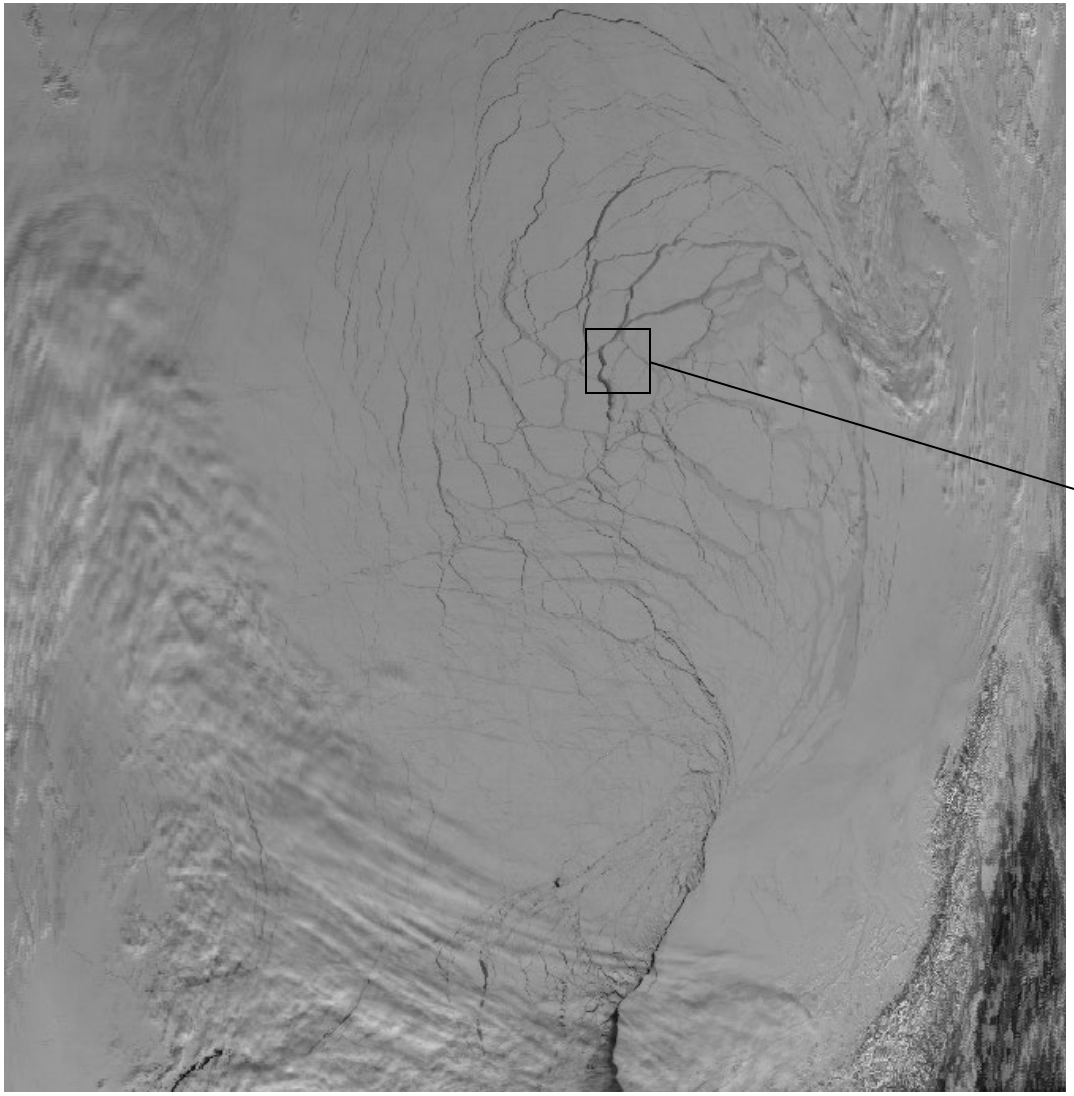

MODIS Full Resolution, 250 m Pixels

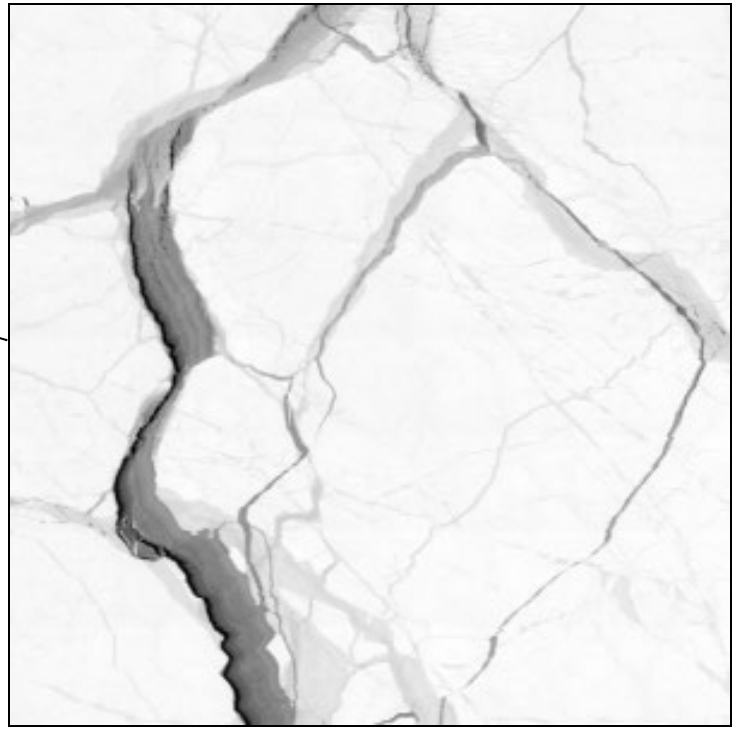

Sea ice monitoring – Gulf of St. Lawrence (02/10/03)

Iceberg monitoring in Ross Sea, Antarctica (01/28/03)

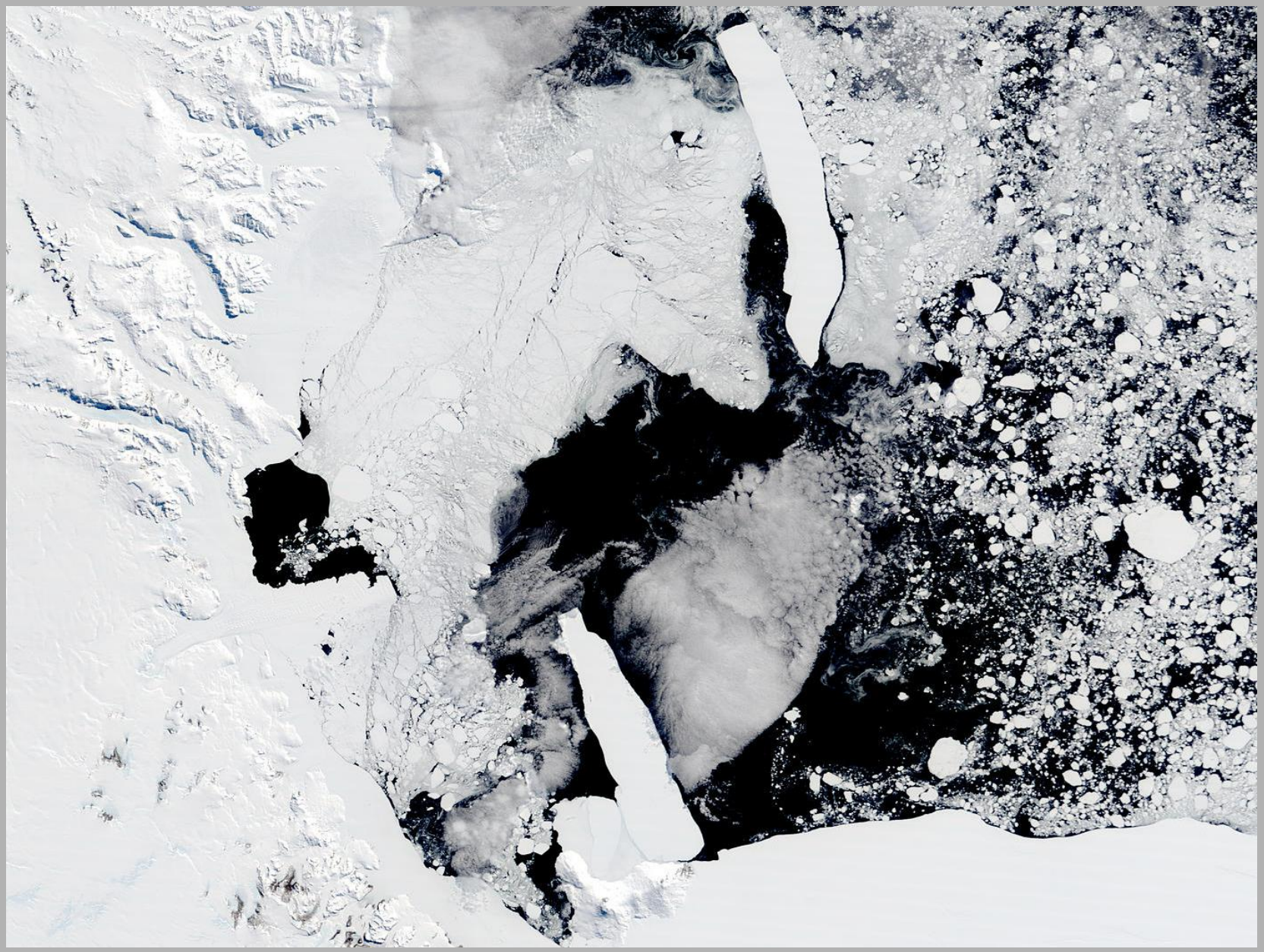

Kuril Islands, Russia (09/17/02)

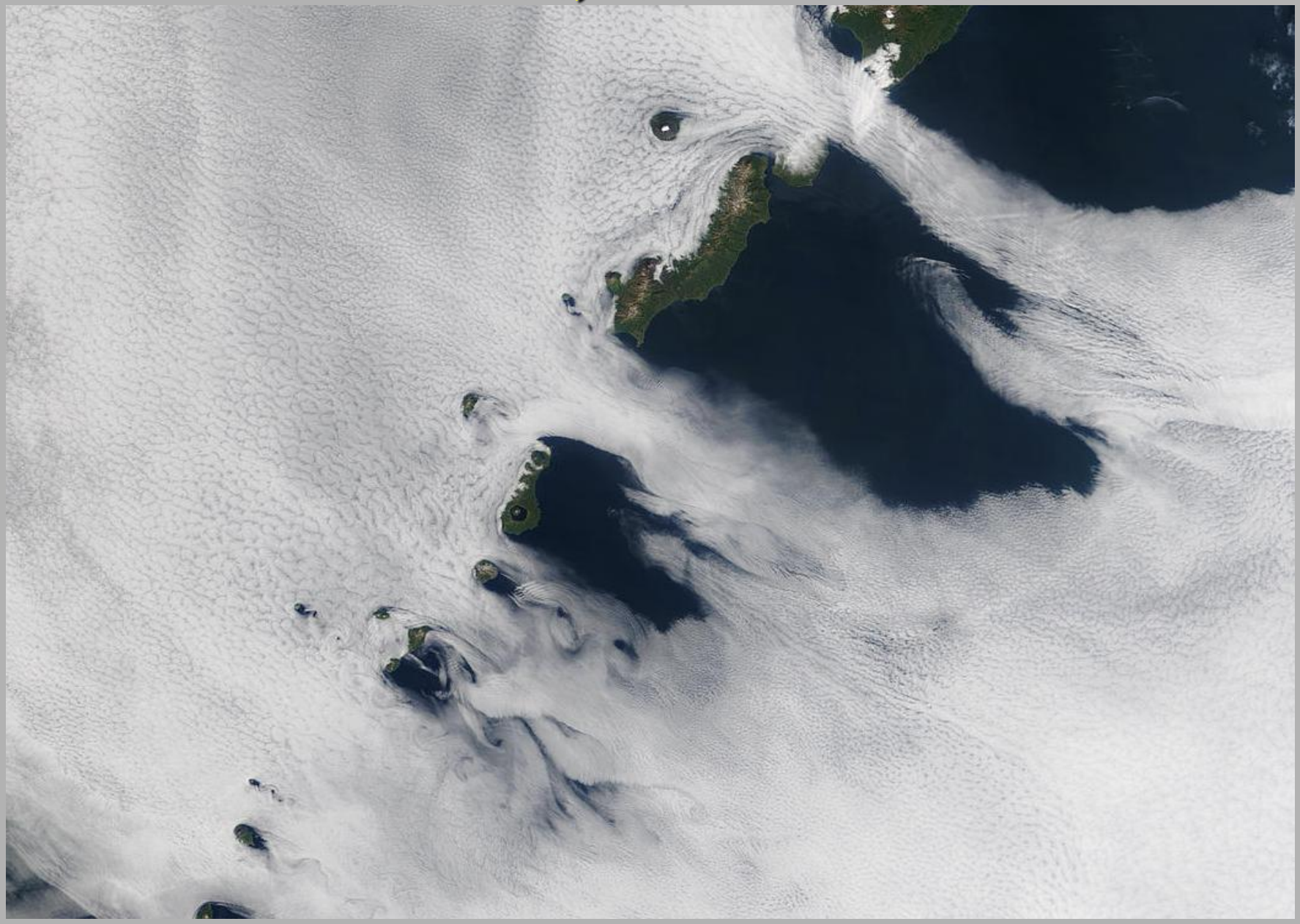

MODIS Image and snow map - November 3, 2000

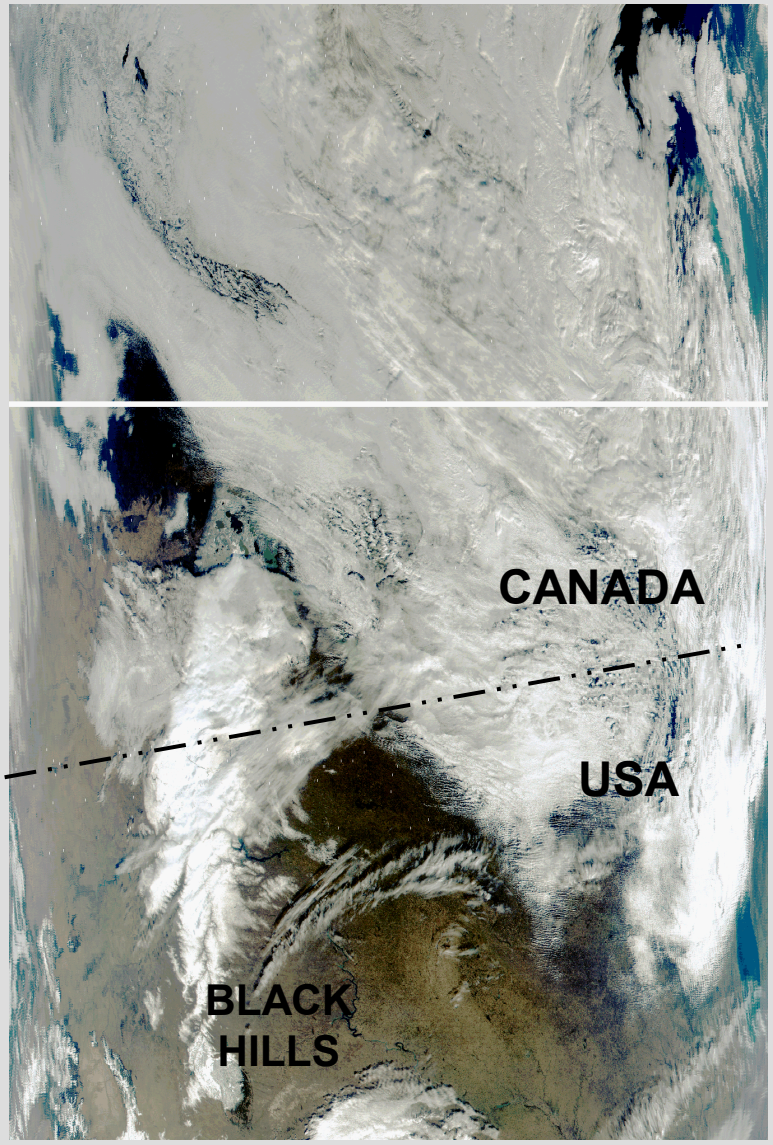

MODIS bands 1, 4, 3

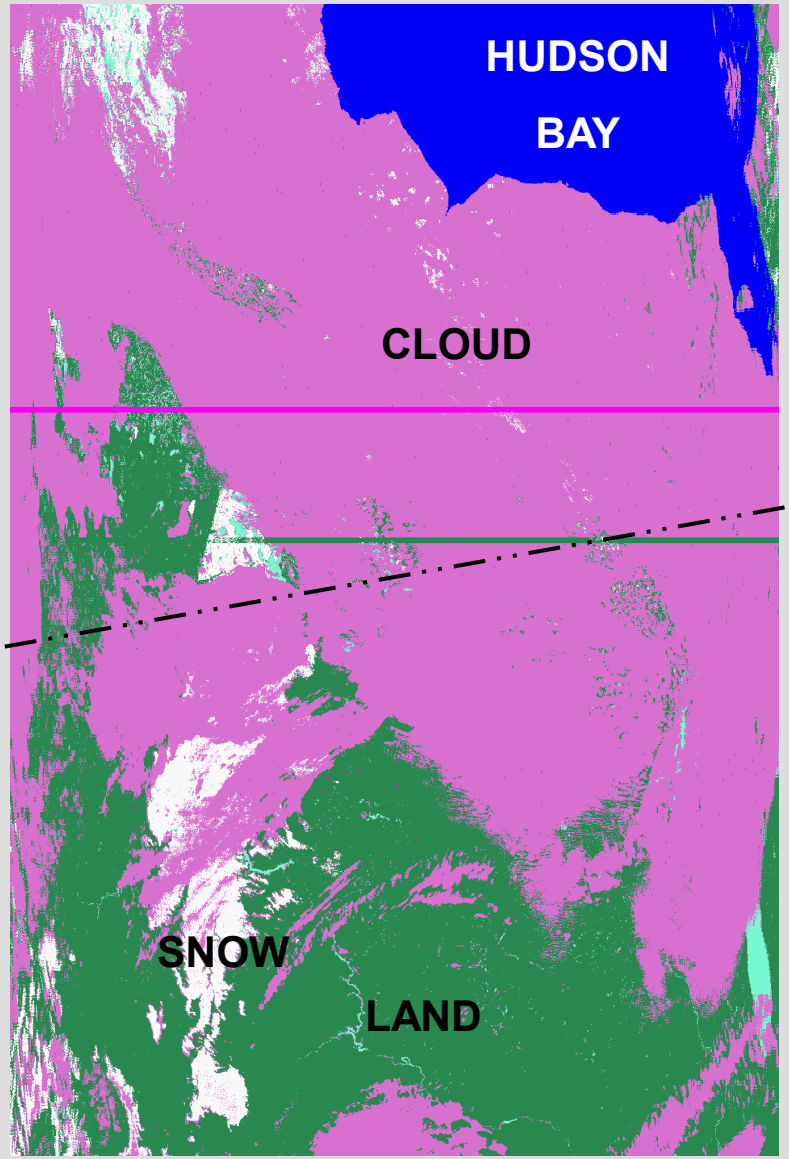

9.0 million sq. km of snow cover

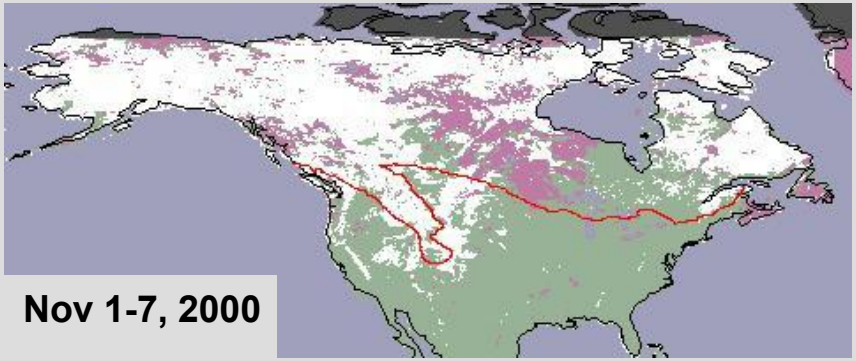

Nov 1-7, 2000

10.8 million sq. km of snow cover

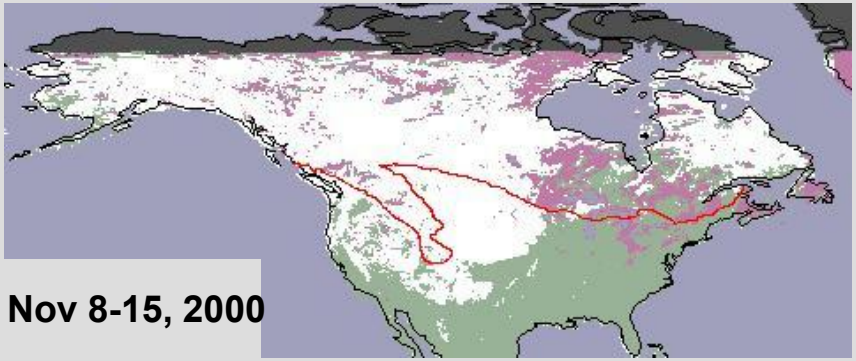

Nov 8-15, 2000

Change in maximum snow extent between two composite periods seen above (1.8 million sq. km)

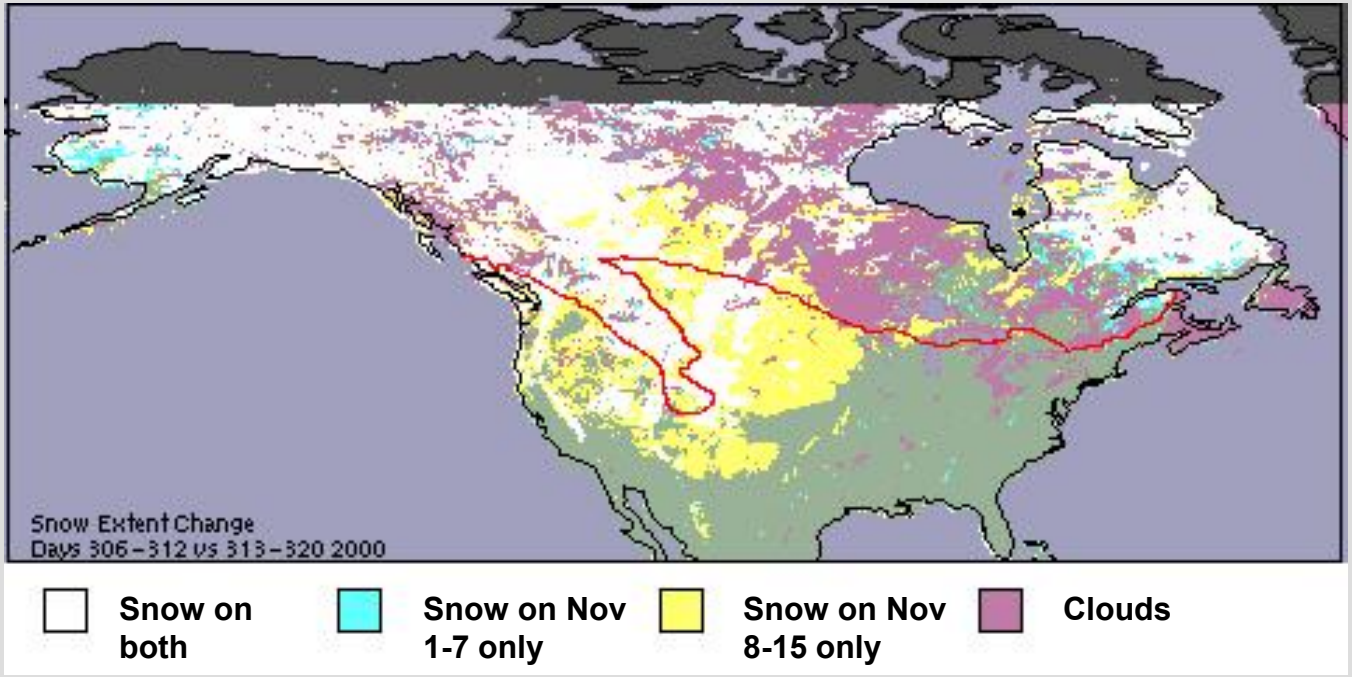

ATMOSPHERE-SOLAR RADIATION

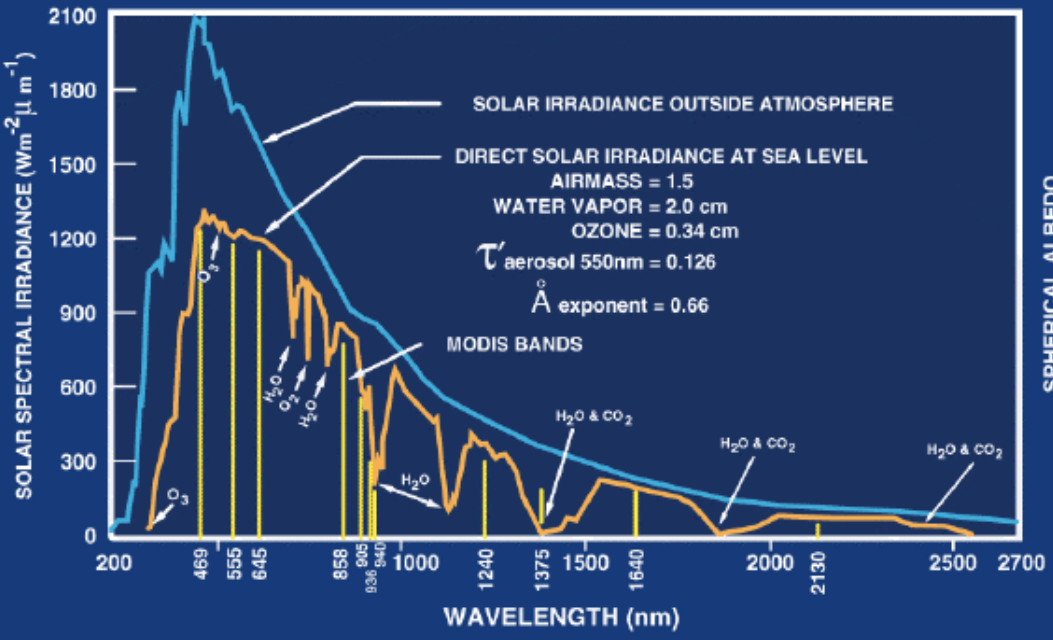

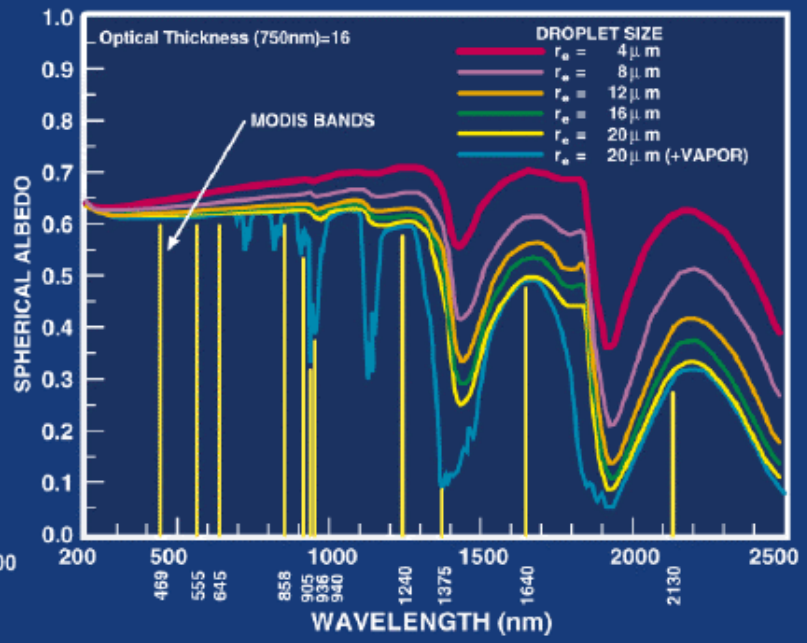

ATMOSPHERE - CLEAR SKY THERMAL EMISSION

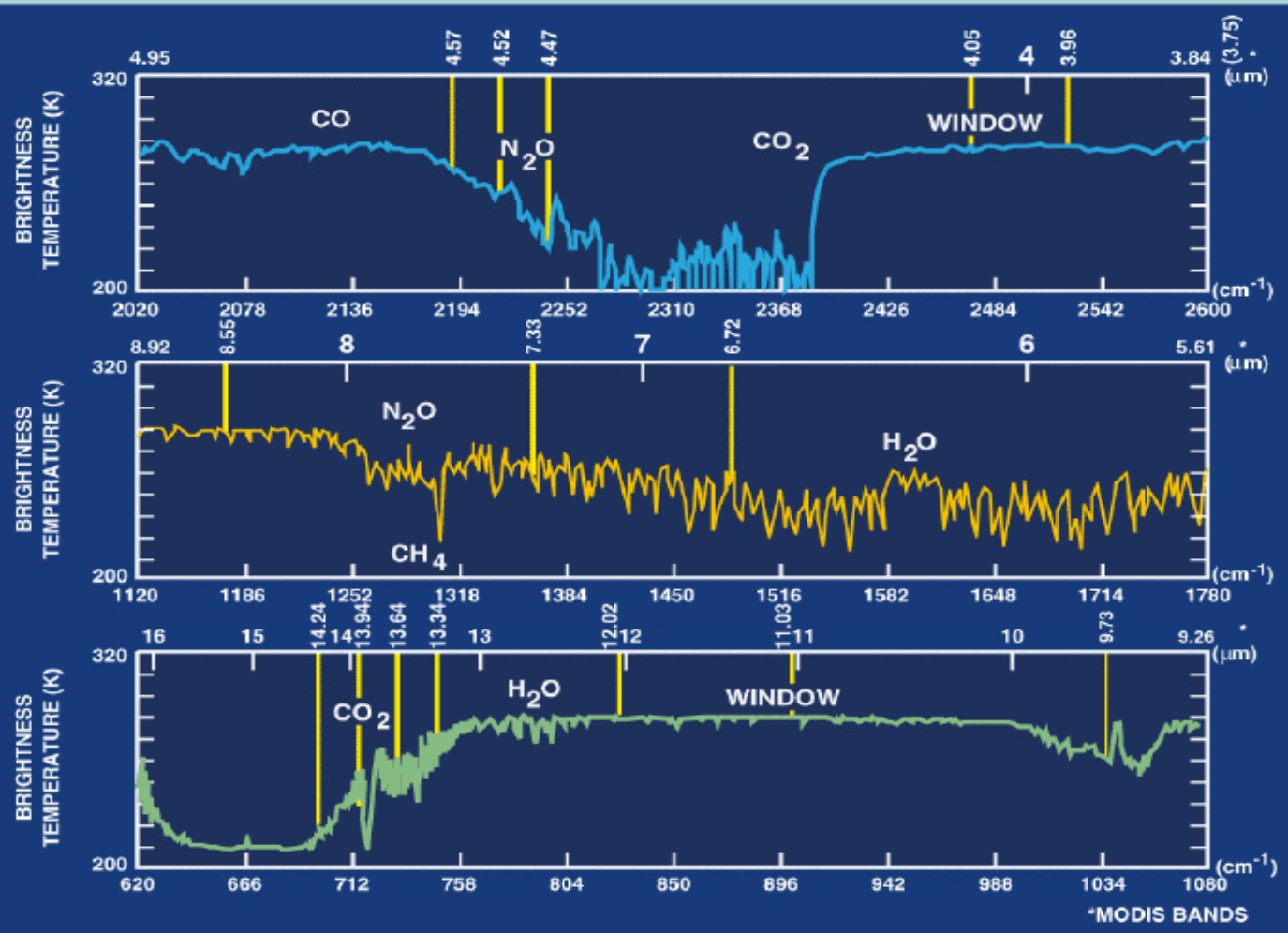

002 11/92

ATMOSPHERE - THERMAL RADIATION

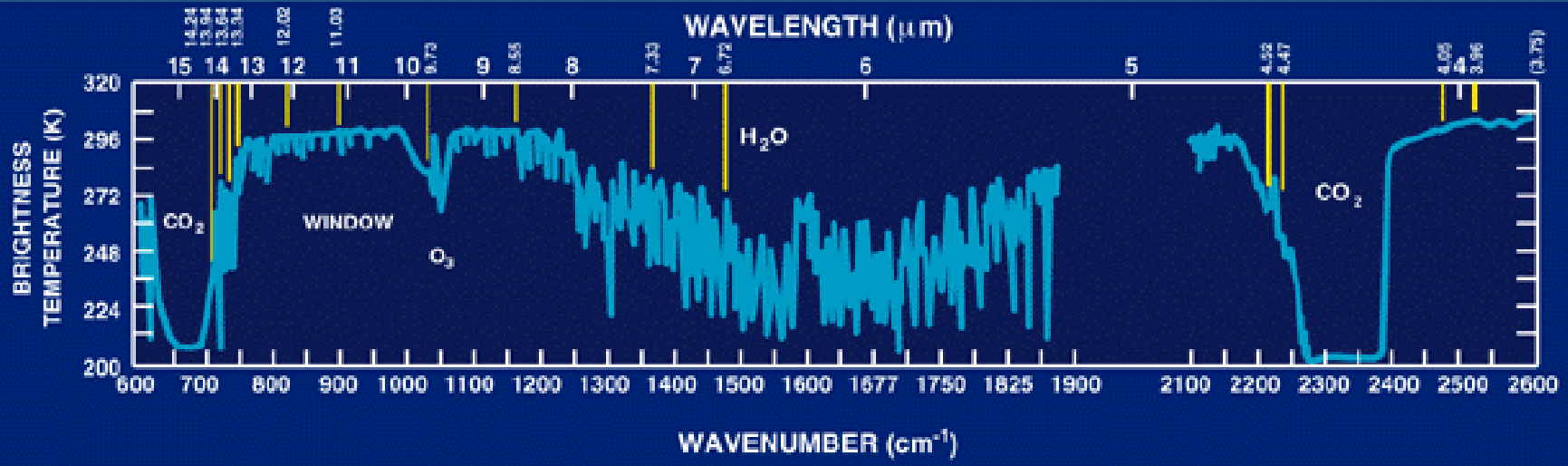

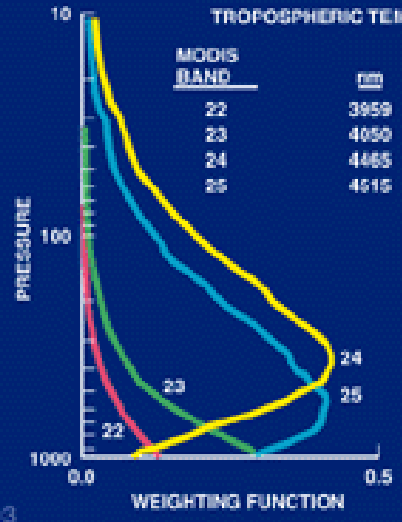

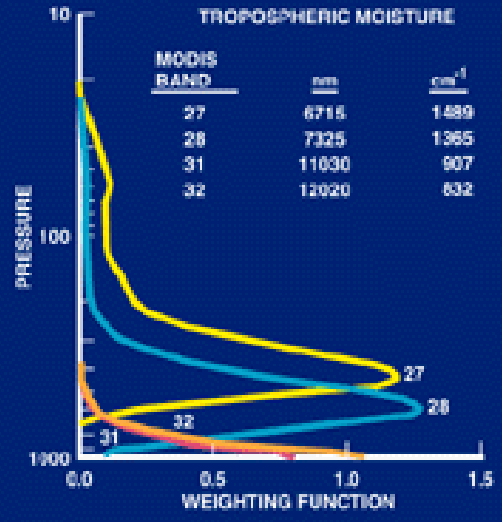

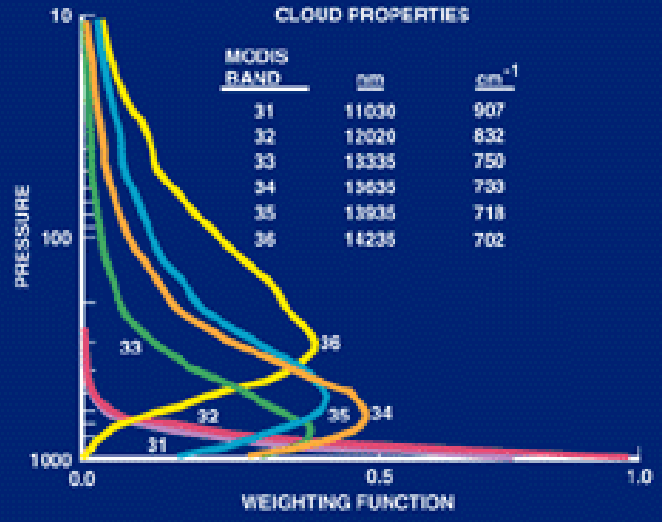

E351.002 5/93

MODIS identifies cloud classes

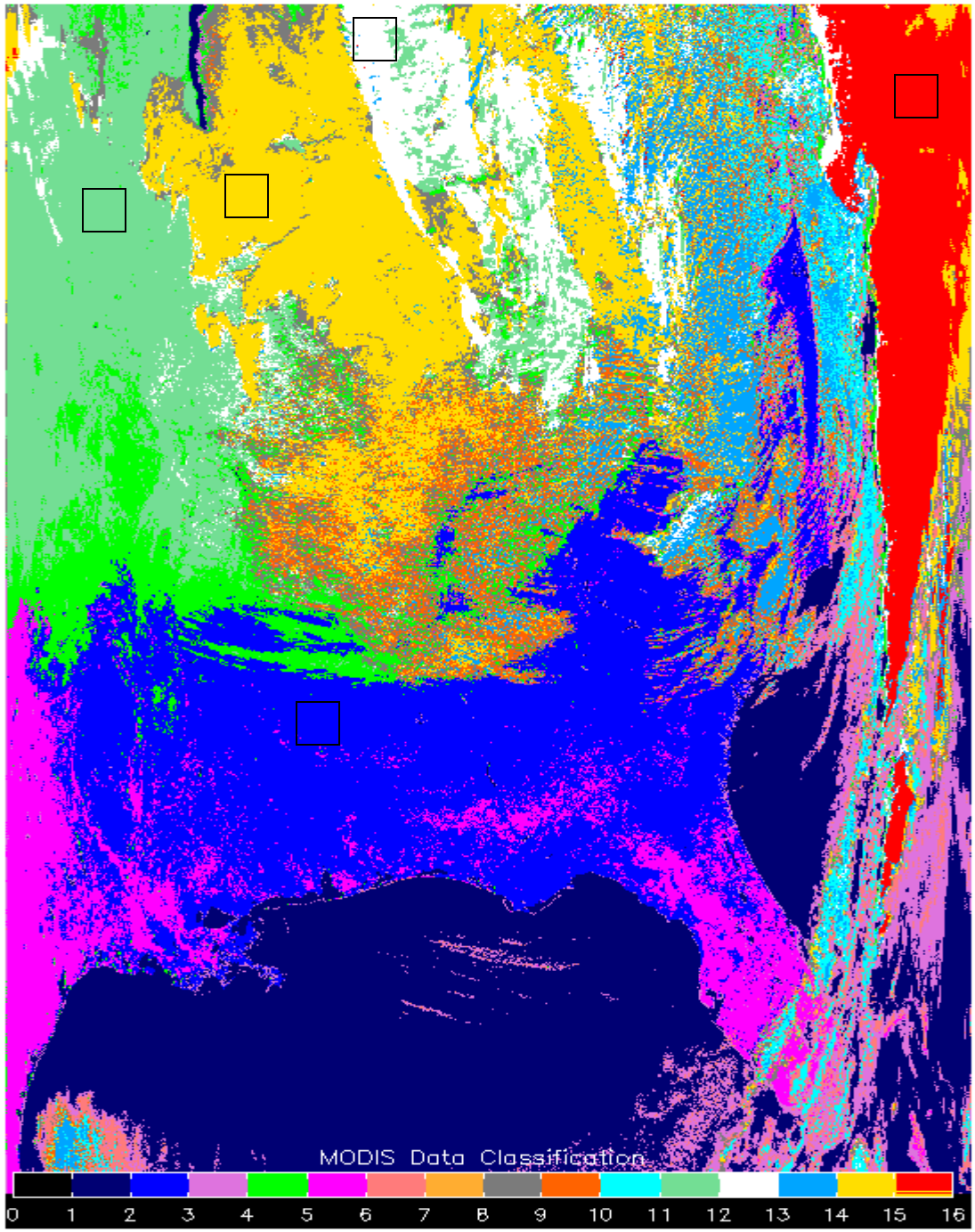

Hi cld

Mid cld

Lo cld

Snow

clr

Clouds separate into classes when multispectral radiance information is viewed

vis

LSD 1.6 um

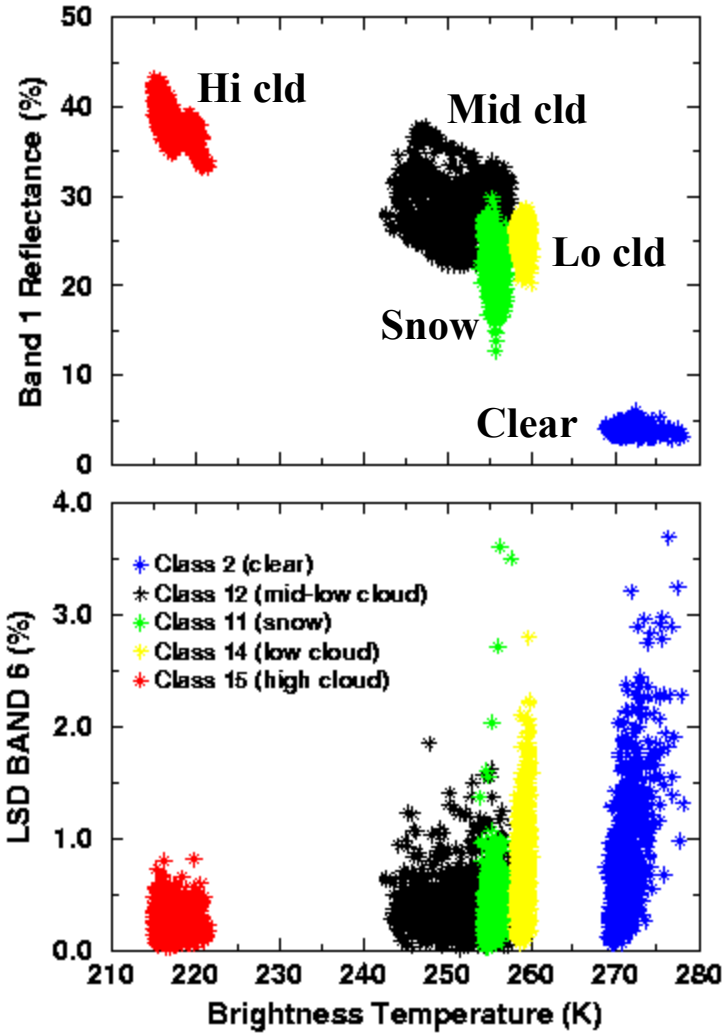

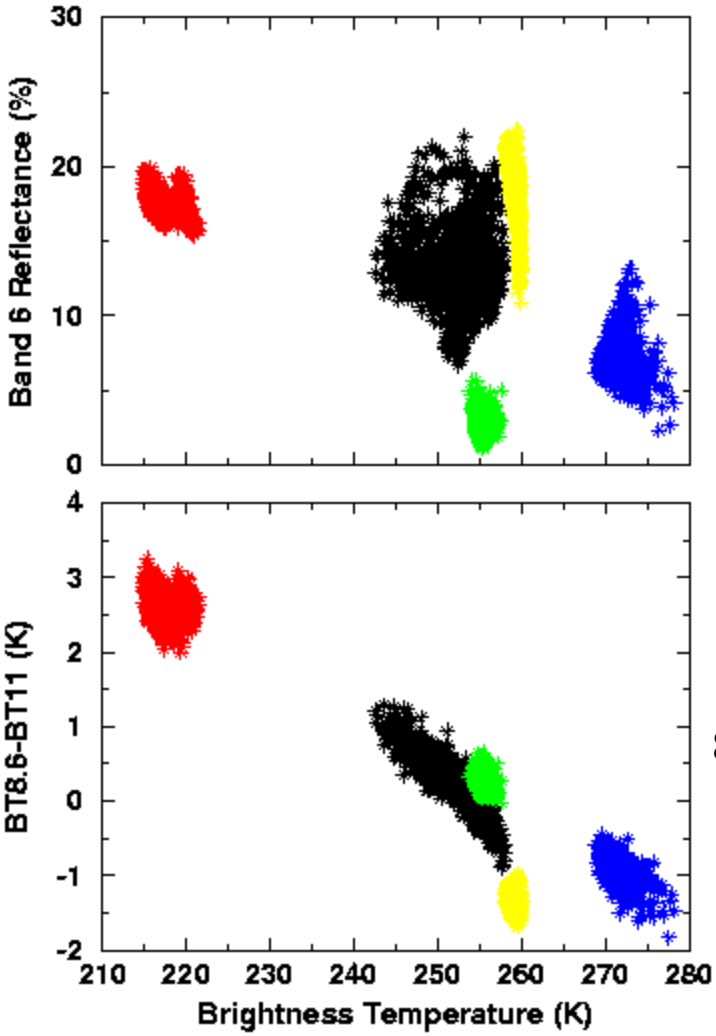

1.6 um

11 um

8.6-11 um

11 um

Cloud Properties

True Color Image
Cloud Mask
Land Classification
Cloud Opt Thickness
Cloud Eff Radius
Cloud Top Temp
Bispectral Phase

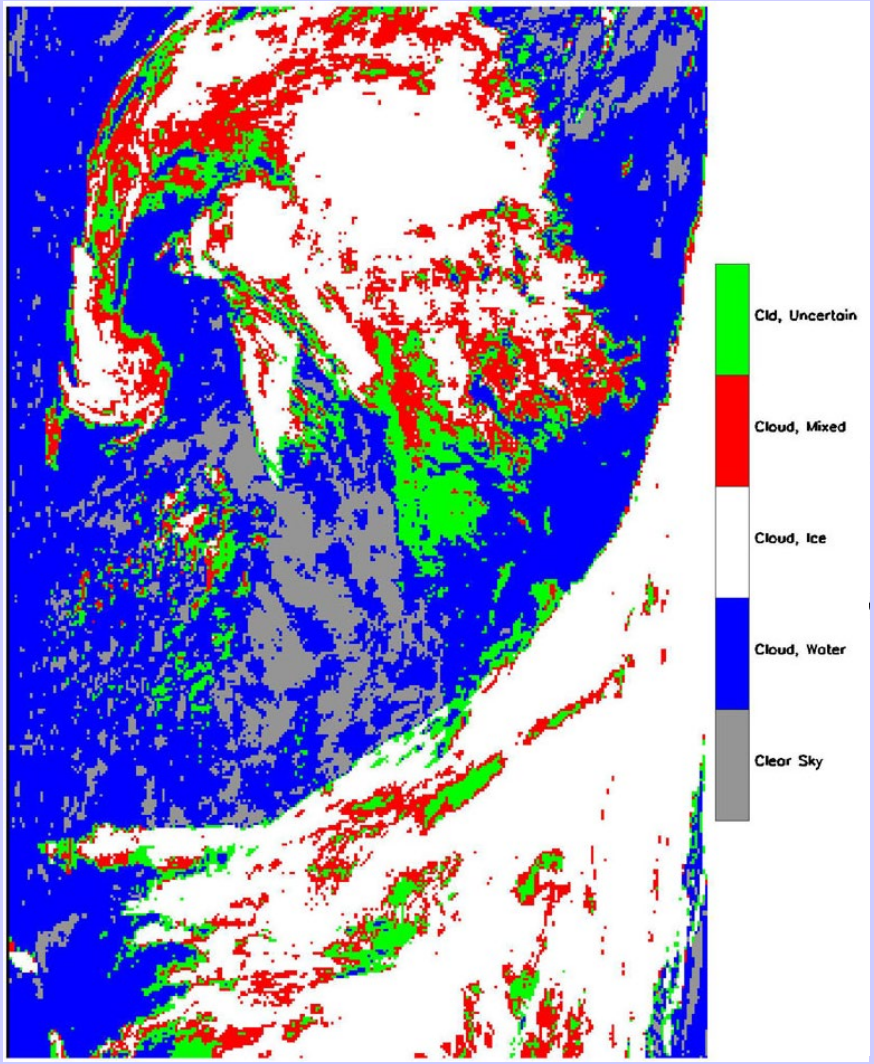

October 1, 2001

Cloud optical, microphysical properties

retrieval space example

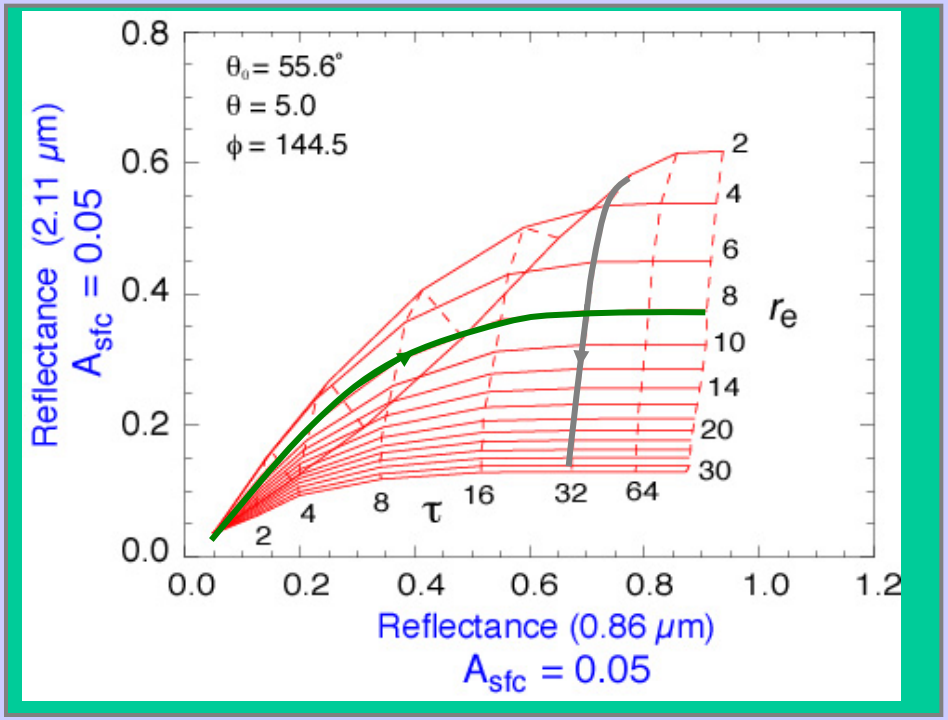

2.1 μm absorption increases with particle size, little effect at 0.86 μm

2.1 μm reflectance reaches limiting values with optical thickness

Liquid water cloud
ocean surface

Cloud Parameter Determinations from Satellite Measured Radiances
for a given field of view (FOV) partly clear and partly cloudy

Radiance from a partly cloudy FOV

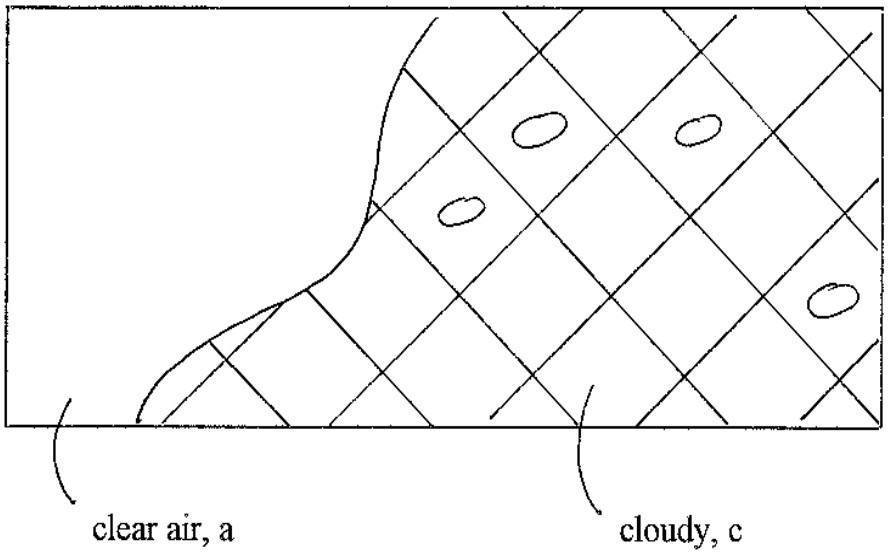

$$R = [1 - N] R_a + N R_c$$

but if b indicates opaque "black" cloud

$$R_c = [1 - \varepsilon] R_a + \varepsilon R_b(p_c)$$

so together

$$R = [1 - N\varepsilon] R_a + N\varepsilon R_b(p_c)$$

Two unknowns, ε and Pc, require two measurements

CO2 channels see to different levels in the atmosphere

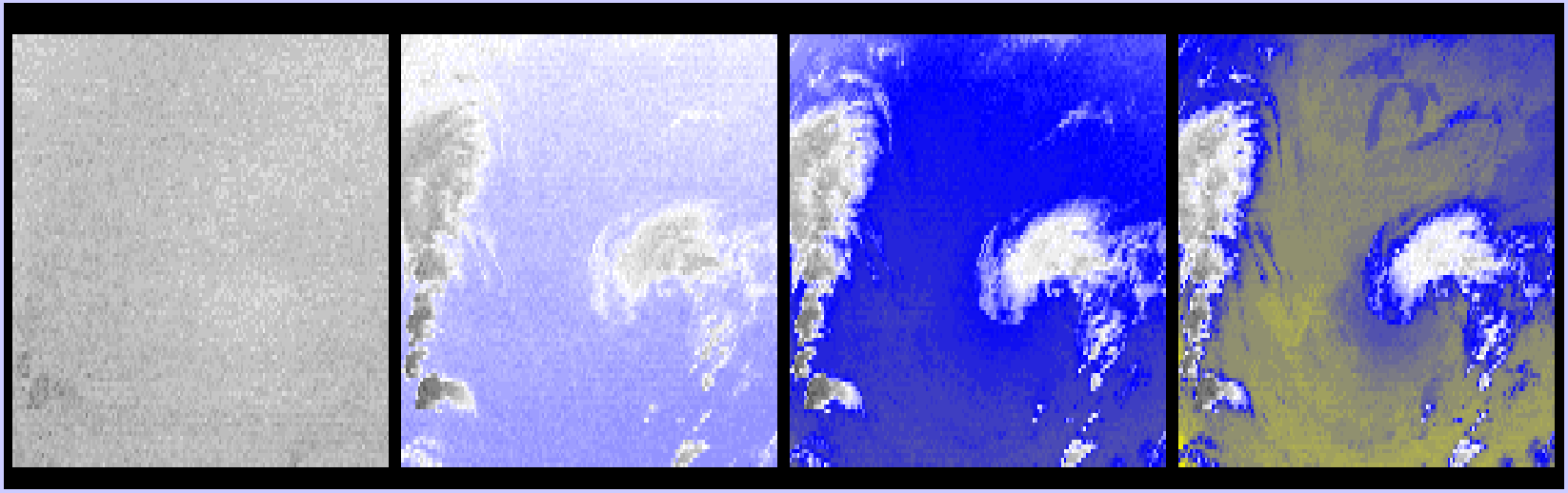

14.2 um 13.9 um 13.6 um 13.3 um

Different ratios reveal cloud properties at different levels

hi - 14.2/13.9
mid - 13.9/13.6
low - 13.6/13.3

Meas **Calc**

$$\frac{(I_{\lambda 1}-I_{\lambda 1}^{clr})}{(I_{\lambda 2}-I_{\lambda 2}^{clr})} = \frac{\eta\varepsilon_{\lambda 1}\int_{p_s}^{p_c}\tau_{\lambda 1}\,dB_{\lambda 1}}{\eta\varepsilon_{\lambda 2}\int_{p_s}^{p_c}\tau_{\lambda 2}\,dB_{\lambda 2}}$$

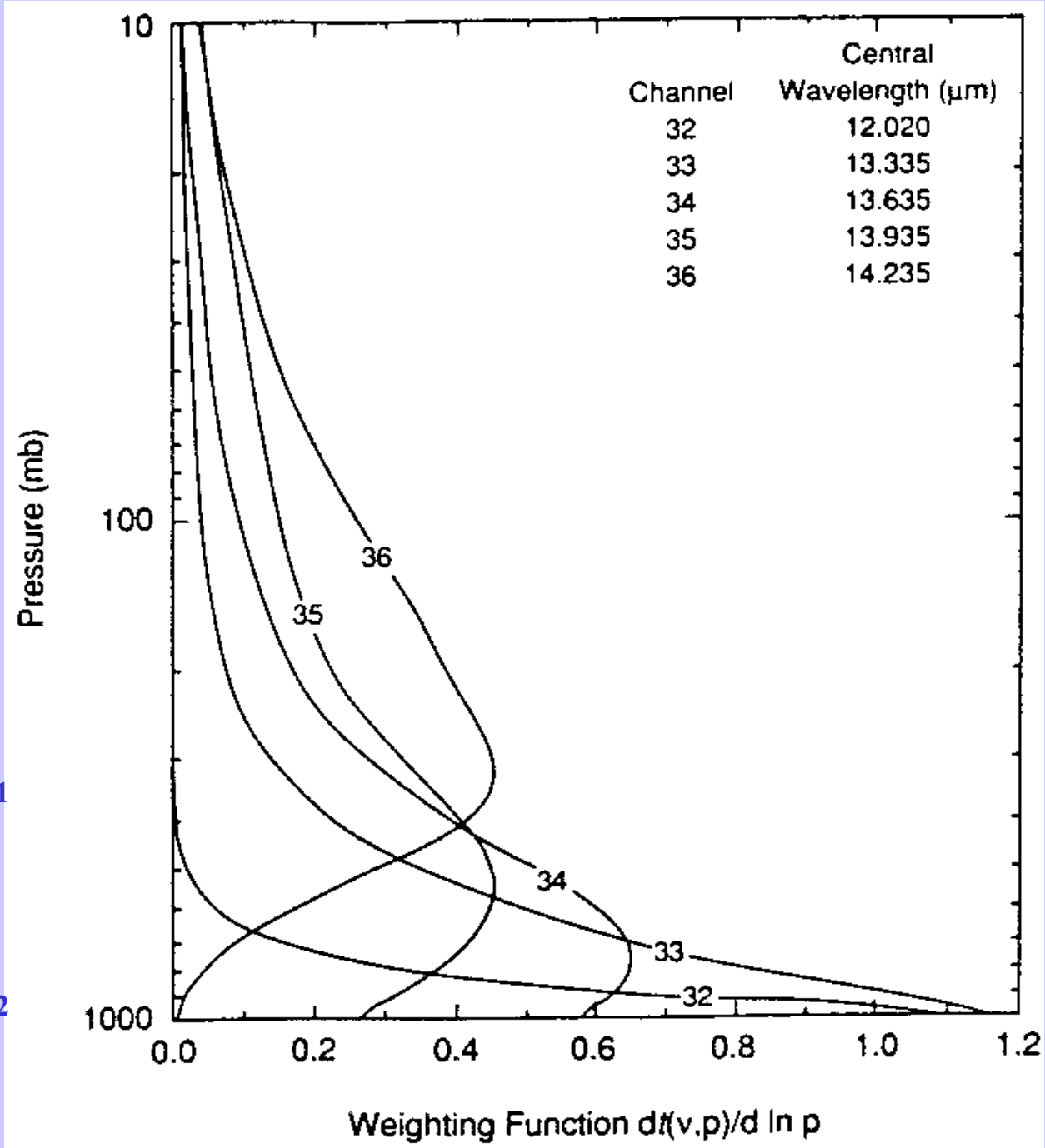

BT in and out of clouds for MODIS CO_2 bands

- demonstrate weighting functions and cloud top algorithm

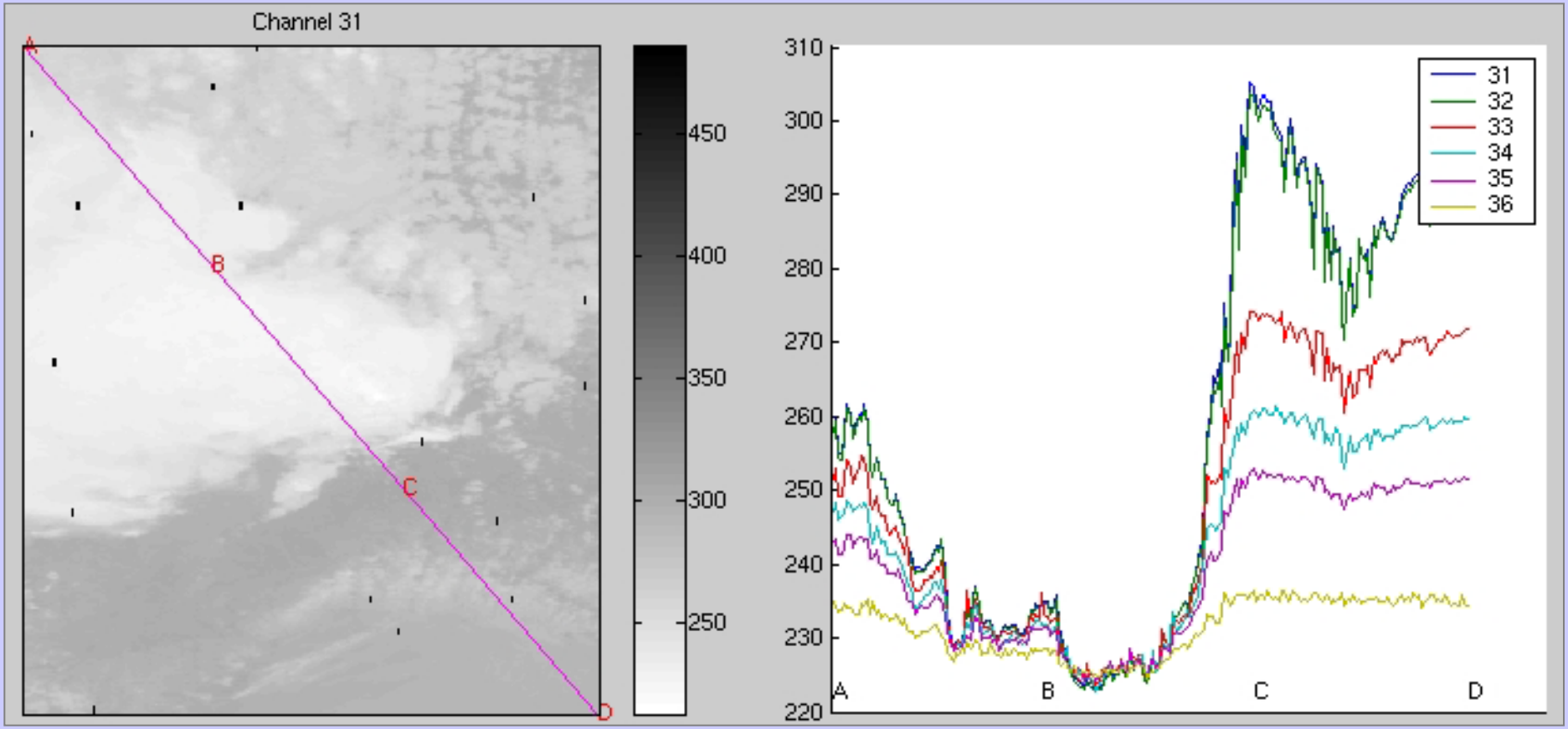

AQUA/MODIS BAND1 2300UTC 8/24/02

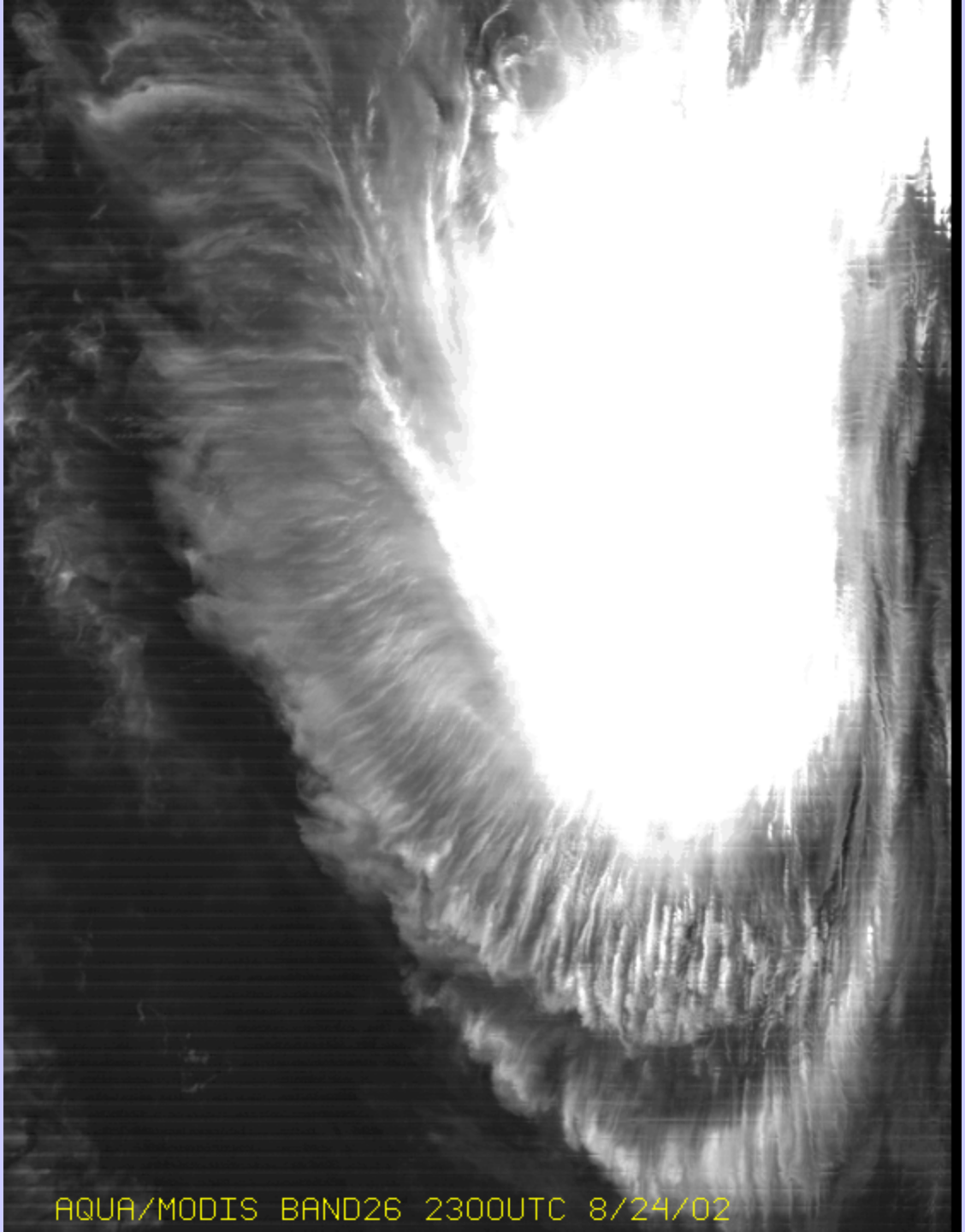
AQUA/MODIS BAND26 2300UTC 8/24/02

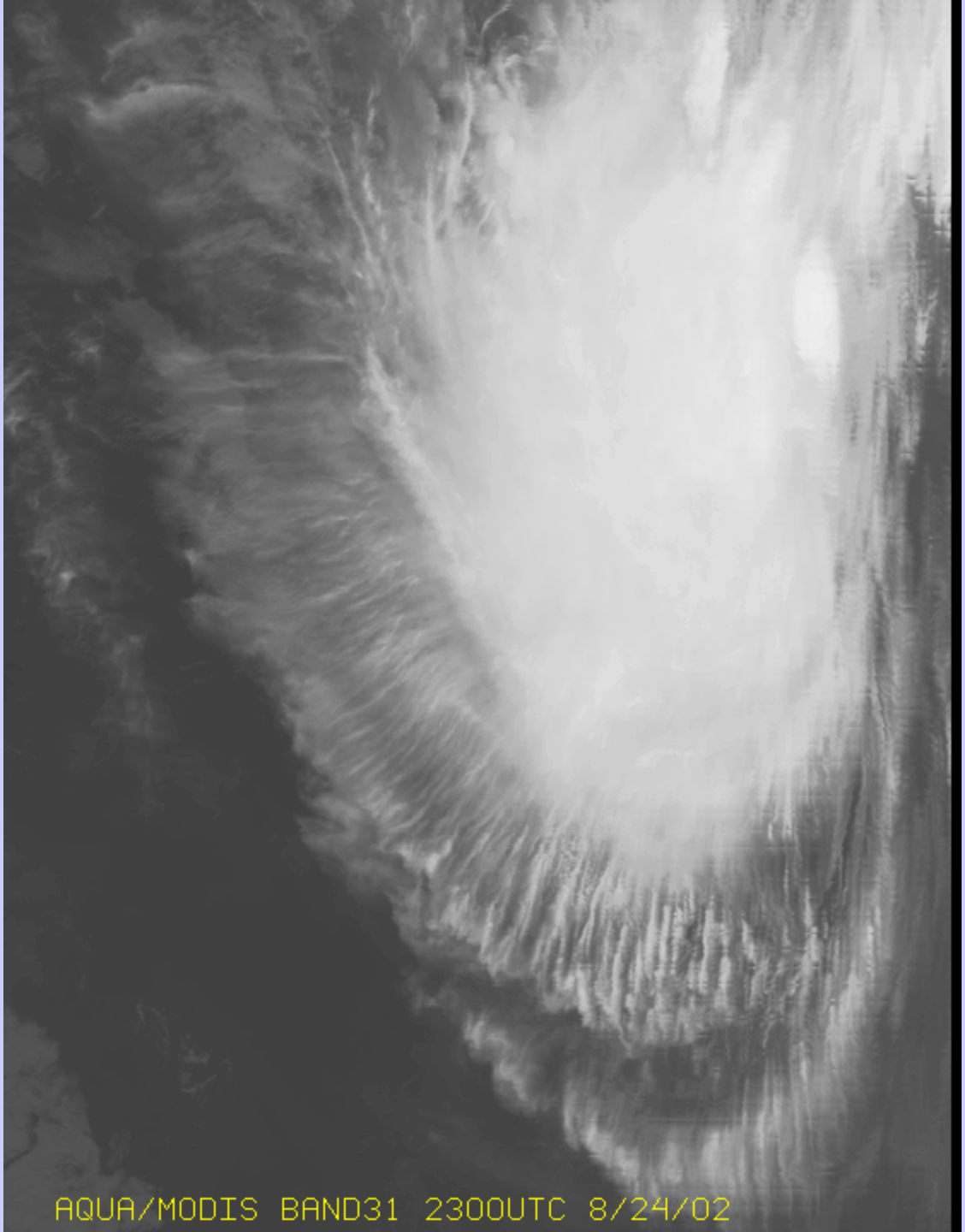
AQUA/MODIS BAND31 2300UTC 8/24/02

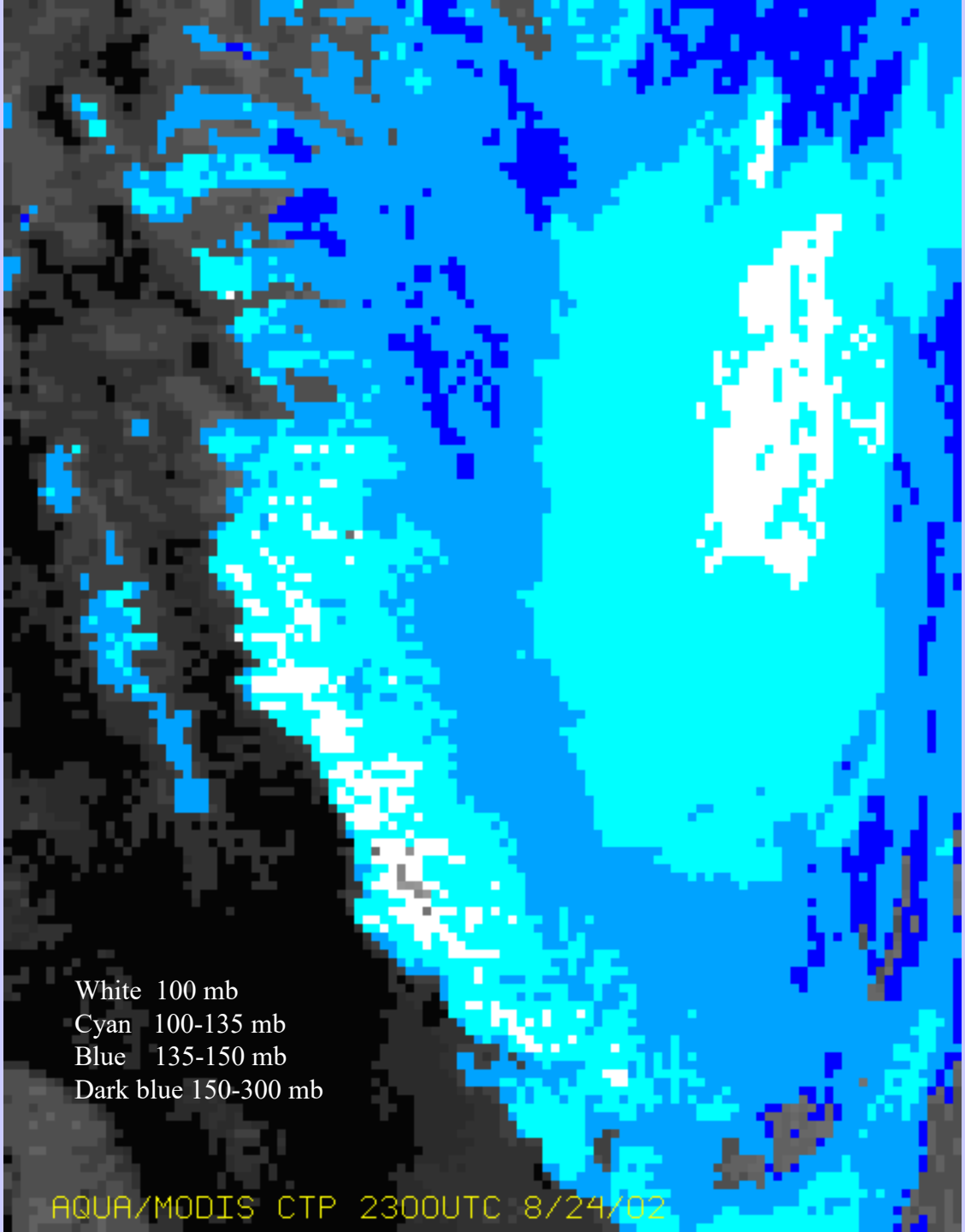
White 100 mb
Cyan 100-135 mb
Blue 135-150 mb
Dark blue 150-300 mb
AQUA/MODIS CTP 2300UTC 8/24/02

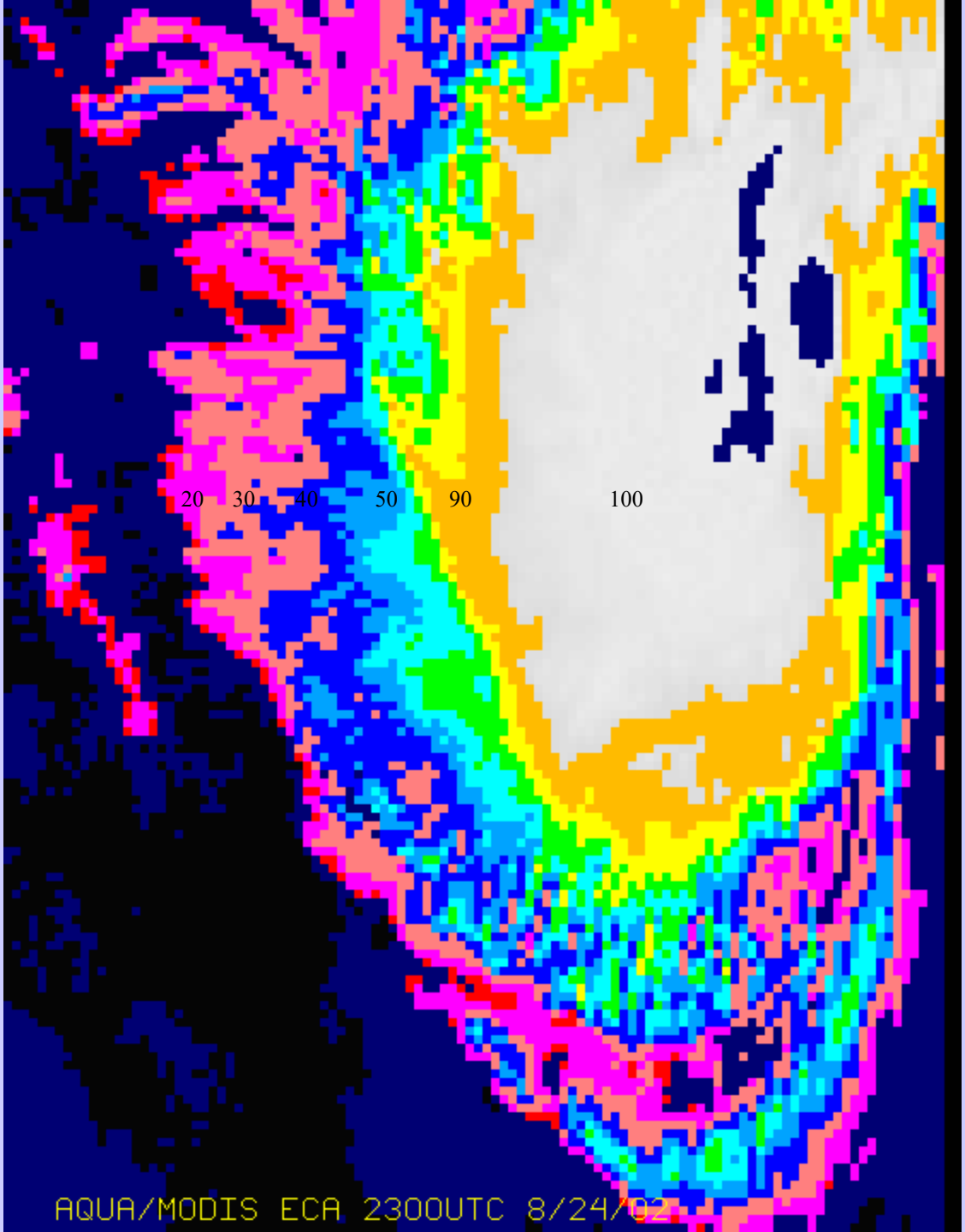
L
20
30
40
50
90
100
AQUA/MODIS ECA 2300UTC 8/24/02

January 2001: MODIS High Clouds (0–400 mb)

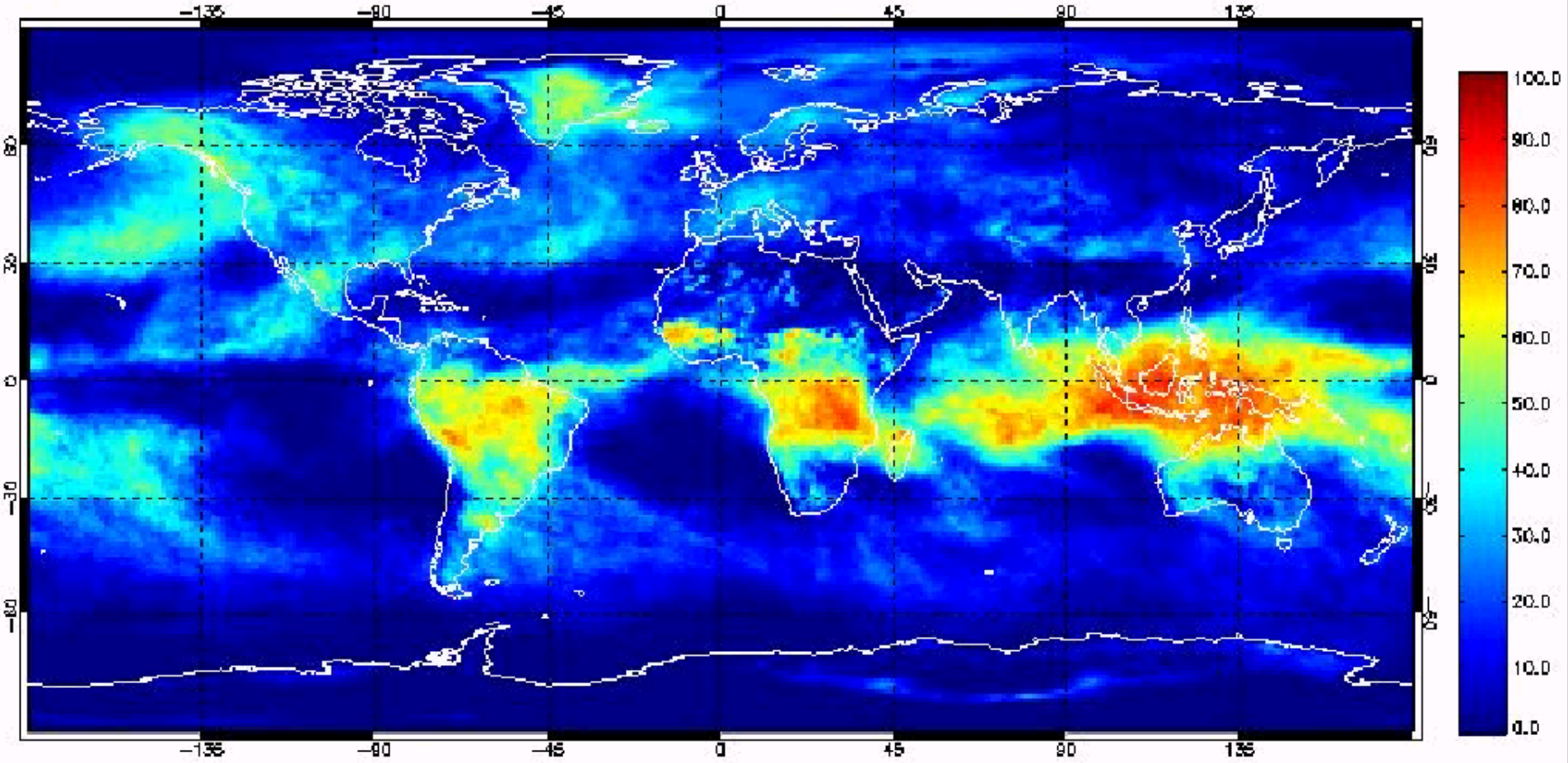

Simulations of Ice and Water Phase Clouds
8.5 - 11 μm BT Differences

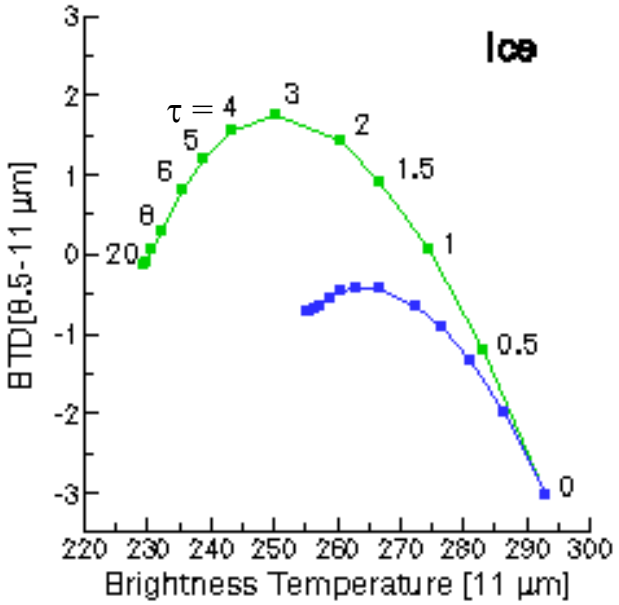

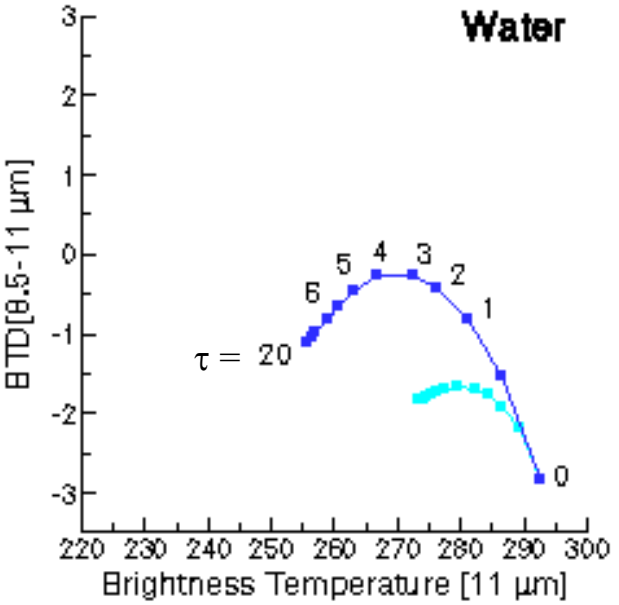

High Ice clouds

• BTD[8.5-11] > 0 over a large range of optical thicknesses τ
•T_{cld} = 228 K

Midlevel clouds

• BTD[8.5-11] values are similar (*i.e.*, negative) for both water and ice clouds
•T_{cld} = 253 K

Low-level, warm clouds

• BTD[8.5-11] values always negative
•T_{cld} = 273 K

Ice: Cirrus model derived from FIRE-I in-situ data (Nasiri et al, 2002)
Water: r_e=10 μm
Angles: θ_o = 45°, θ = 20°, and ϕ = 40°
Profile: midlatitude summer

MODIS Direct Broadcast

May 14, 2003 at 1458 UTC (Terra)
1-km resolution

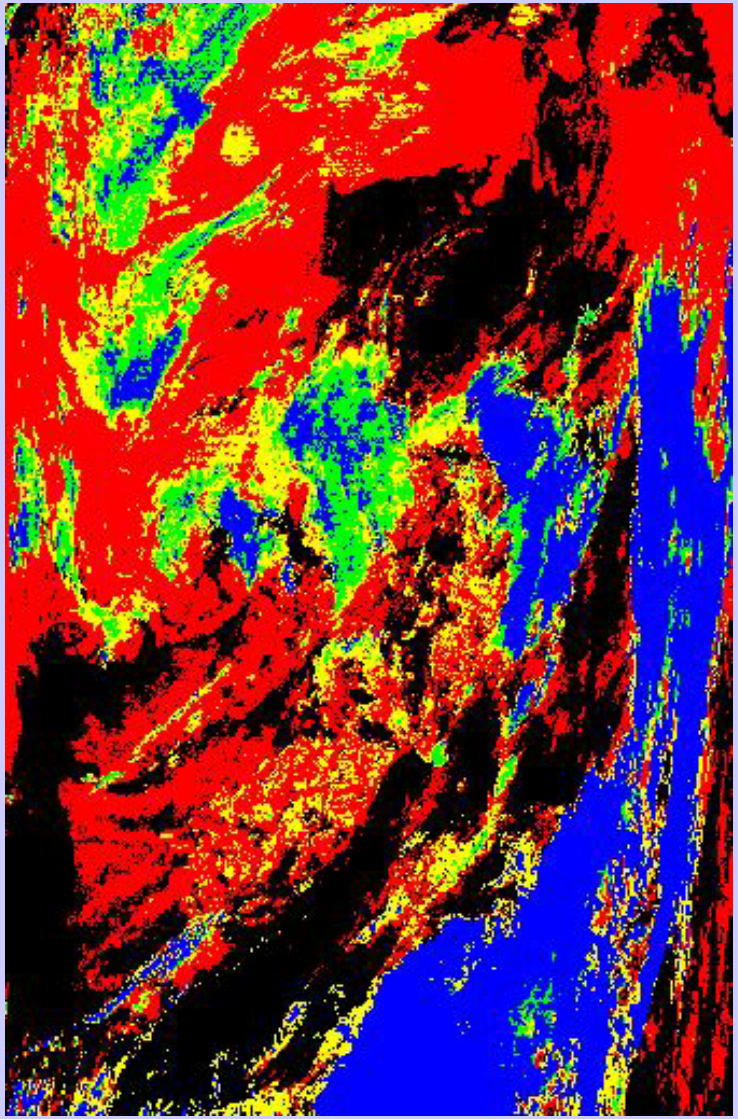

Cloud Phase

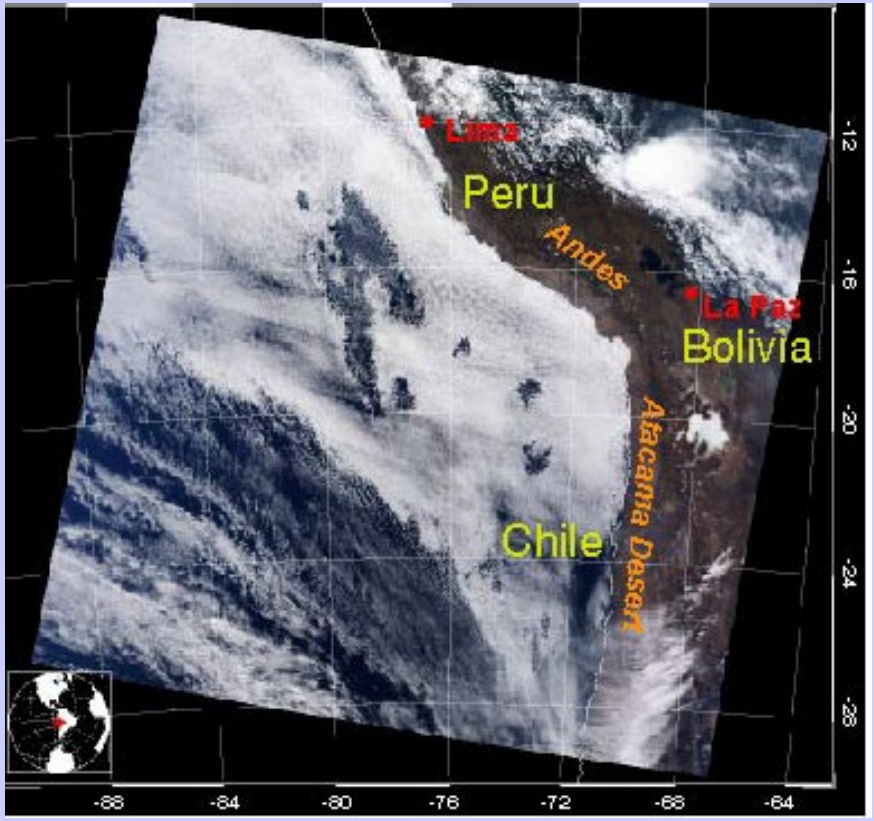

18 July 2001

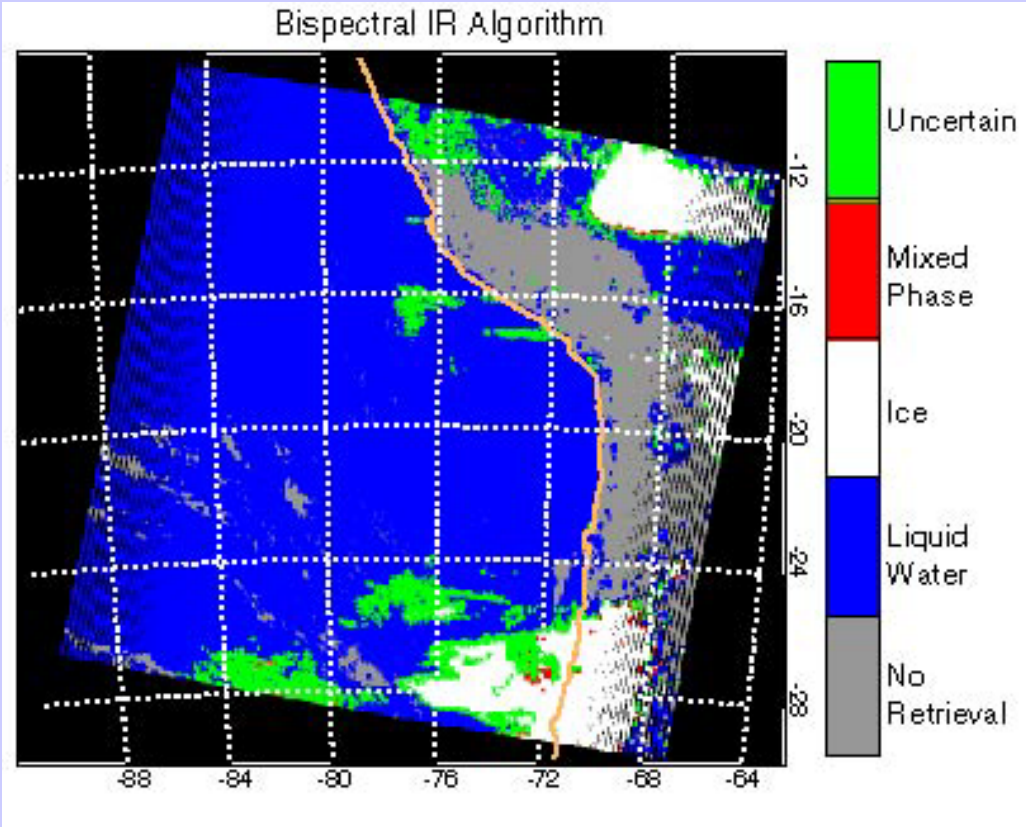

Multilayered Clouds

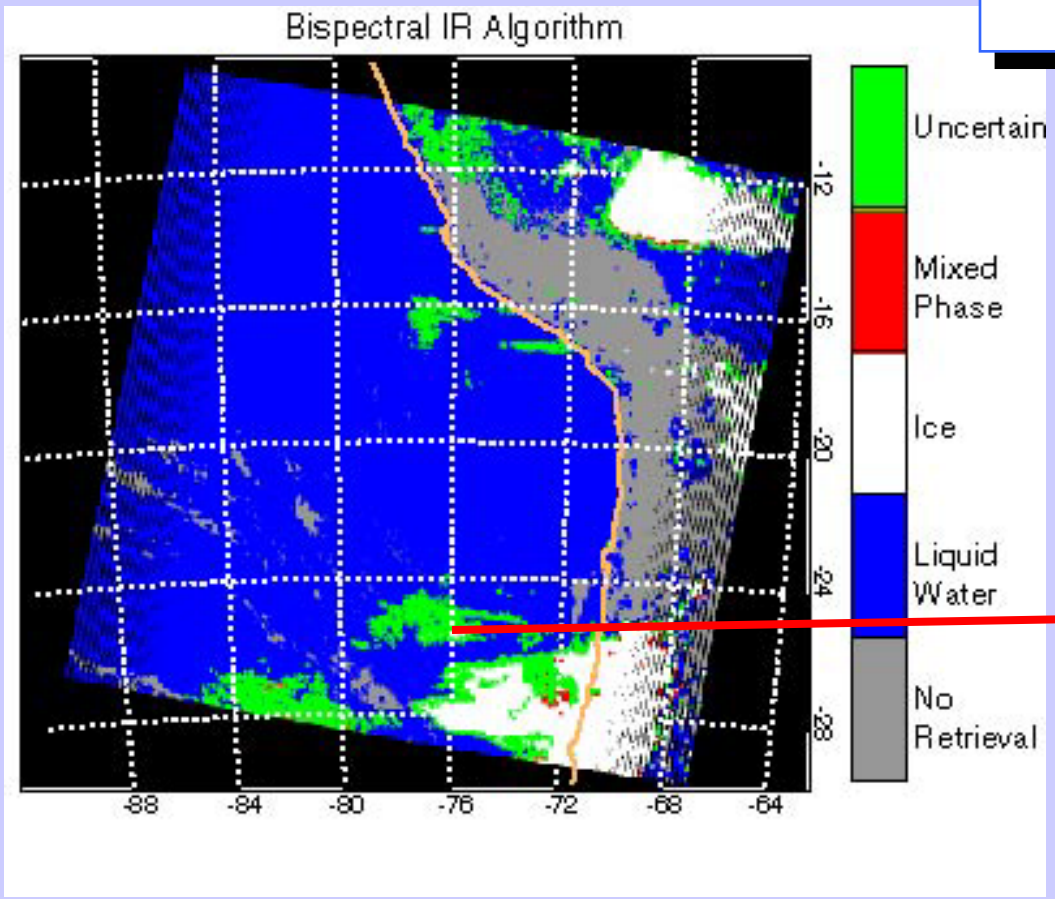

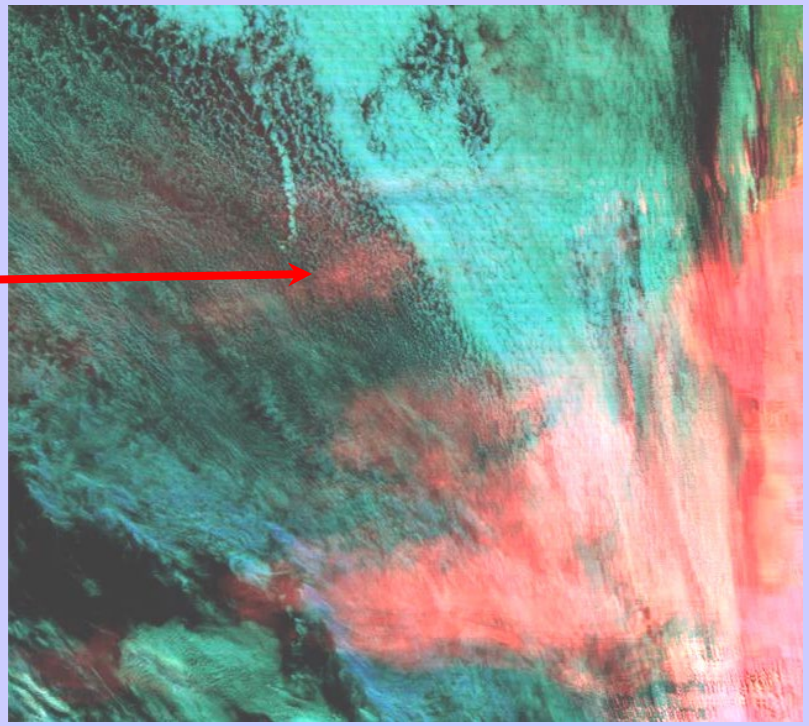

MODIS Cloud Thermodynamic Phase
Percentage Ice and Water Cloud
05 Nov. 2000 -Daytime Only

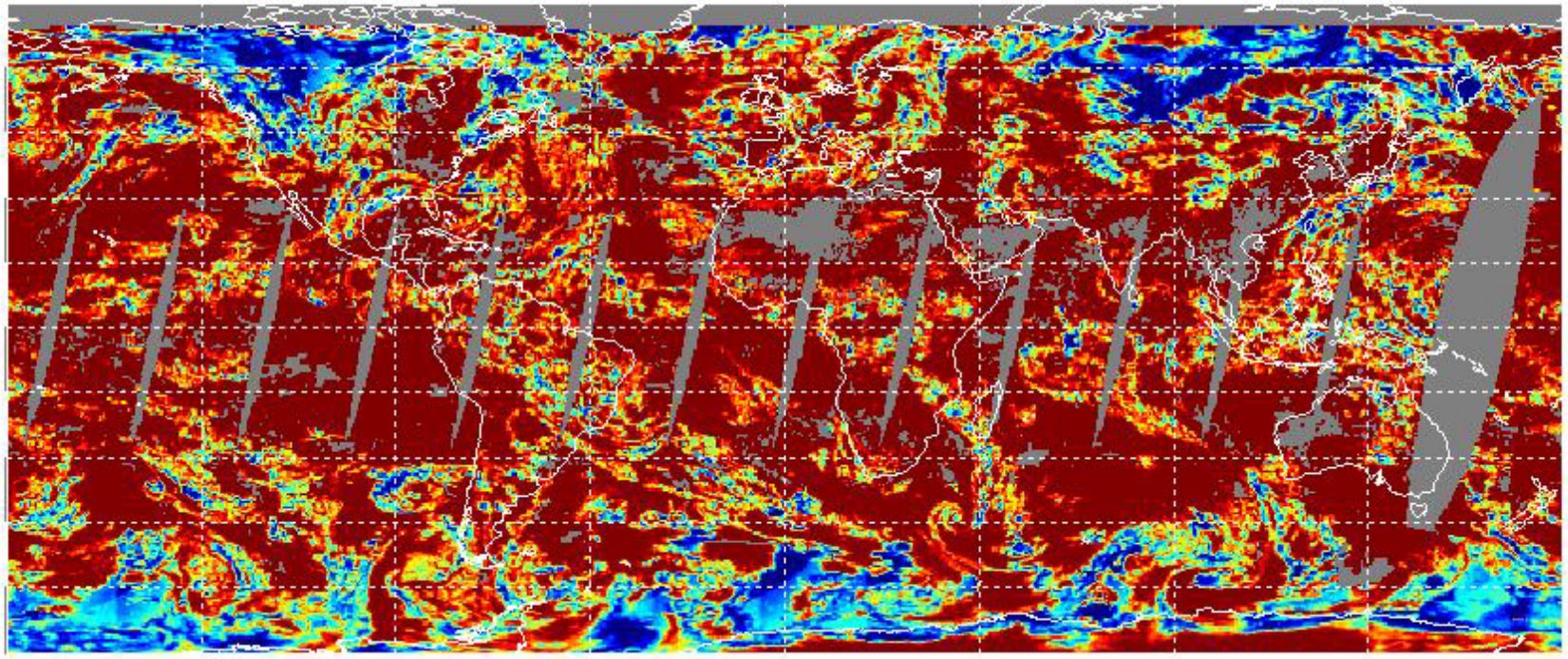

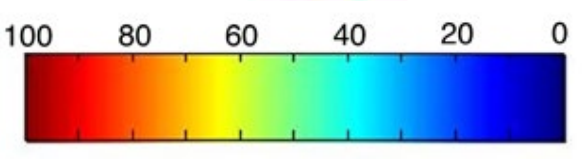

frequency of occurrence in percent (%)

MODIS Cloud Thermodynamic Phase
Percentage Ice and Water Cloud
05 Nov. 2000 - Nighttime Only

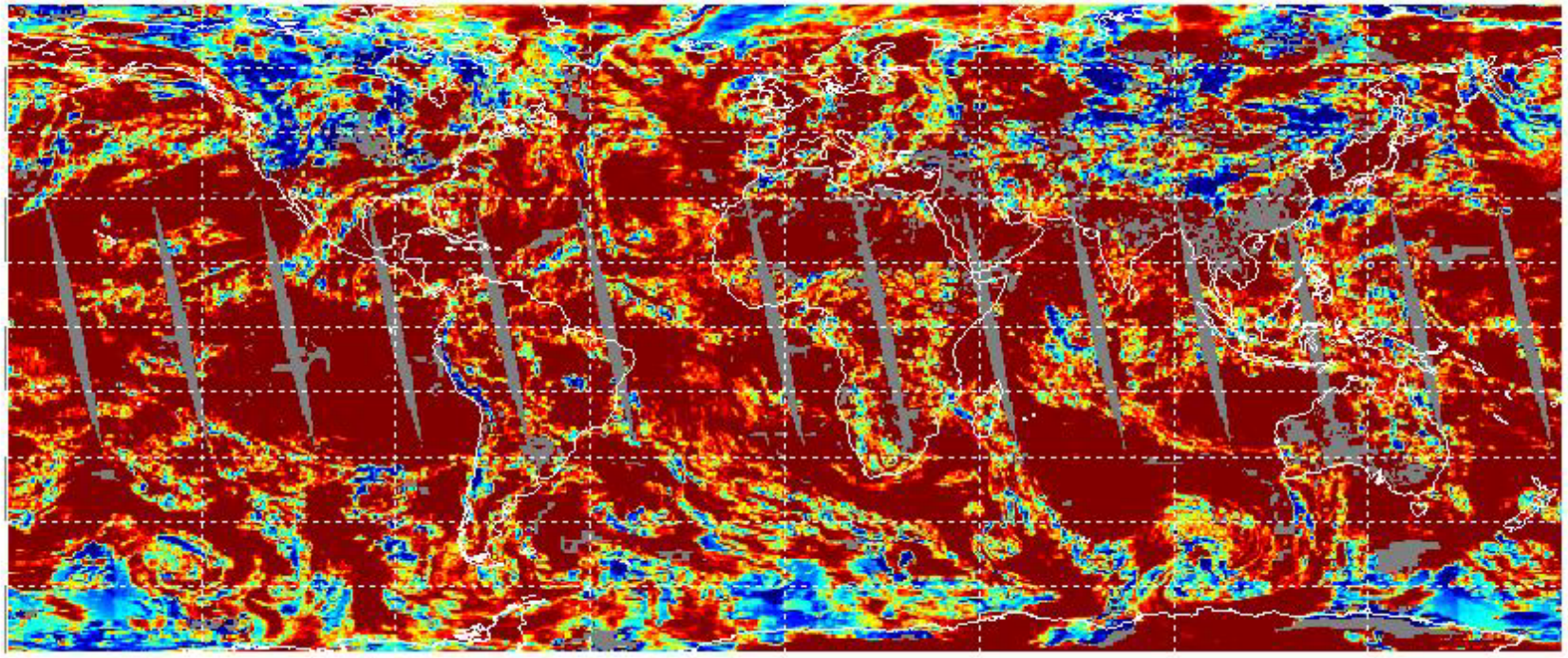

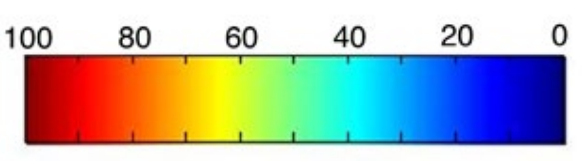

frequency of occurrence in percent (%)

MODIS Frequency of Co-occurrence Water Phase with 253 K < T_{cld} < 268 K 05 Nov. 2000 - Daytime Only

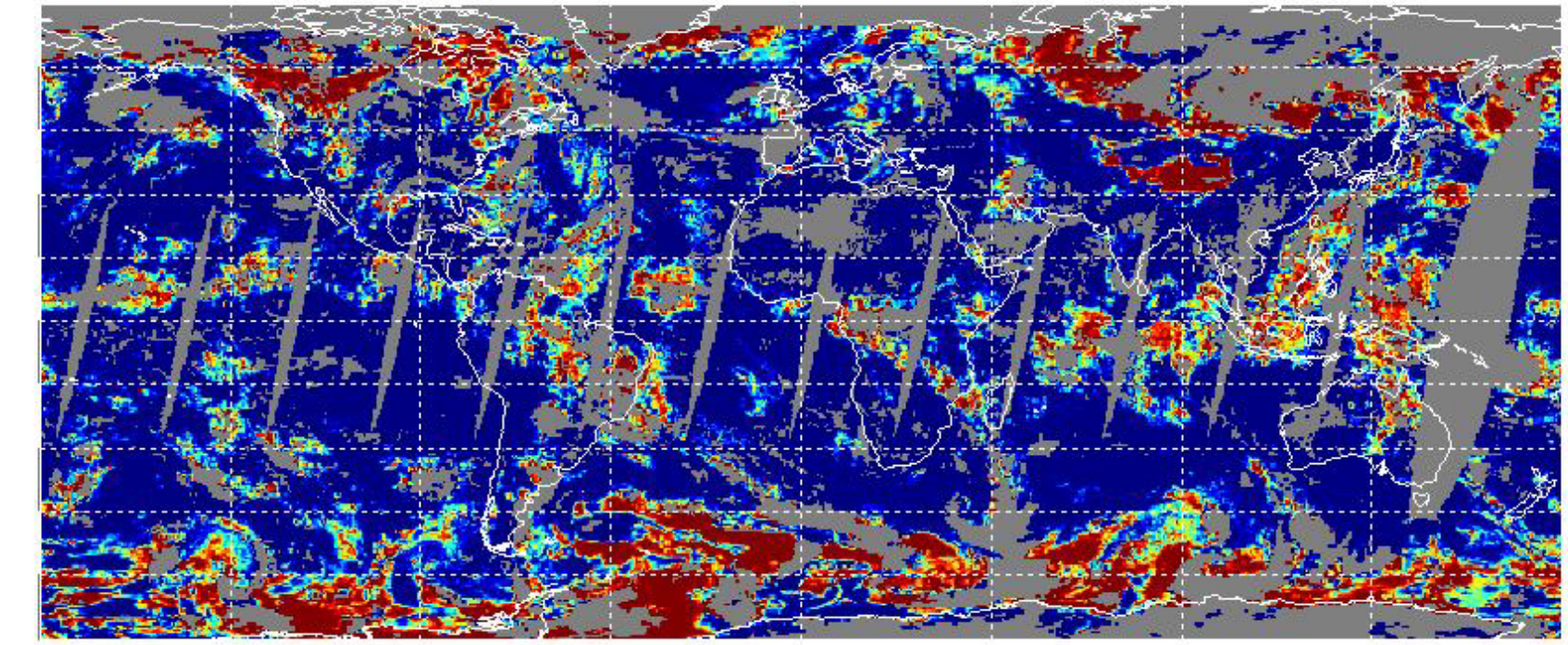

frequency of occurrence in percent (%)

MODIS Frequency of Co-occurrence
Water Phase with 253 K < T_{cld} < 268 K
05 Nov. 2000 - Nighttime Only

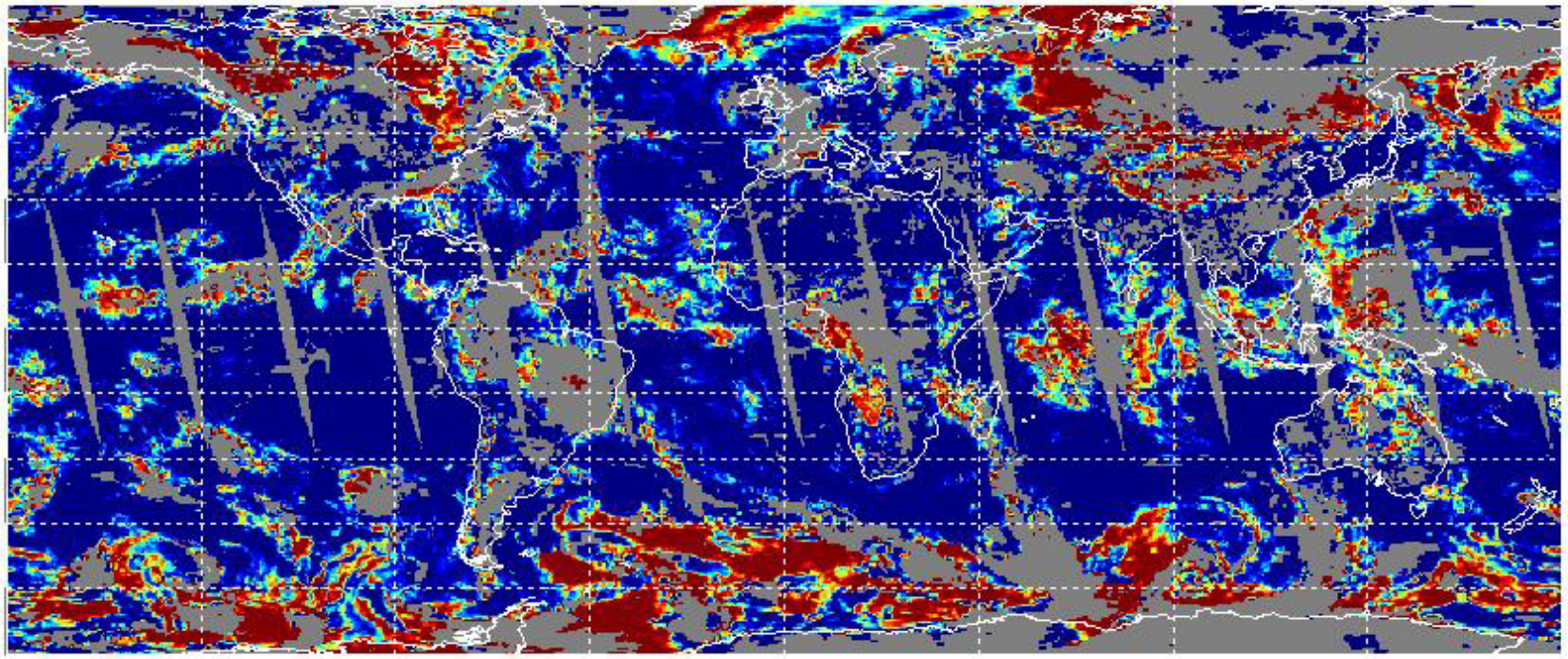

frequency of occurrence in percent (%)

Aerosol Types and Origin

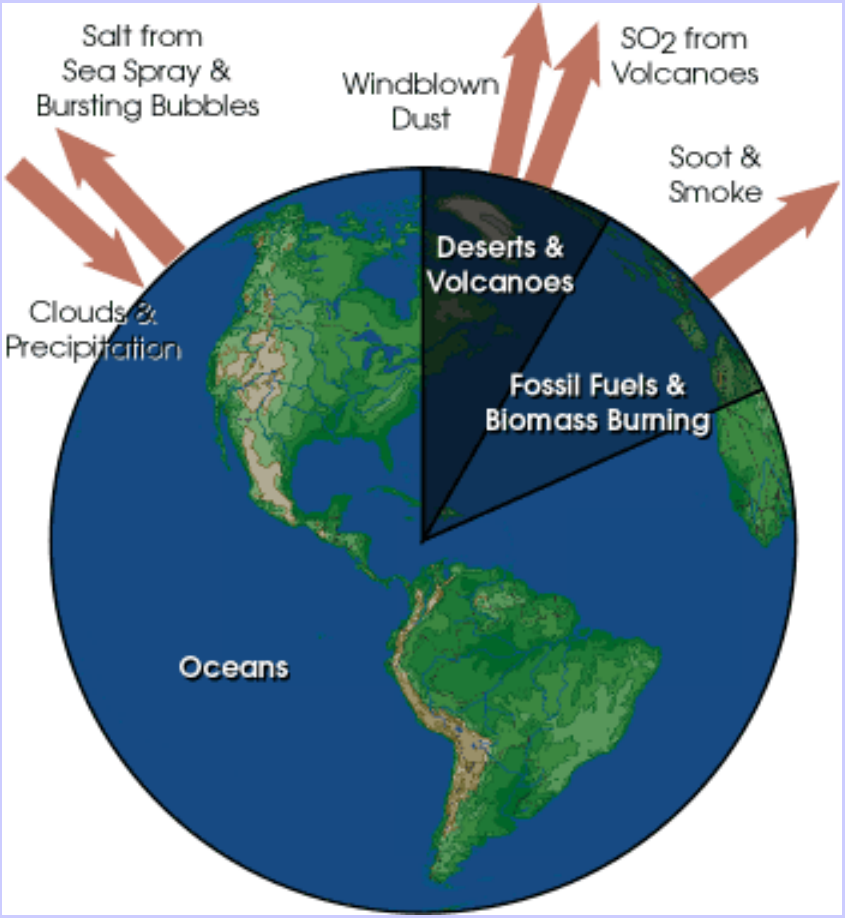

- Aerosol particles larger than about 1 μm in size are produced by windblown dust and sea salt from sea spray and bursting bubbles
- Aerosols smaller than 1 μm are mostly formed by condensation processes such as conversion of sulfur dioxide (SO2) gas (released from volcanic eruptions) to sulfate particles and by formation of soot and smoke during burning processes.
- After formation, aerosols are mixed and transported by atmospheric motions and are primarily removed by clouds and precipitation.

Aerosol Size Distribution

There are 3 modes :

- « **nucleation** »: radius is between 0.002 and 0.05 µm. They result from combustion processes, photo-chemical reactions, etc.

- « **accumulation** »: radius is between 0.05 µm and 0.5 µm. Coagulation processes.

- « **coarse** »: larger than 1 µm. From mechanical processes like aeolian erosion.

« fine » particles (nucleation and accumulation) result from anthropogenic activities, coarse particles come from natural processes.

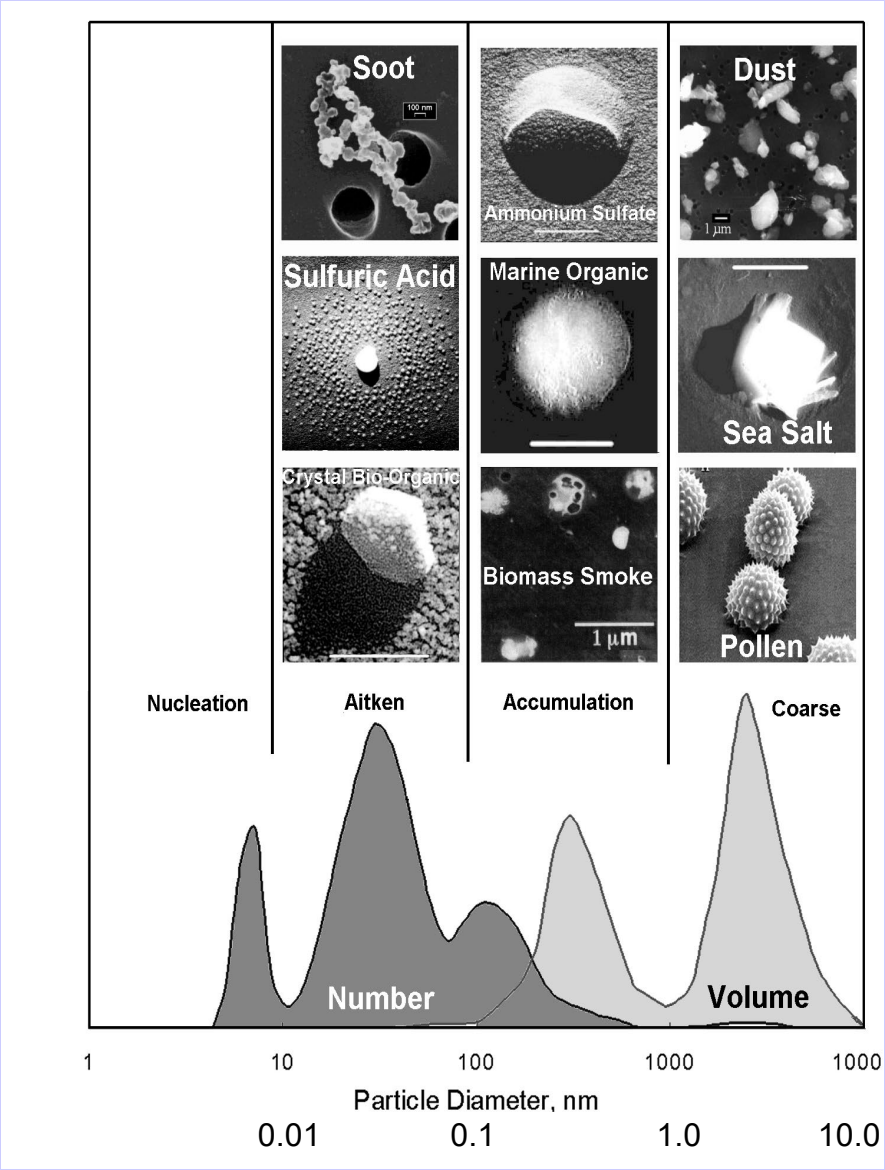

Dust Storm off Morocco (03/12/03)

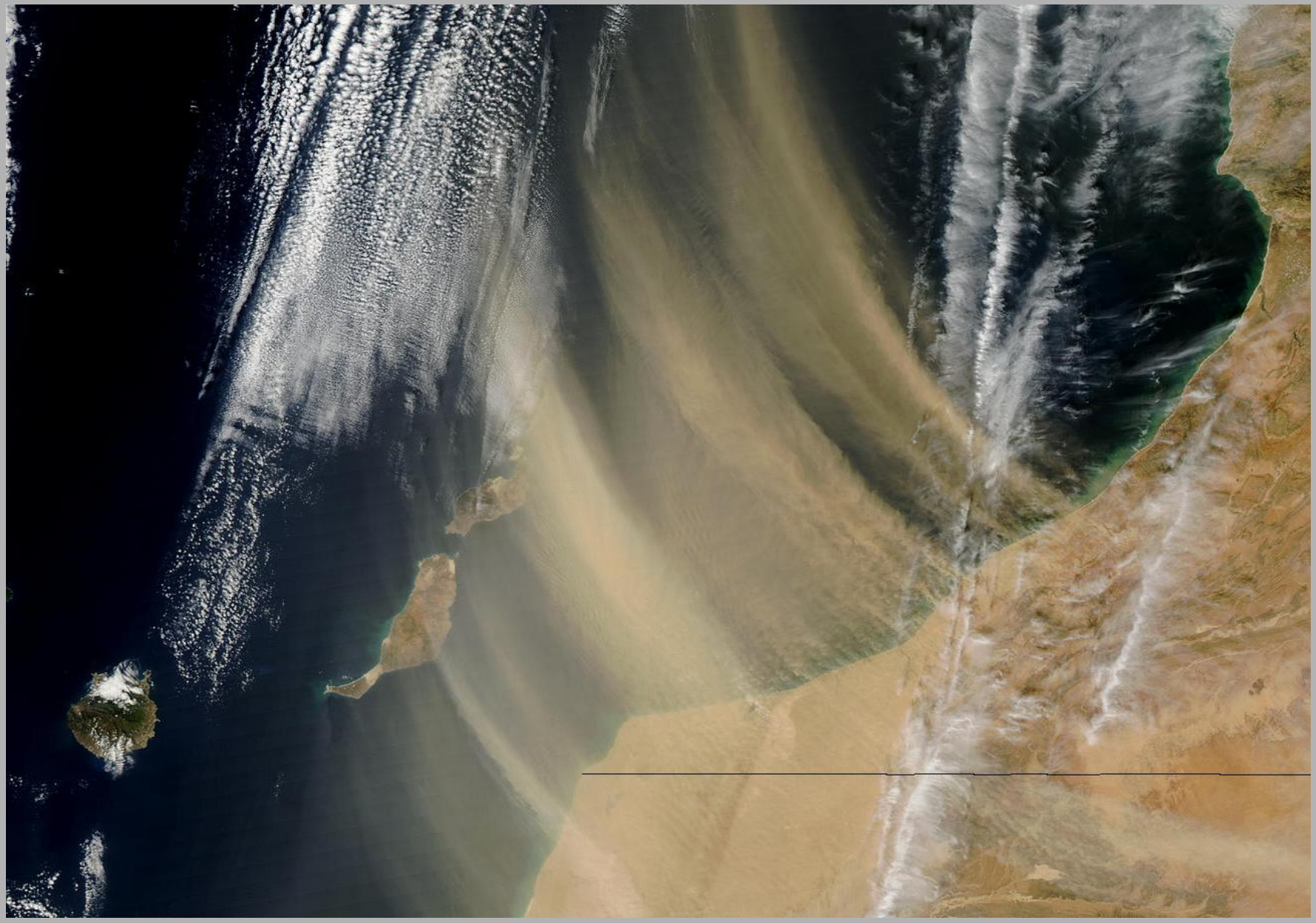

Dust Storm off West Africa (03/02/03)

Pollution off Northeast United States (08/14/02)

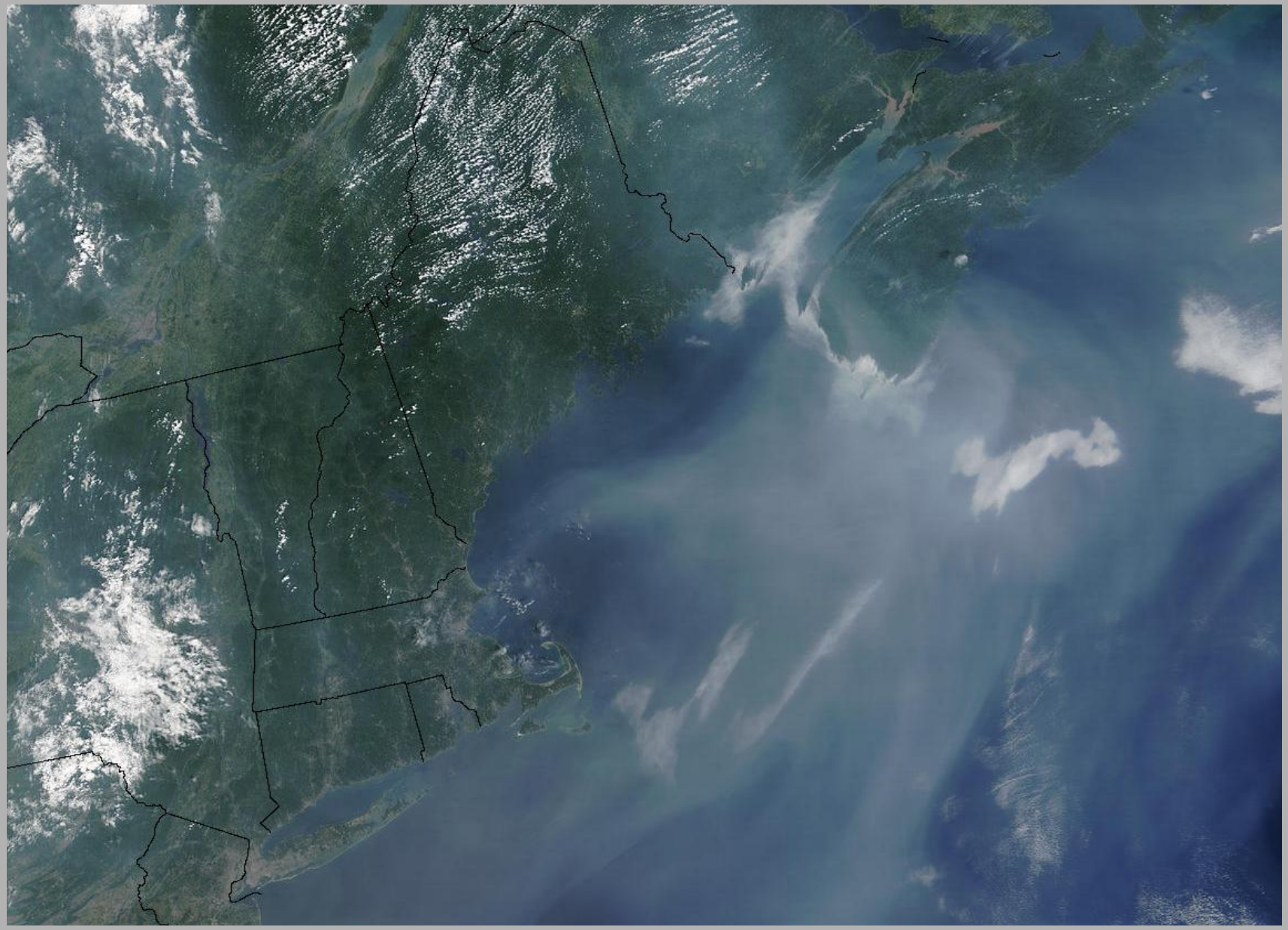

True color composite

AOT (0.55 um)

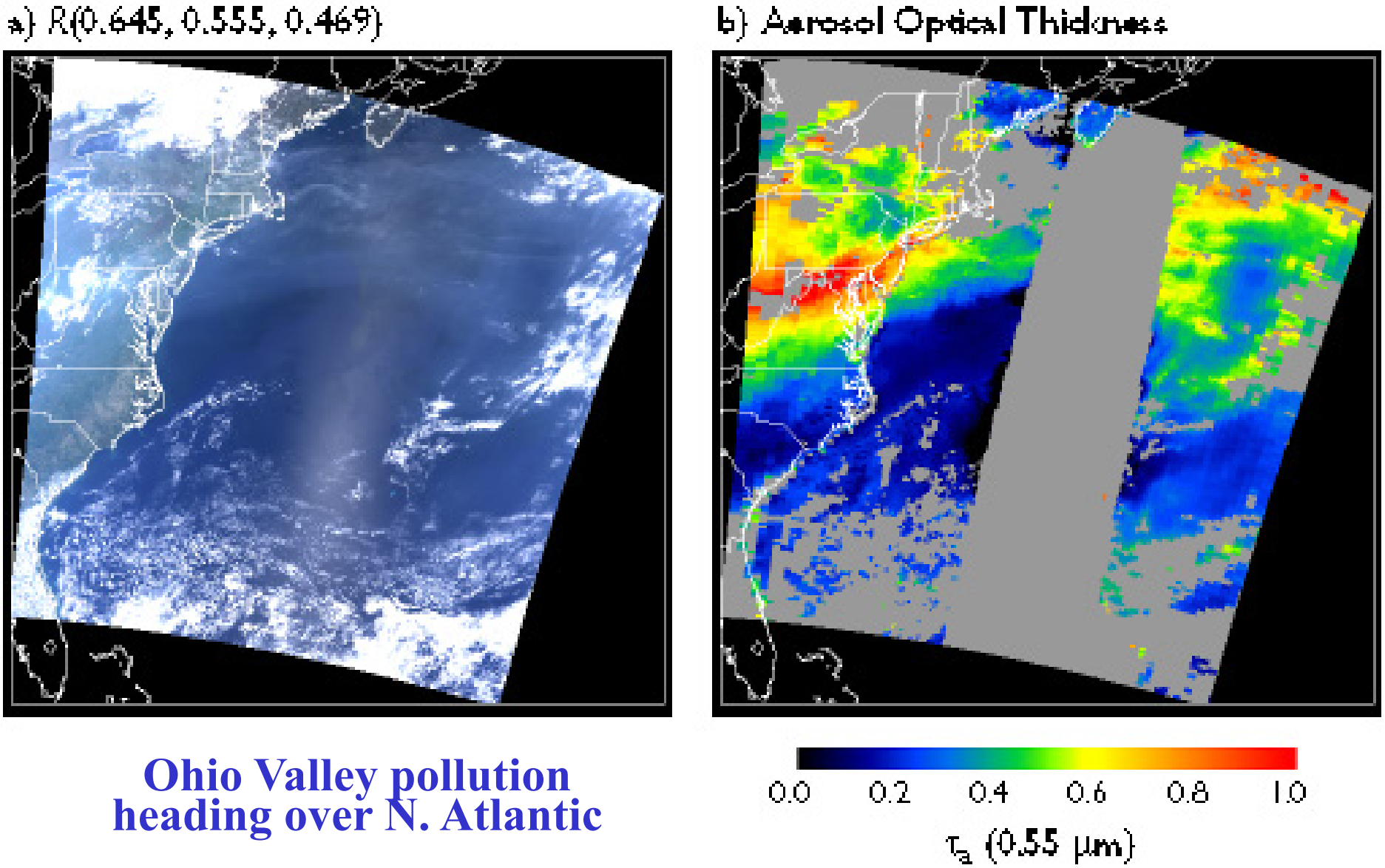

Ohio Valley pollution heading over N. Atlantic

- Effect of aerosol on climate:

Cooling past climates, possibly warming future climates

- Effect of aerosol on hydrologic cycle:

Less evaporation from cooler land and ocean, more stable atmosphere, less clouds and precipitation.

- Effect of aerosol on health: May be more important then ozone in causing cancer and heart problems.

- **Effect on agriculture, vegetation**: Shift of precipitation away from polluted land, less sunlight to vegetation

Aerosol, their sources and effects on climate

Properties	Net effect	Aerosol type	Main Source
Reflect sunlight	Cool the earth	Desert dust, sulfate smog	dry lake beds industry
Absorb sunlight	**Heat the earth & atmosphere reduce cloudiness**	**Black carbon**	**biomass burning dirty engines**
Cloud Condensation Nuclei	brighter clouds less precipitation	sulfate smog smoke	industry fires

Remote sensing of Aerosol

Open questions: - Where does aerosol begin and cloud ends?
- Does aerosol in cloud free area represent the aerosol that interacts with clouds?
- How to handle the spatial and temporal variability of aerosol properties?

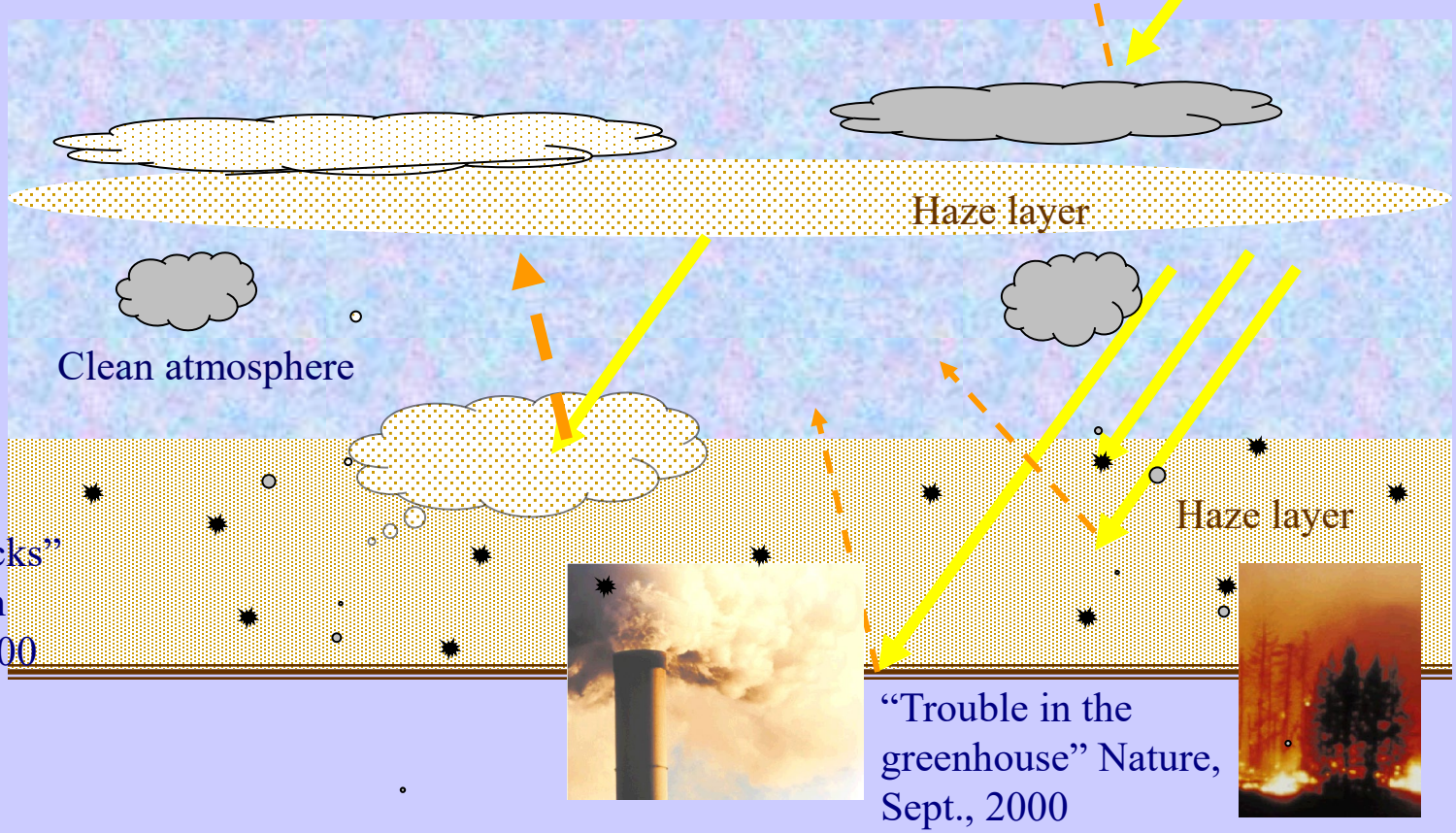

”Toxic trucks” Washington Post 11/19/00

“Trouble in the greenhouse” Nature, Sept., 2000

Does Population cause Pollution ?

POLDER aerosol index Feb. 1997 & population density

(Kaufman, Tanré & Boucher, Nature 2002)

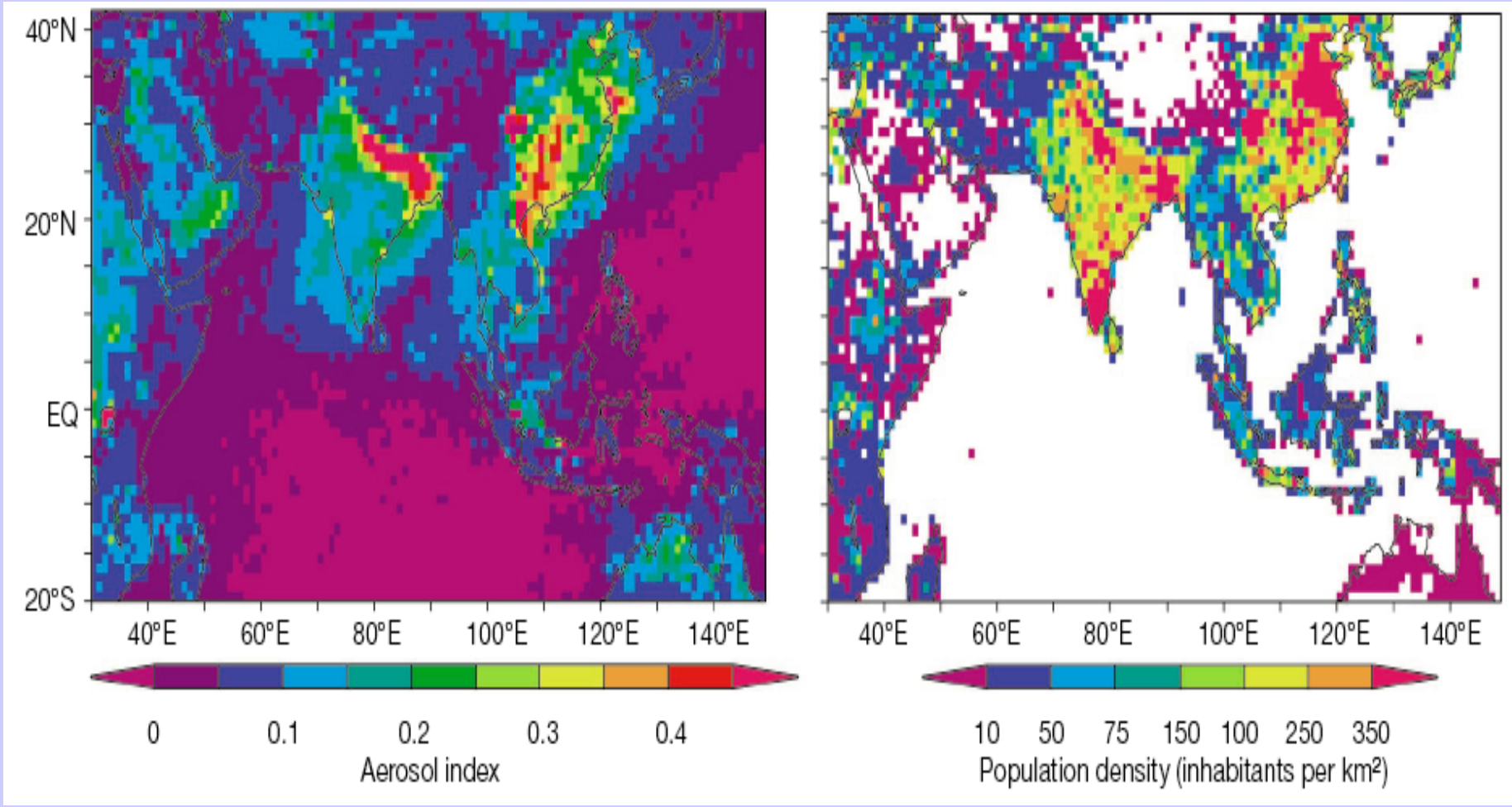

Aerosol Optical Thickness
(Coarse Particle Mode)

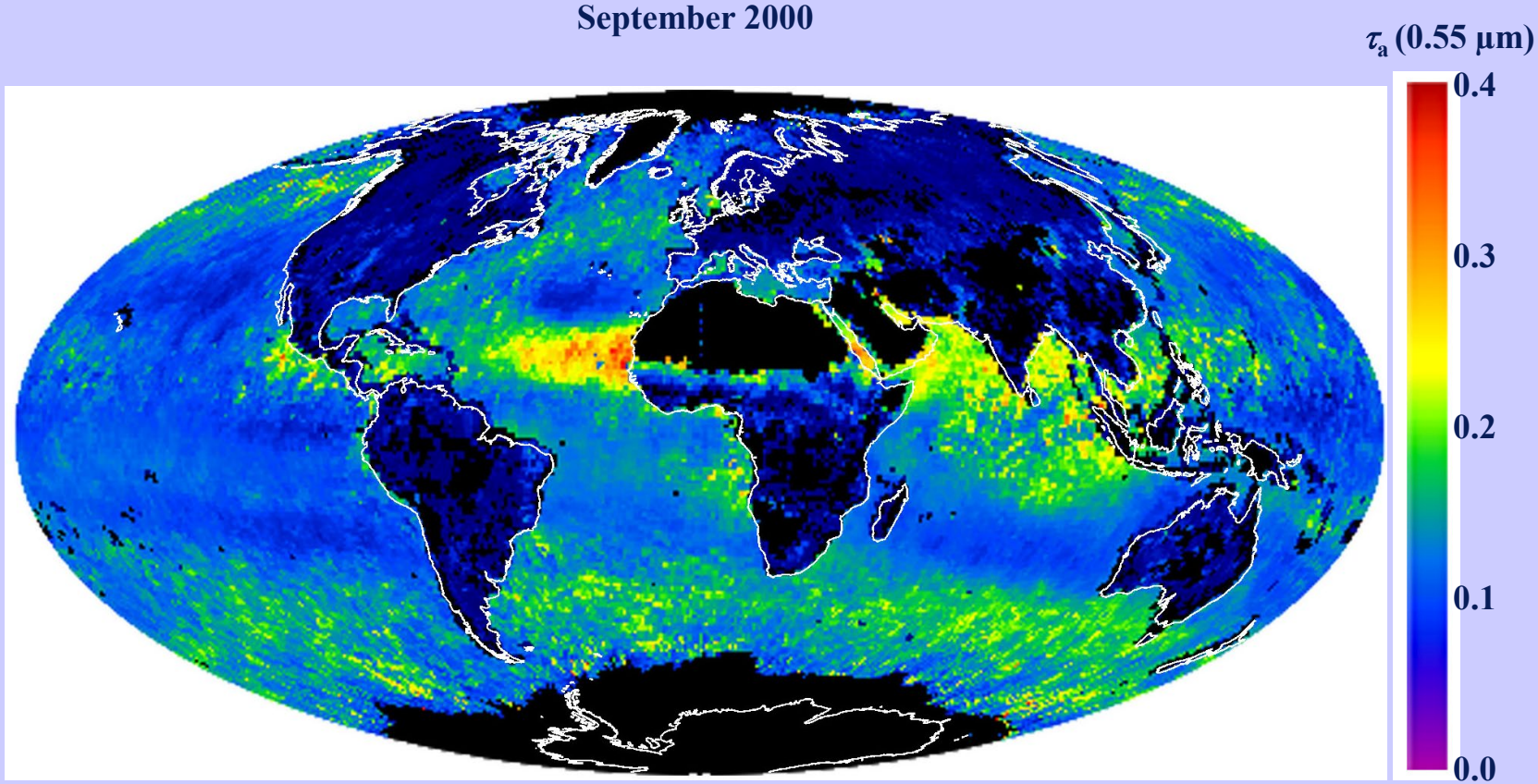

bands for aerosol retrieval over ocean (550, 660, 865, 1230, 1640, 2130 nm)

Global AOT for April 1997

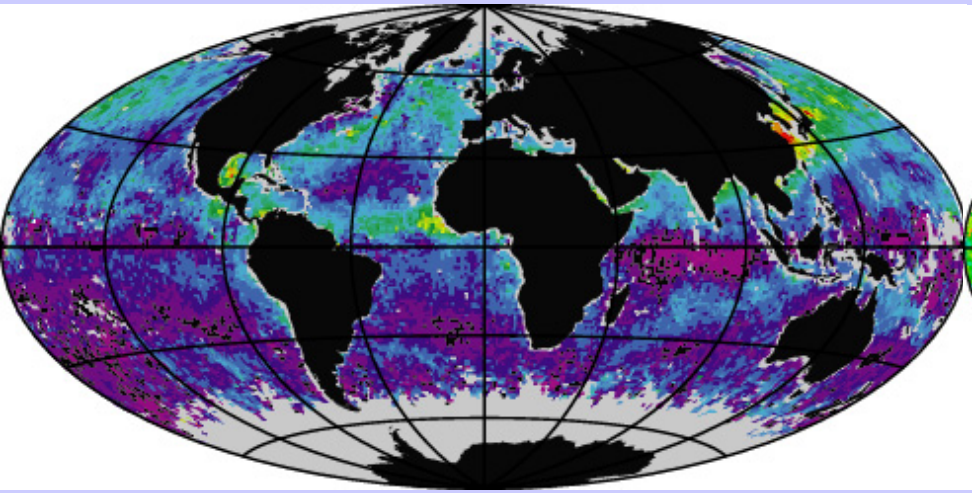

0 AVHRR @ 0.63um .5

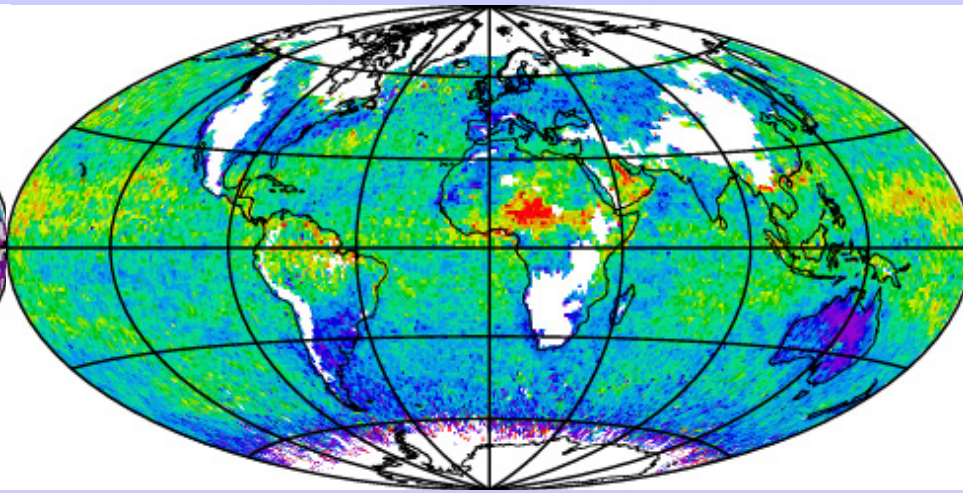

0 TOMS @ 0.38um 1.0

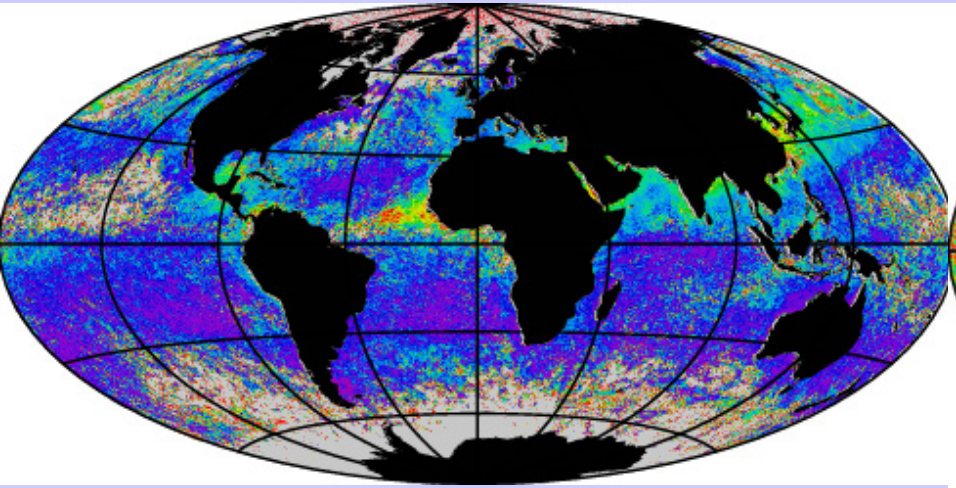

0 POLDER @ 0.865um .5

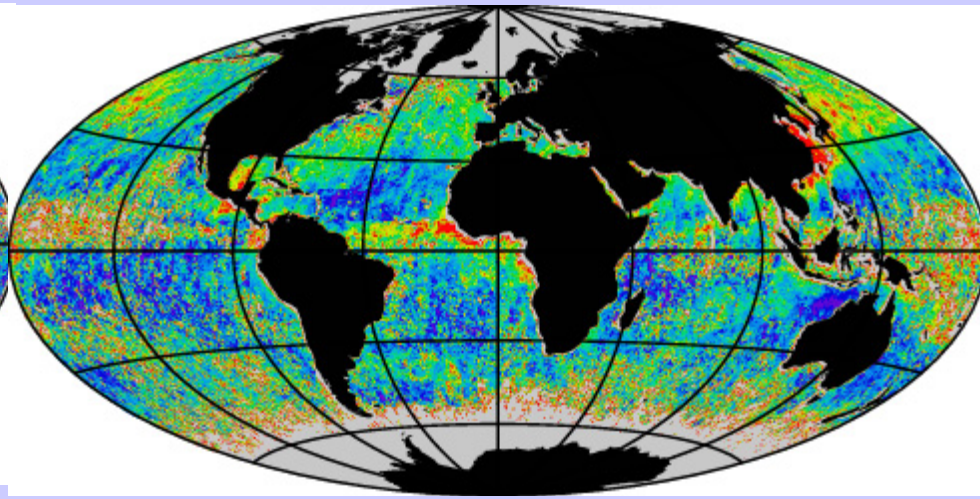

0 OCTS @ 0.50um 1.0

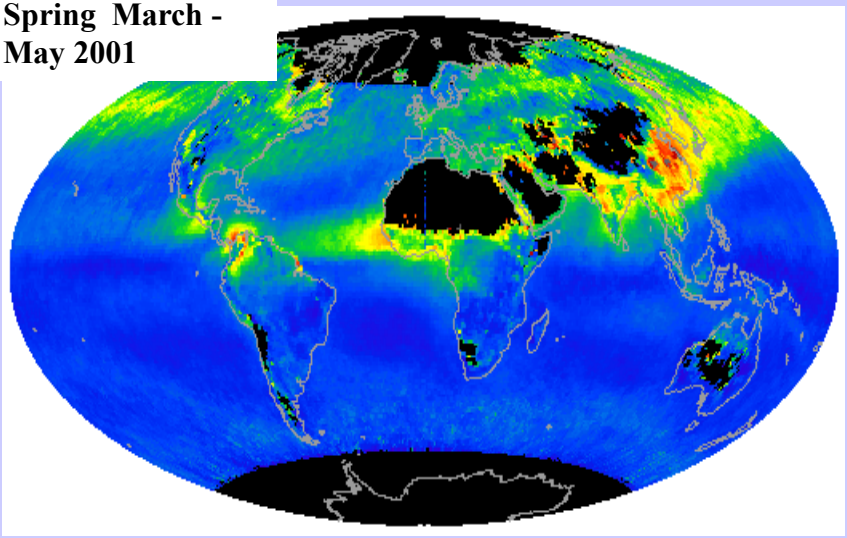

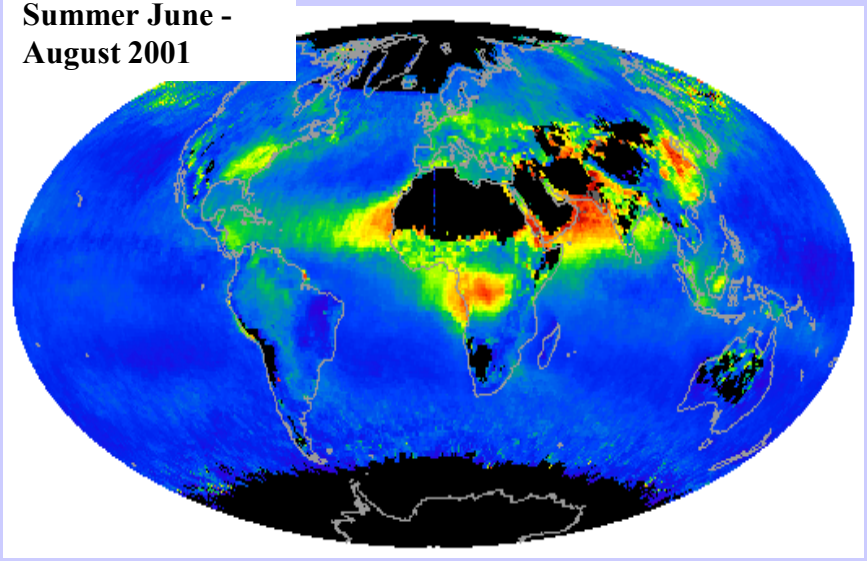

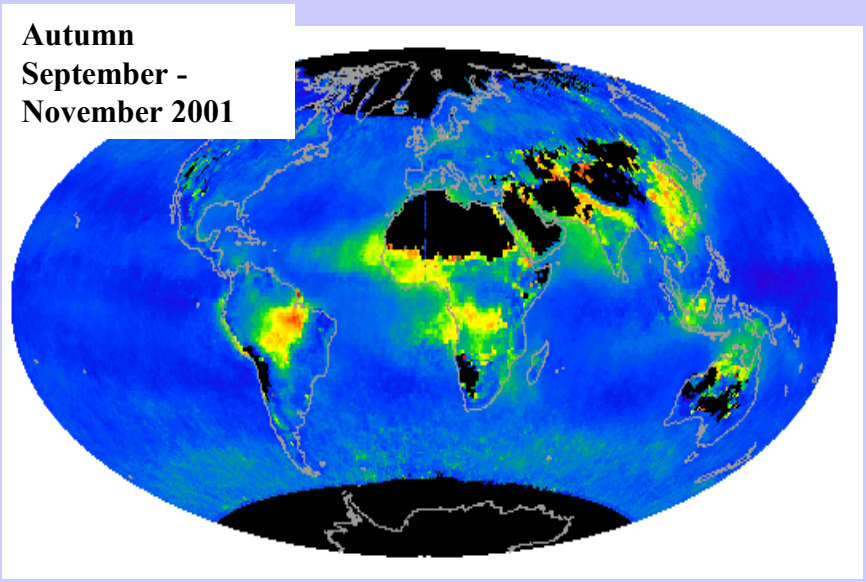

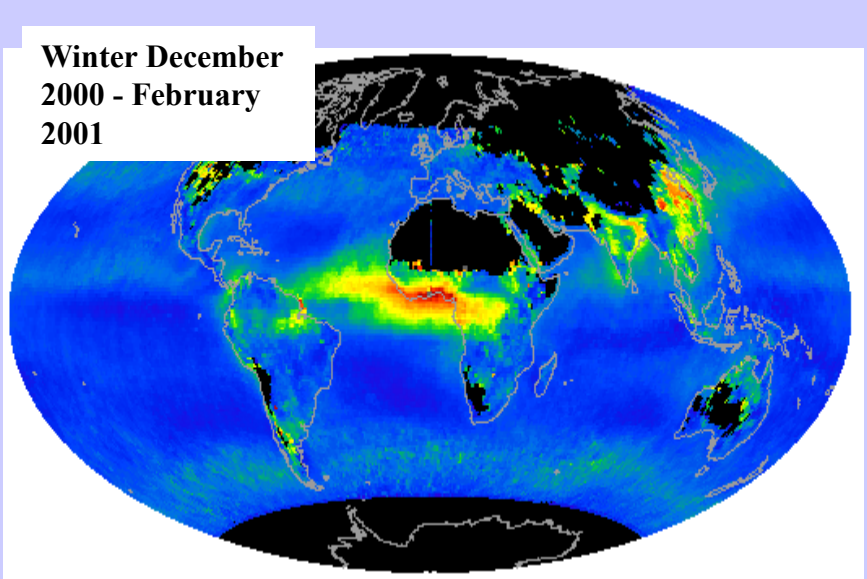

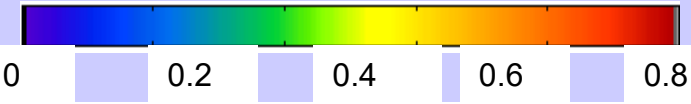

Average optical thickness

Example: pollution accumulating under the Alps

600 km

MODIS aerosol optical thickness

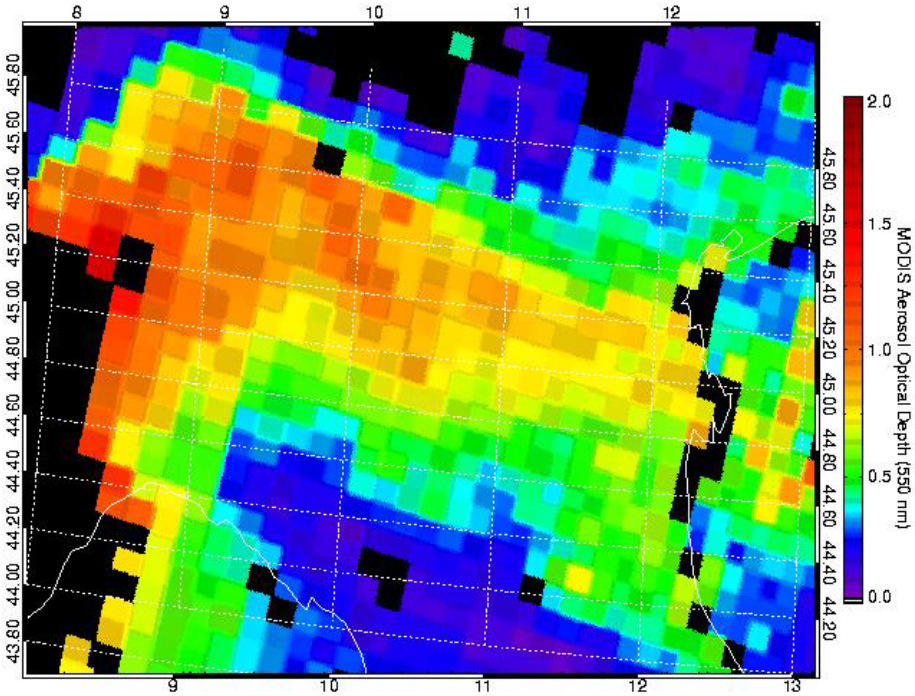

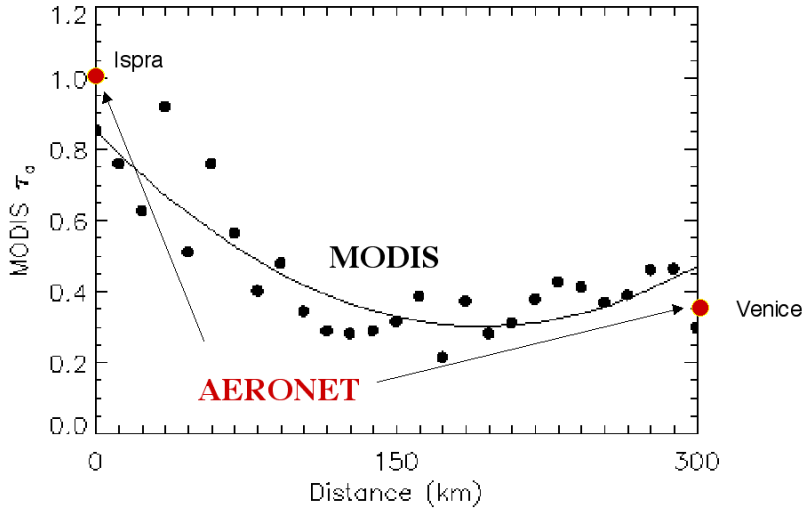

Allen Chu, SSAI/GSFC

Example: Los Angeles

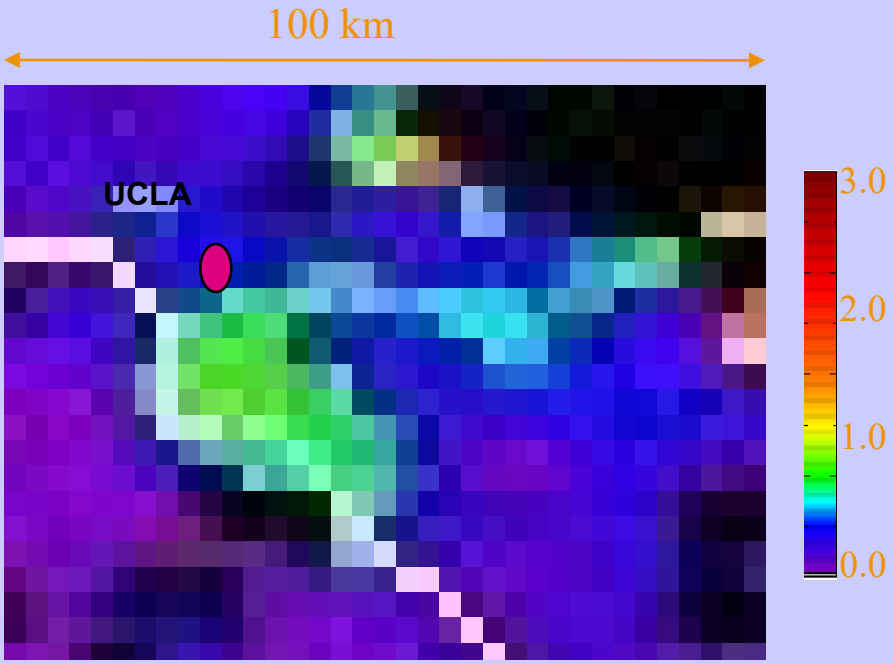

Measurements in the Solar Reflected Spectrum across the region covered by AVIRIS

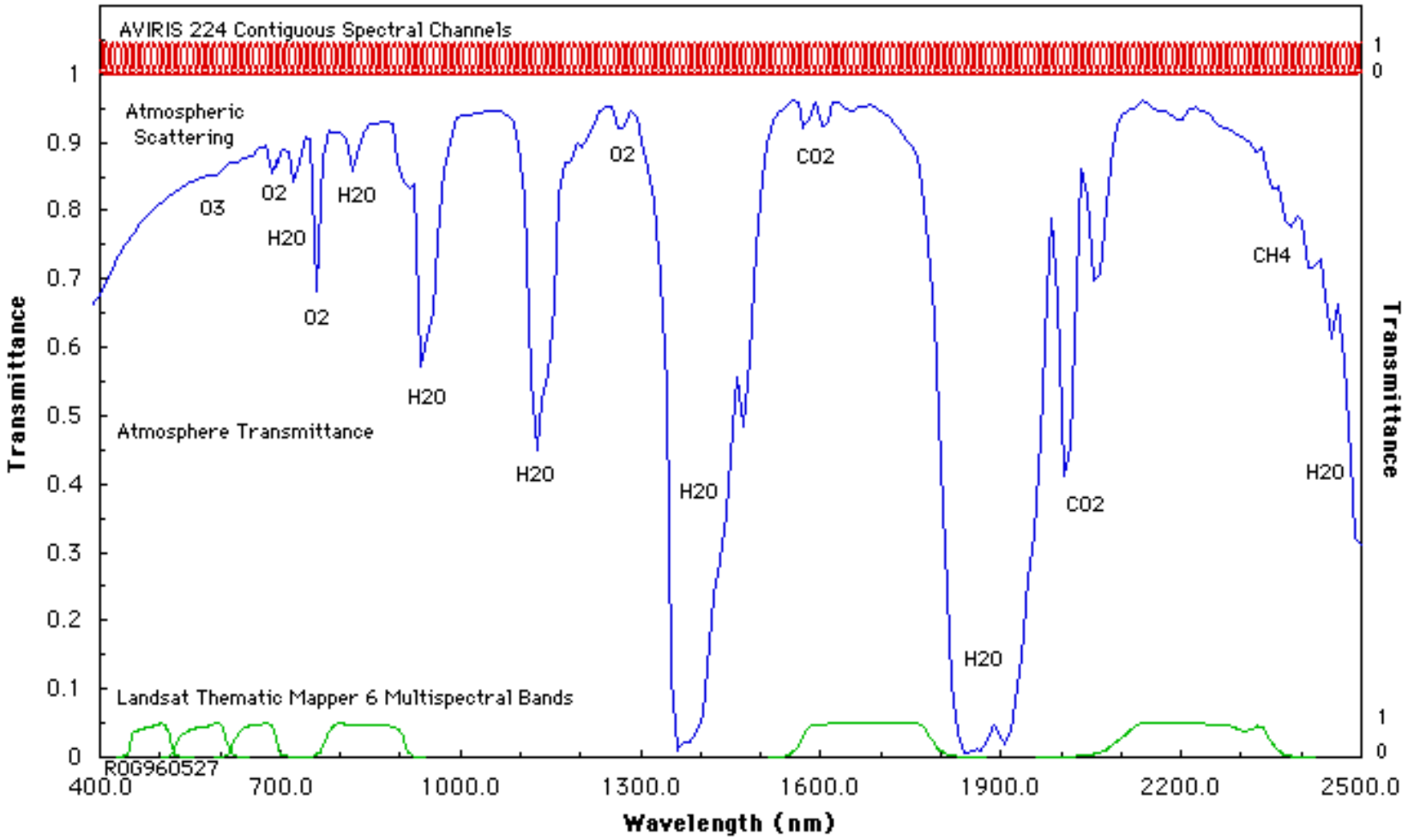

AVIRIS Movie #1

AVIRIS Image - Linden CA 20-Aug-1992
224 Spectral Bands: 0.4 - 2.5 μm
Pixel: 20m x 20m Scene: 10km x 10km

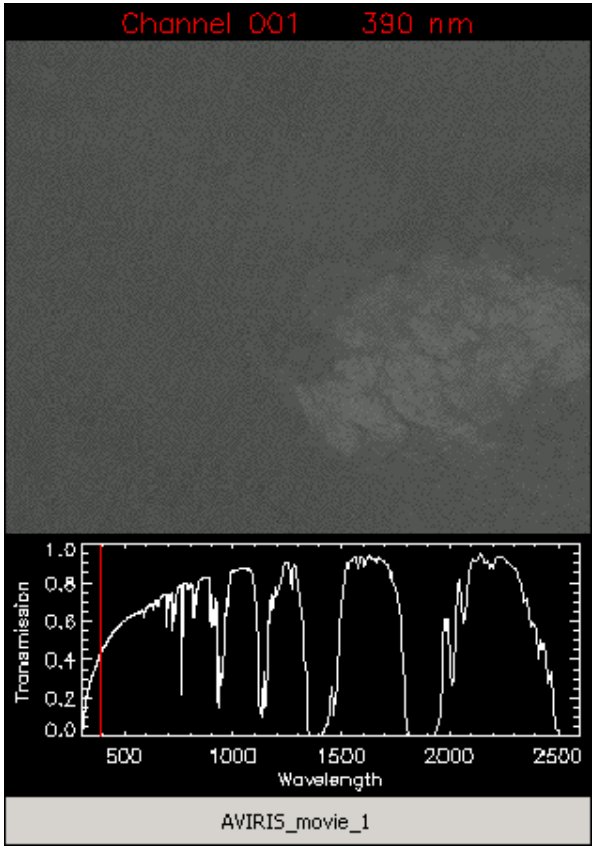

Cuiaba Brazil mosaic on 25 August 1995 shows a forest clearing fire. True color image, and single band images in black and white.

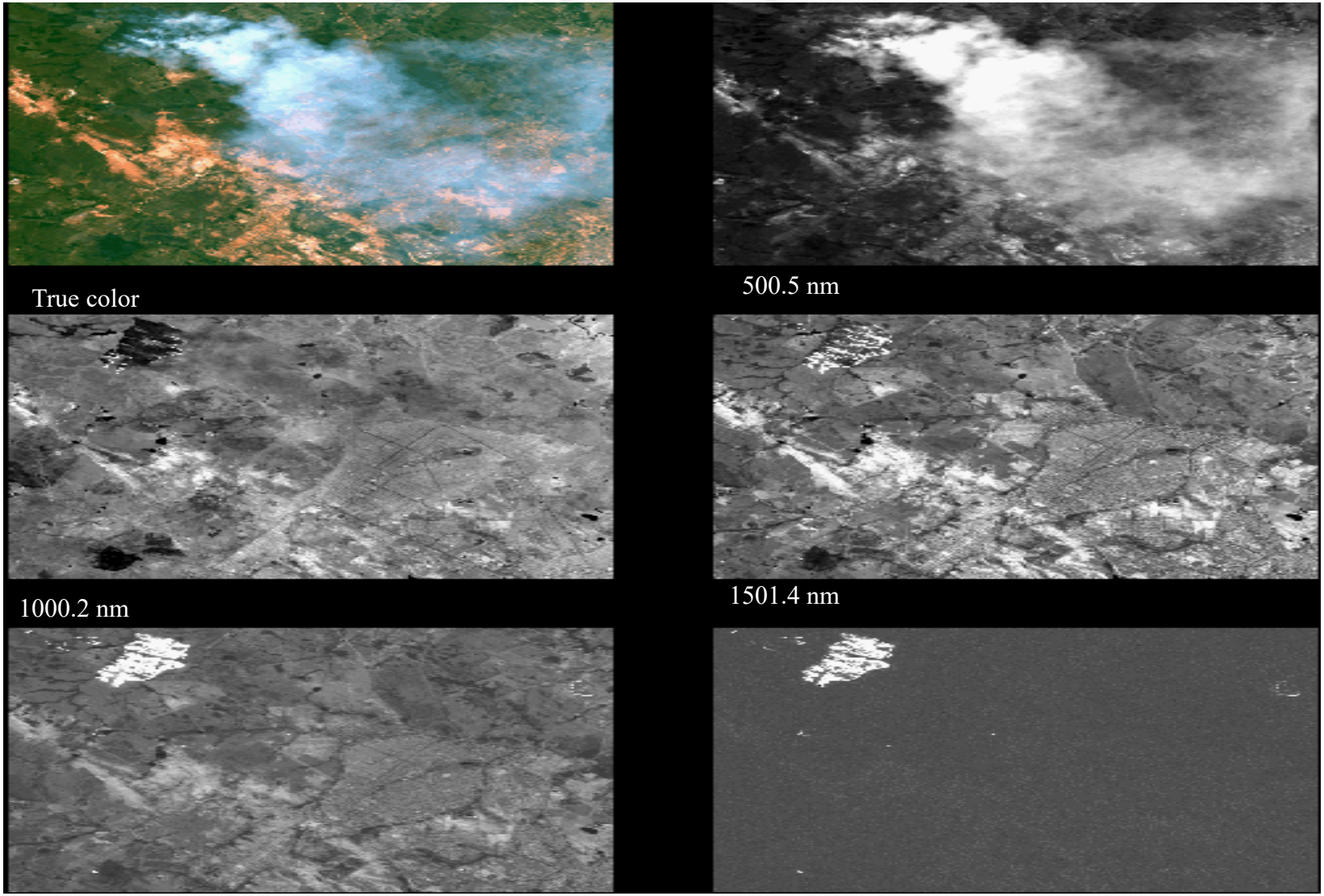

Active Fire Detection

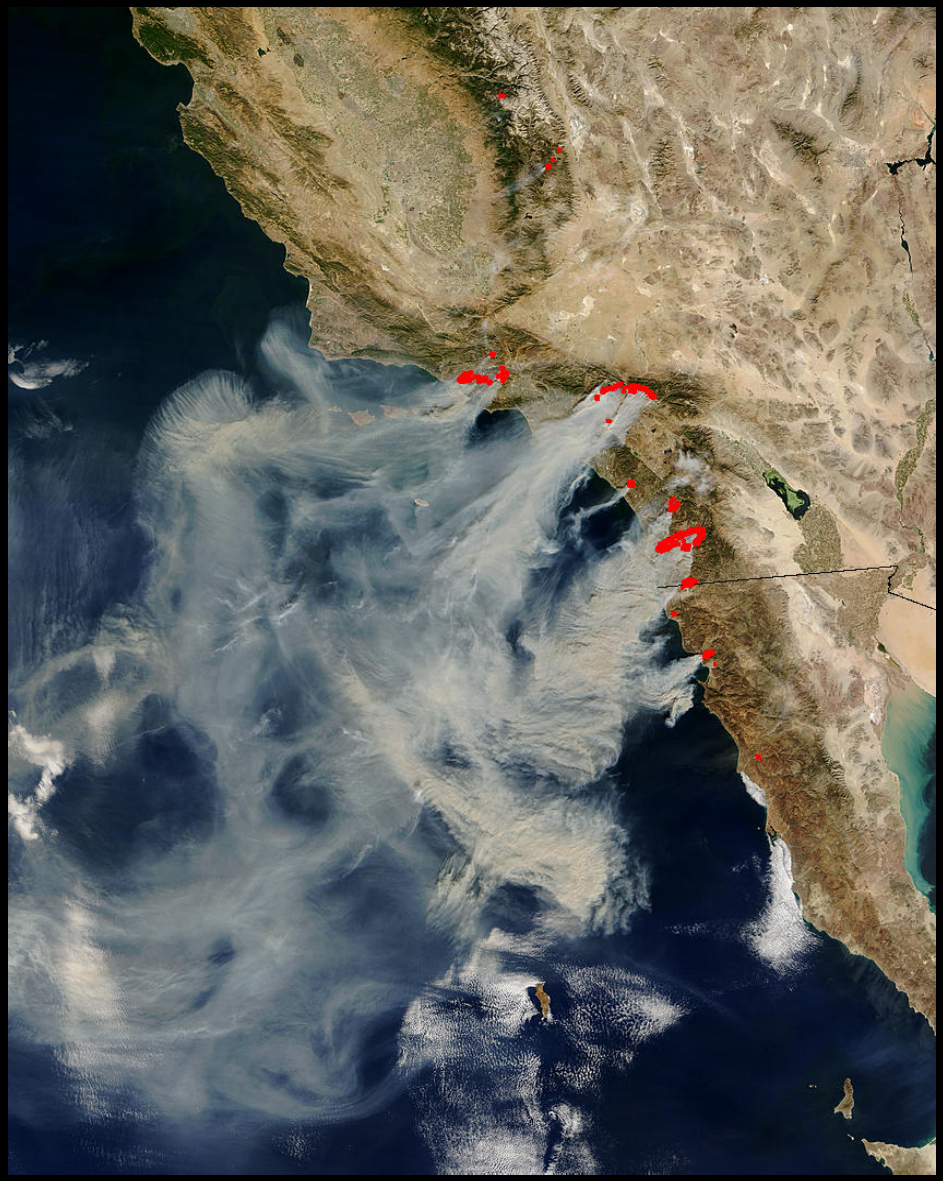

- Same code as the "offical" MOD14 thermal anomalies product
- Contextual algorithm (Giglio et al., 2003)
- The algorithm considers the spectral signature (in middle and thermal infrared) of each pixel and compares it to the non-burning surrounding pixels
- The natural variability of the surrounding background is taken into account
- Fewer false detections than traditional threshold-based algorithms
- Sensitive enough to detect small fires
- Current version: v4.3.2 (March 2003)

Biscuit and Tiller Fires in California and Oregon (08/14/02)

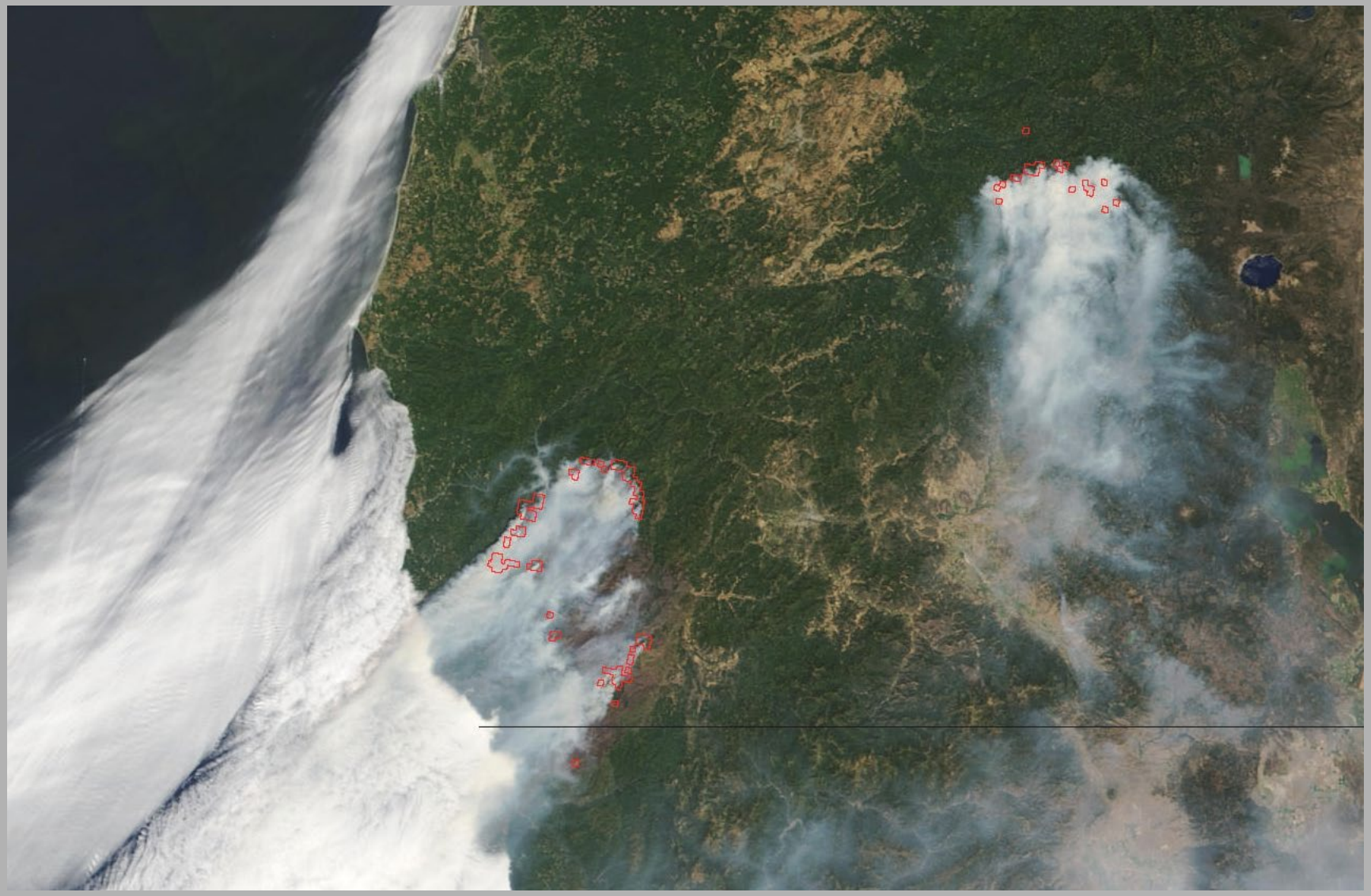

Fire Monitoring: http://rapidfire.sci.gsfc.nasa.gov/realtime

Cooperative Development of Advanced Products

Mapping Burn Severity With MODIS

The Devil Fire Susanville, California May 2001

These MODIS images were obtained shortly after containment of the 4,200 acre Devil Fire on June 3, 2001.

Two models were run on the subset area using Erdas Imagine:

- NDVI (Normalized Difference Vegetation Index)
- NDBR (Normalized Difference Burn Ratio), developed by the USGS.

Unsupervised classifications were then performed on these 2 images as well as on the false color NIR image.

Ground truthing would be required to determine the accuracy of each technique as well as the burned severity of the perimeter area.

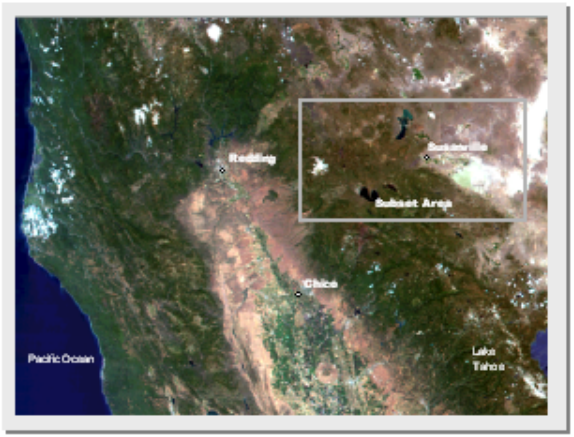

True Color MODIS Image of Northern California June 3, 2001

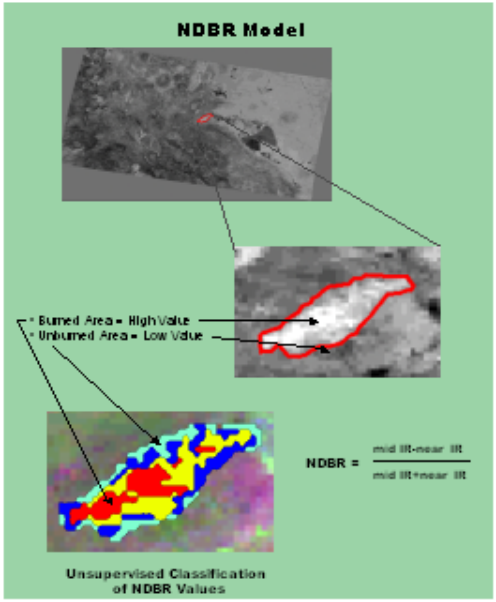

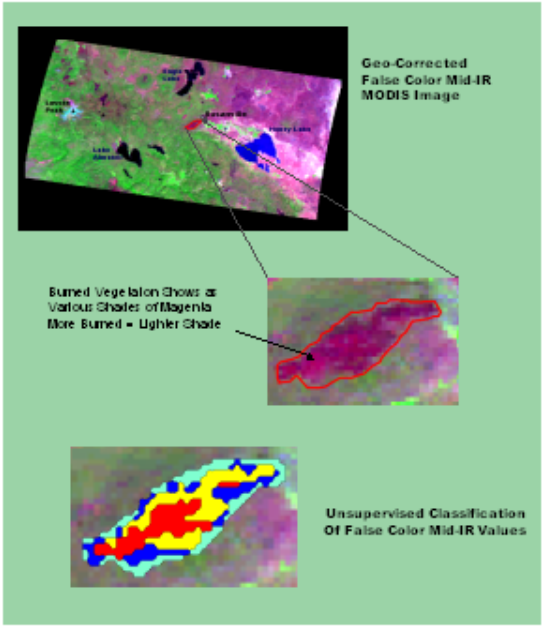

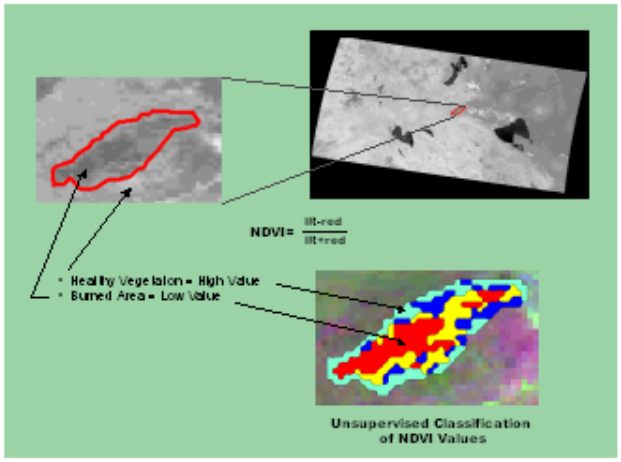

The fire extent and temperature within a field of view can be determined by considering the upwelling thermal radiance values obtained by both channels (Matson and Dozier, 1981; Dozier, 1981). For a given channel, λ, the radiative transfer equation indicates

$$R_\lambda(T) = \varepsilon_\lambda B_\lambda(Ts)\, \tau_\lambda(s) + \int_0^1 B_\lambda(T)\, d\tau_\lambda$$

When the GOES radiometer senses radiance from a pixel containing a target of blackbody temperature T_t occupying a portion p (between zero and one) of the pixel and a background of blackbody temperature T_b occupying the remainder of the pixel (1-p), the following equations represent the radiance sensed by the instrument at 4 and 11 micron.

$$R_4(T_4) = p\, R_4(T_t) + \varepsilon_4\, (1-p)\, R_4\, (T_b) + (1-\varepsilon_4)\, \tau_4(s)\, R_4(solar)$$

$$R_{11}(T_{11}) = p\, R_{11}(T_t) + \varepsilon_{11}\, (1-p)\, R_{11}(T_b)$$

The observed short wave window radiance also contains contributions due to solar reflection that must be distinguished from the ground emitted radiances; solar reflection is estimated from differences in background temperatures in the 4 and 11 micron channels. Once T_b is estimated from nearby pixels, these two nonlinear equations can be solved for T_t and p. In this study, the solution to the set of equations is found by applying a globally convergent bisection technique followed by Newton's method.

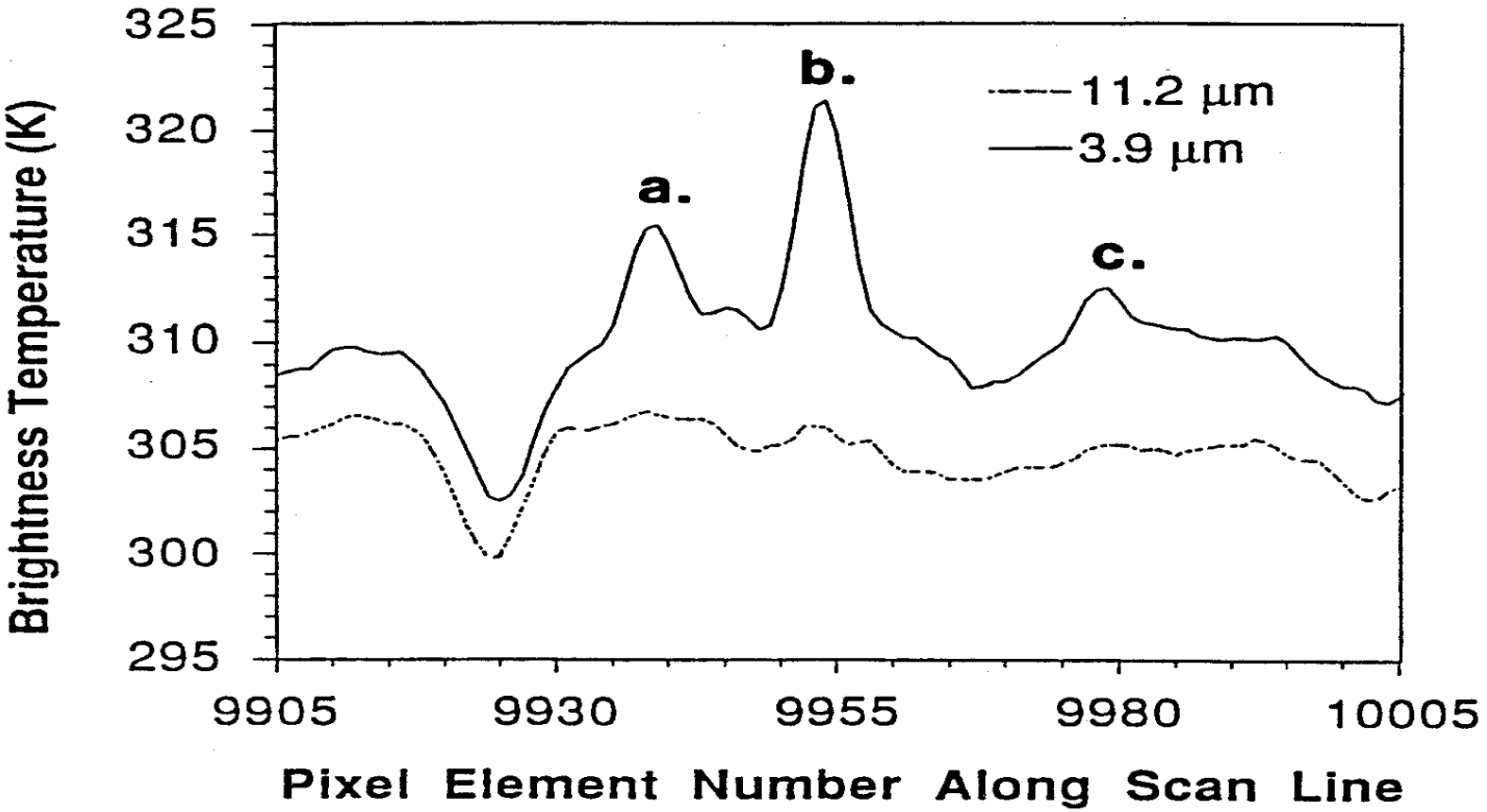

3.9 and 11.2 microns plotted for one scan line over grassland burning in South America; fires are likely at a, b, and c.

GOES-8 Wildfire ABBA Monitors Rapid Intensification of Rodeo/Chediski Fire

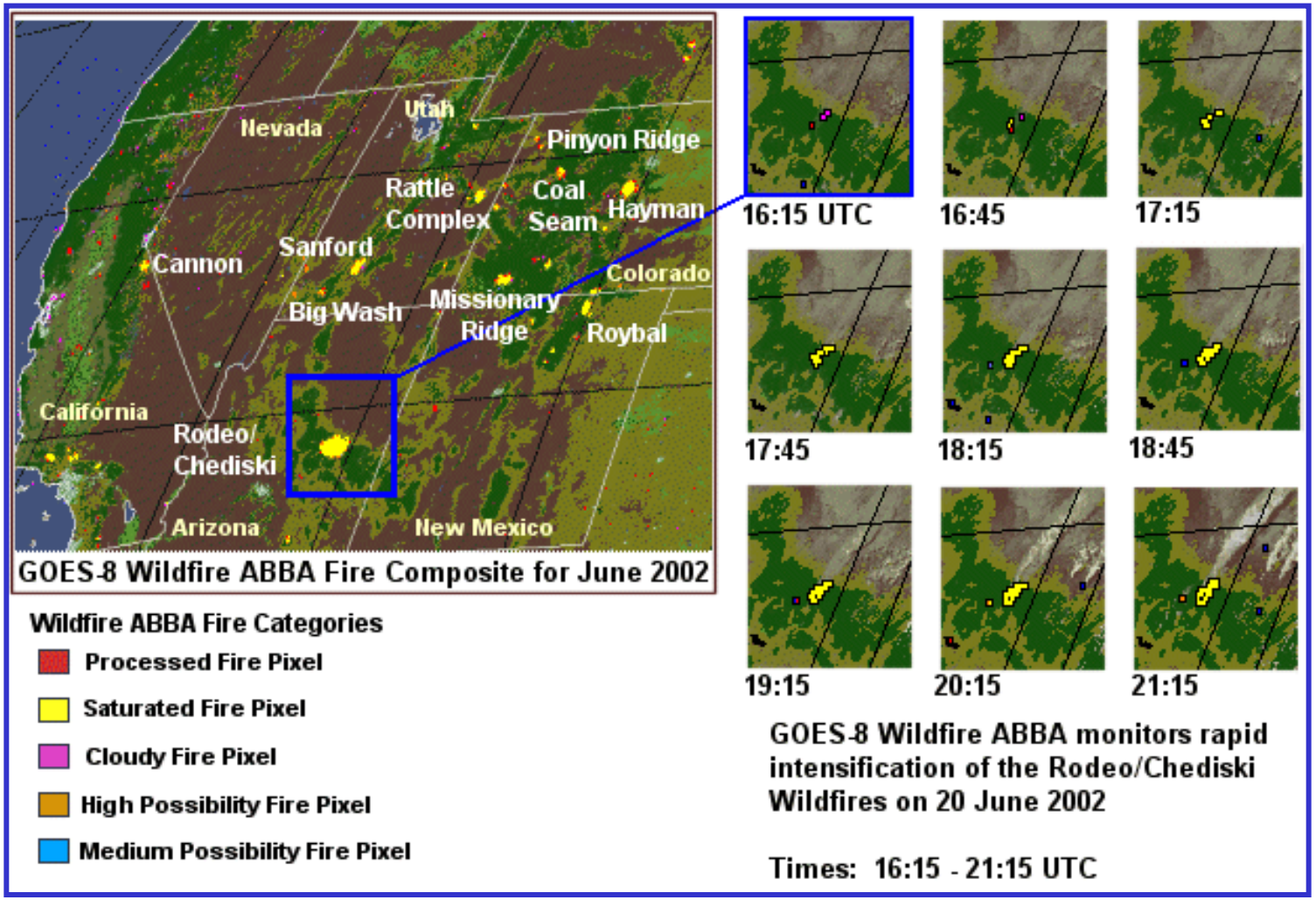

International Global Geostationary Active Fire Monitoring: Geographical Coverage

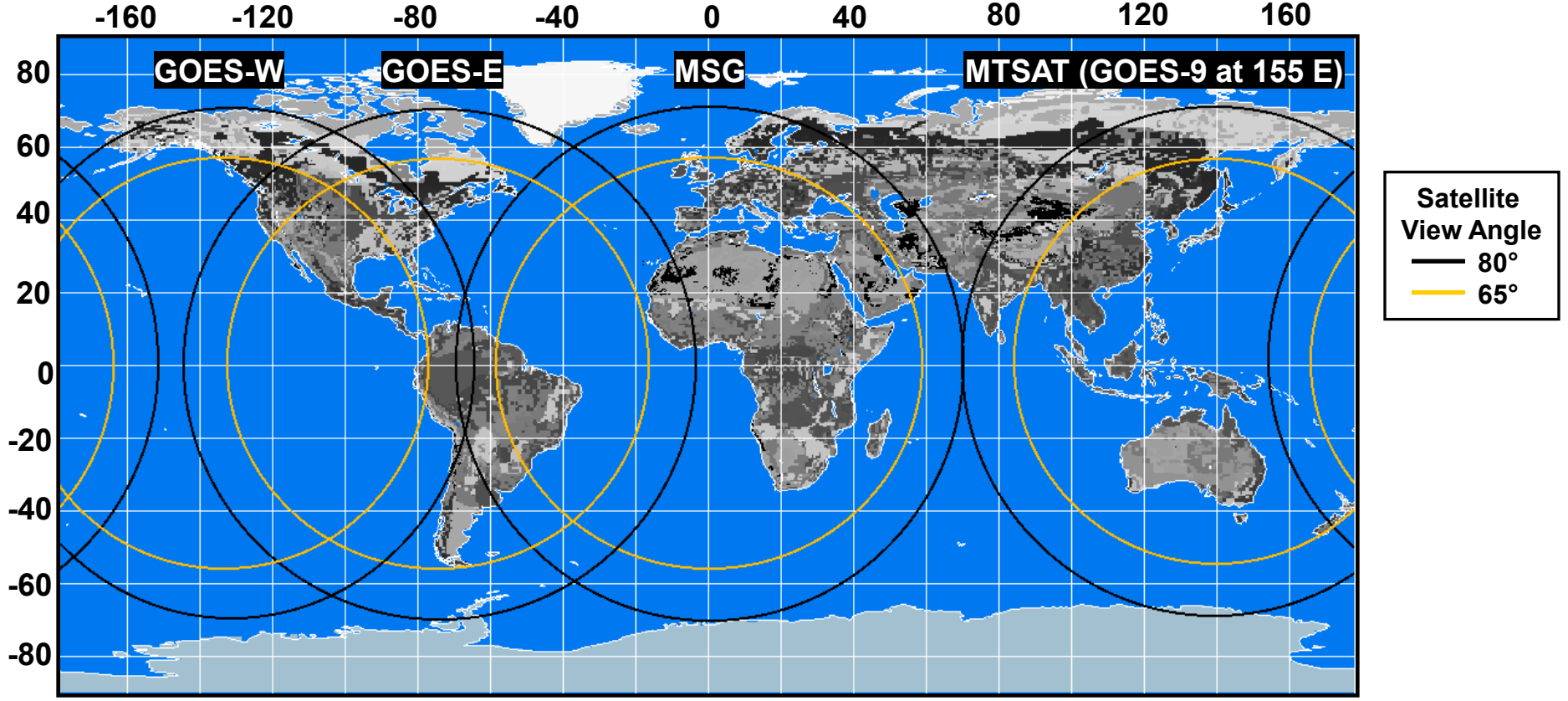

Satellite	Spectral Bands	Resolution IGFOV (km)	SSR (km)	Full Disk Coverage	4 μm Saturation Temperature (K)	Minimum Fire Size at Equator (at 750 K)
GOES-E	1 visible 4 IR	1.0 4.0 (8)	0.57 2.3	3 hours	335 K	0.15
GOES-W	1 visible 4 IR	1.0 4.0 (8)	0.57 2.3	3 hours	322	0.15
MSG SEVIRI (2002)	3 visible 1 near-IR 8 IR	1.6 (4.8) 4.8 4.8	1.0 (3.0) 3.0 3.0	15 minutes	> 335	0.22
MTSAT-1R JAMI (2003)	1 visible 4 IR	0.5 2.0		18 minutes	~320	0.03

Ash Plume Detection

Mt. Cleveland Eruption 19 Feb 2001

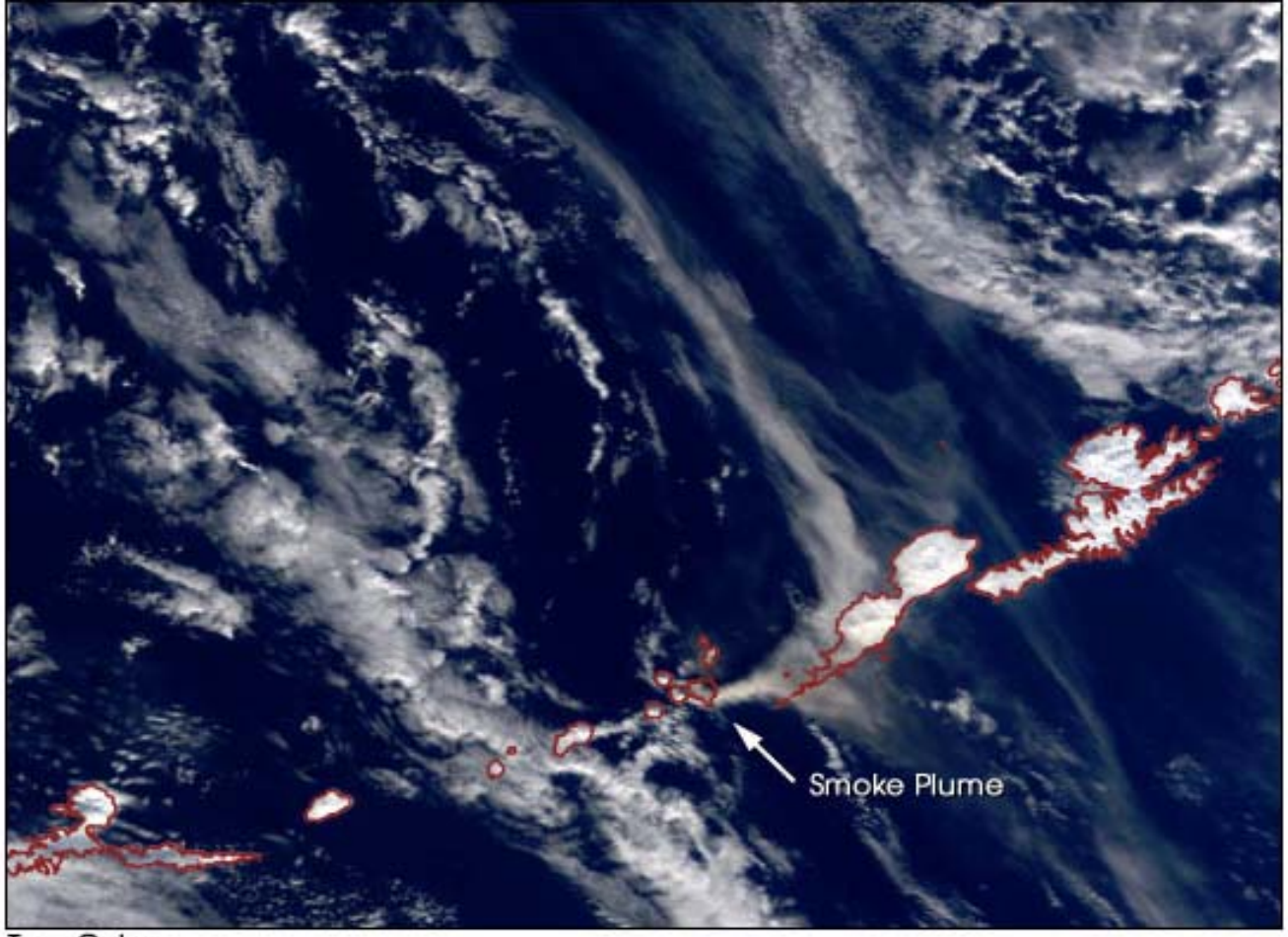

True Color

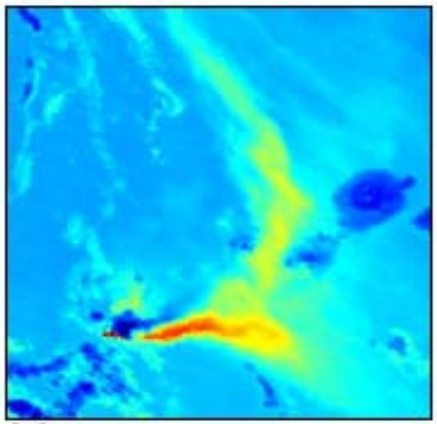

3.9μm

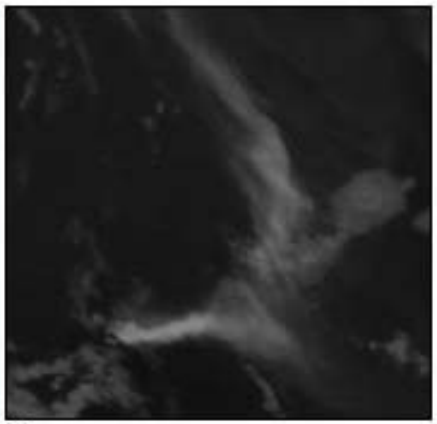

11μm

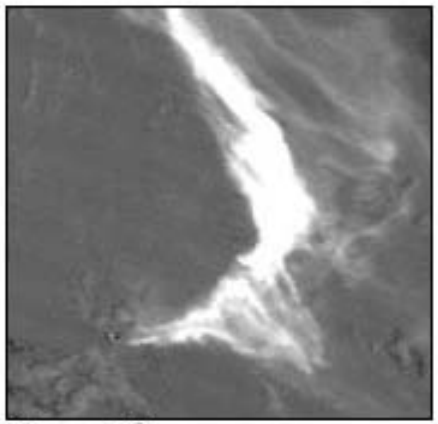

11μm - 12μm

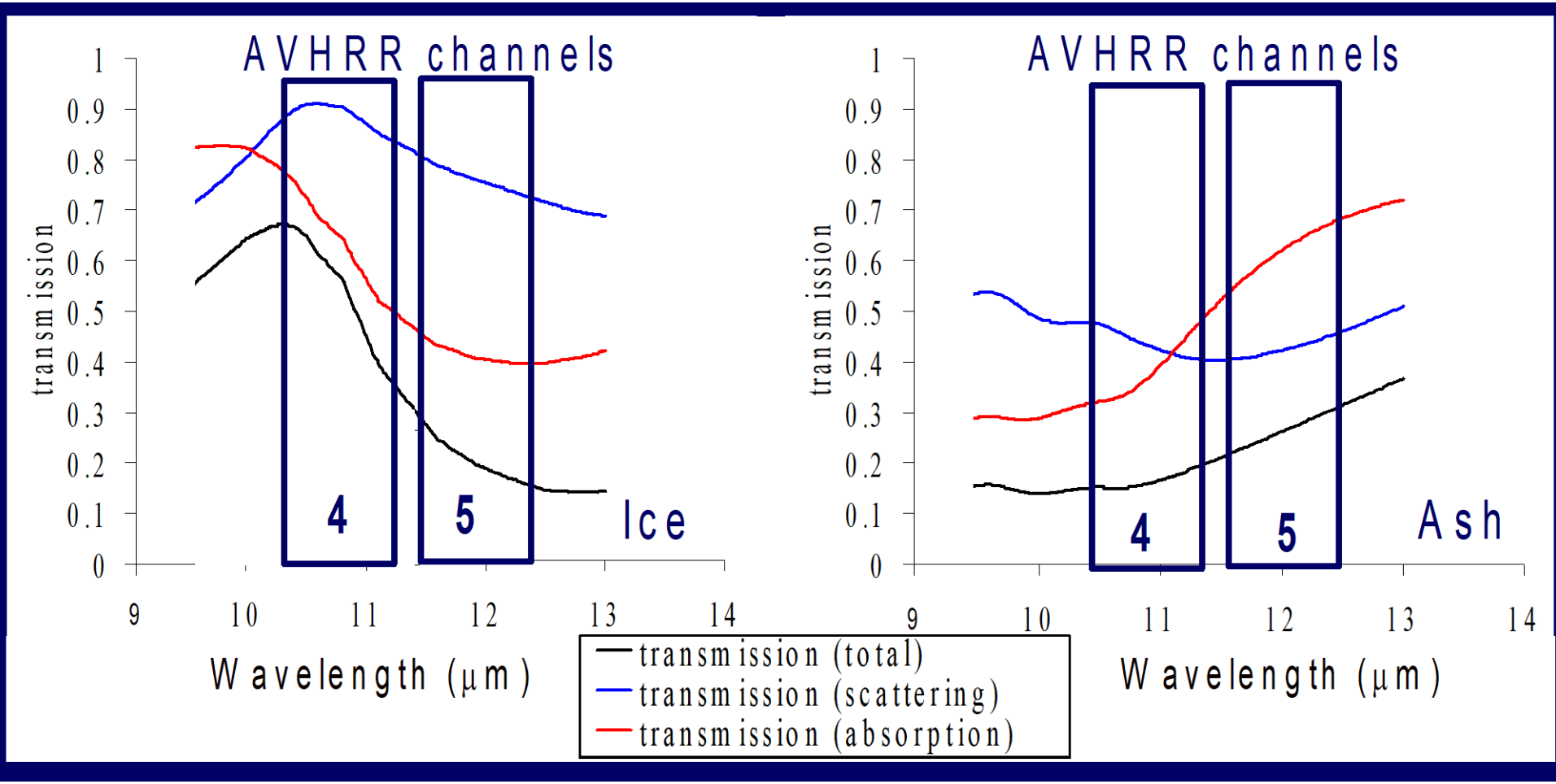

BT11-BT12 > 0 for ice
BT11-BT12 < 0 for volcanic ash

Frank Honey 1980s

MODIS detects ship tracks

Ship Tracks occur in marine stratocumulus regions of the globe

- California, Azores, Namibia, and Peru

Conditions for formation

- High humidity
- Small air-sea temperature difference
- Low wind speed
- Boundary layer between 300 and 750 m deep

Enhanced reflectance of clouds at 3.7 μm

- Larger number of small droplets arising from particulate emission from ships

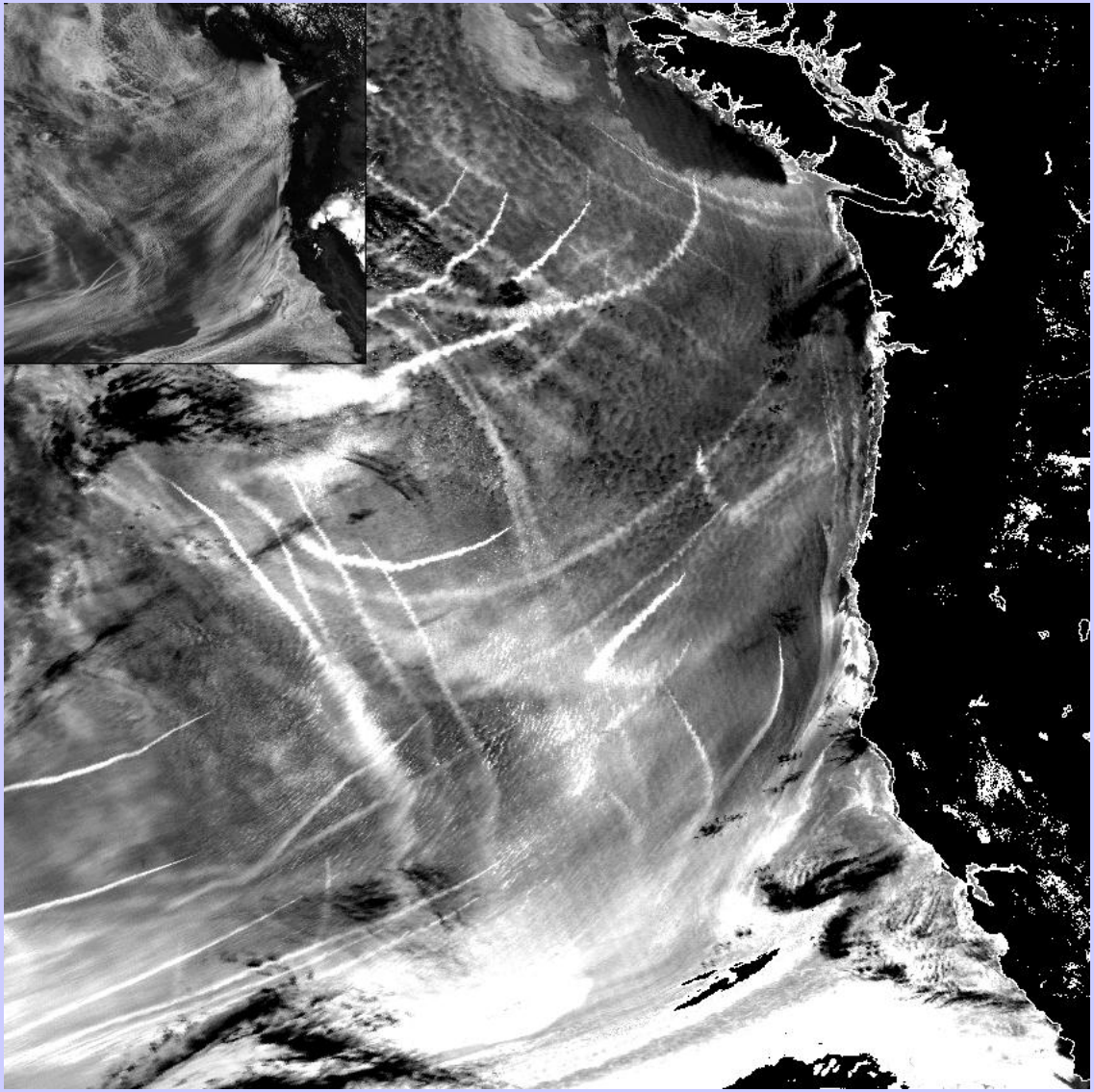

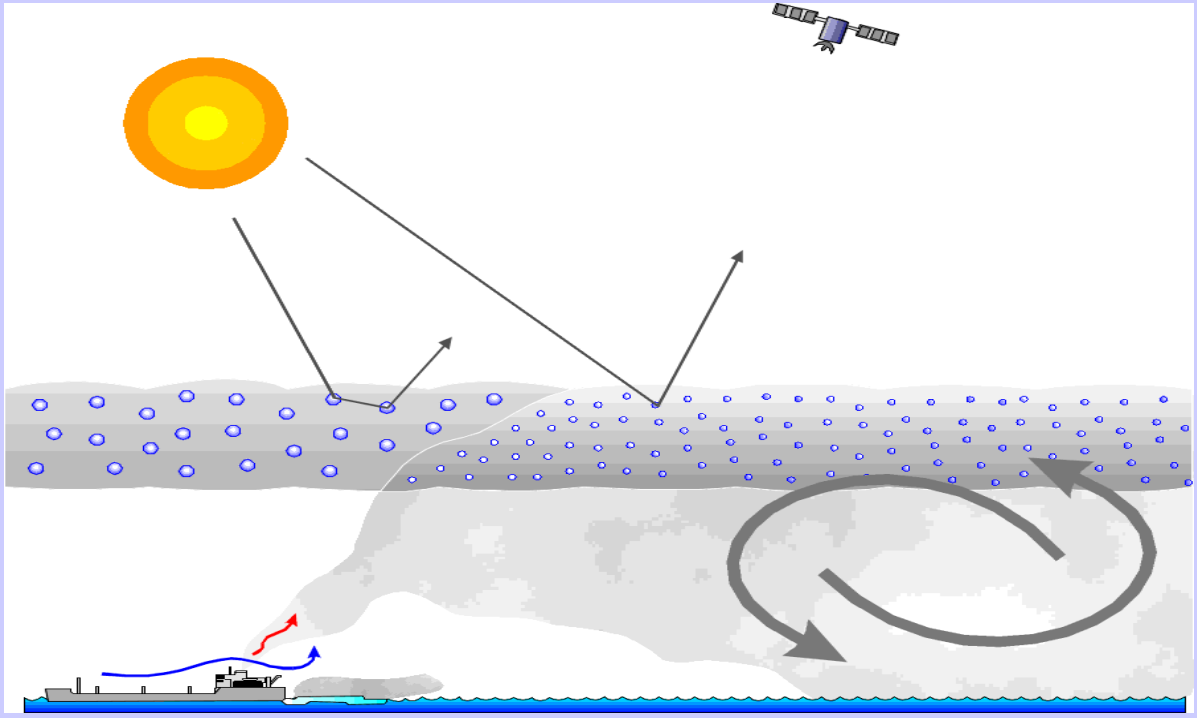

* Particles emitted by ships increase concentration of cloud condensation nuclei (CCN) in the air
* Increased CCN increase concentration of cloud droplets and reduce average size of the droplets
* Increased concentration and smaller particles reduce production of drizzle (100 μm radius) droplets in clouds
* Liquid water content increases because loss of drizzle particles is suppressed
* Clouds are *optically thicker* and brighter along ship track

Ship tracks off France (01/27/03)

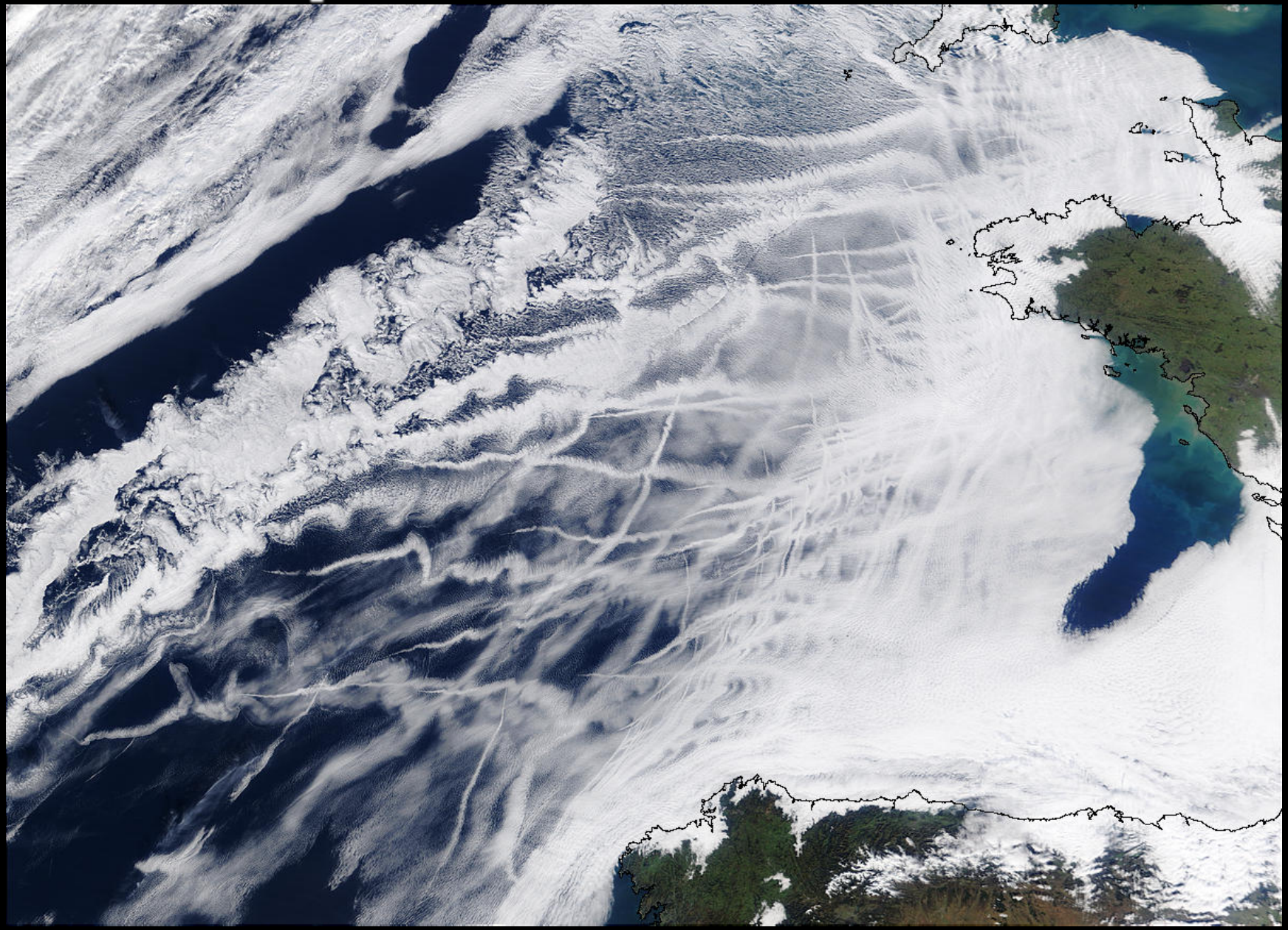

CIRRUS FORMATION BY CONTRAILS OVER CENTRAL U.S. IN GOES-8 IR IMAGERY October 26, 1996

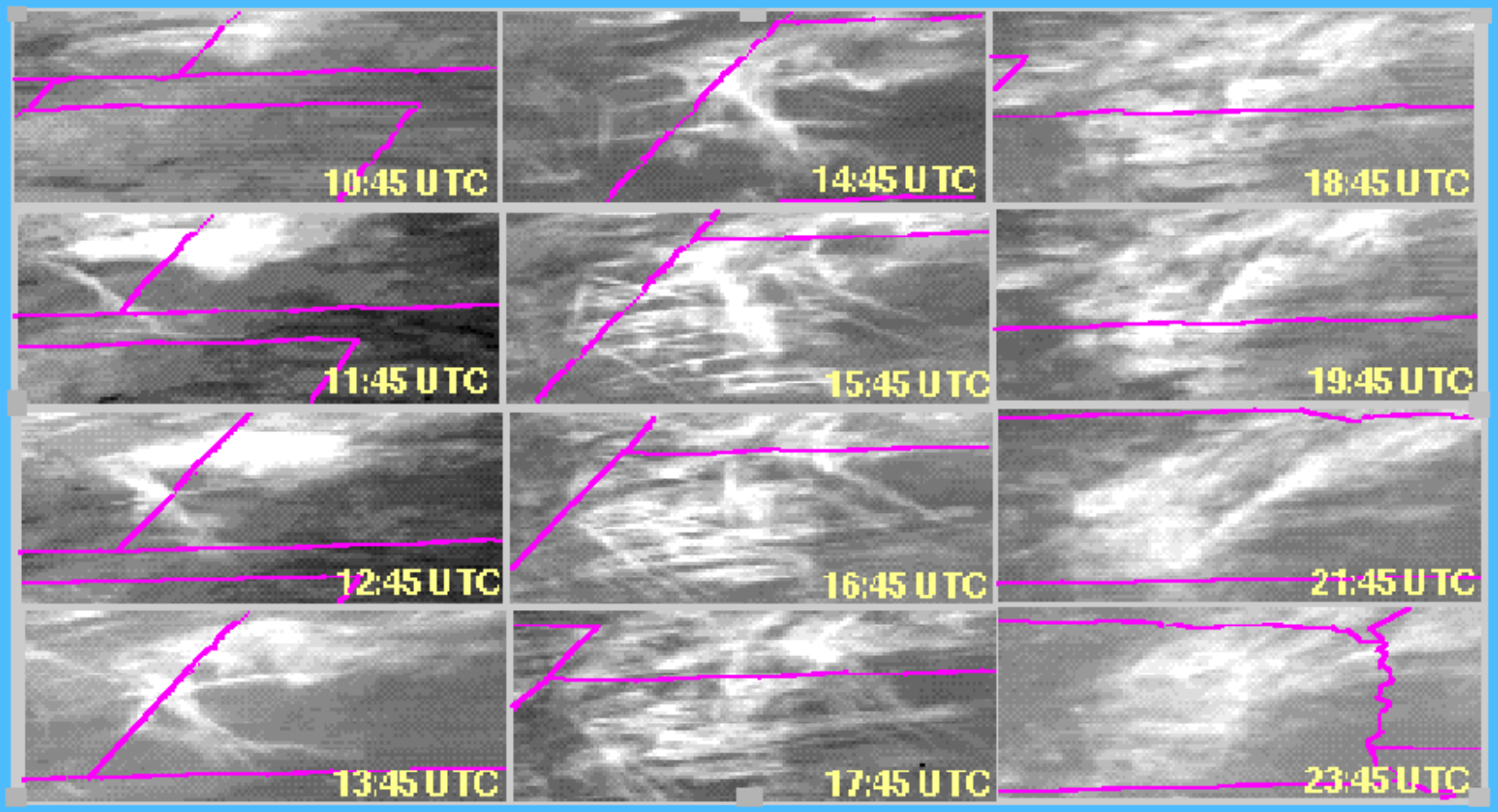

Minnis et al., *Science*, 1999

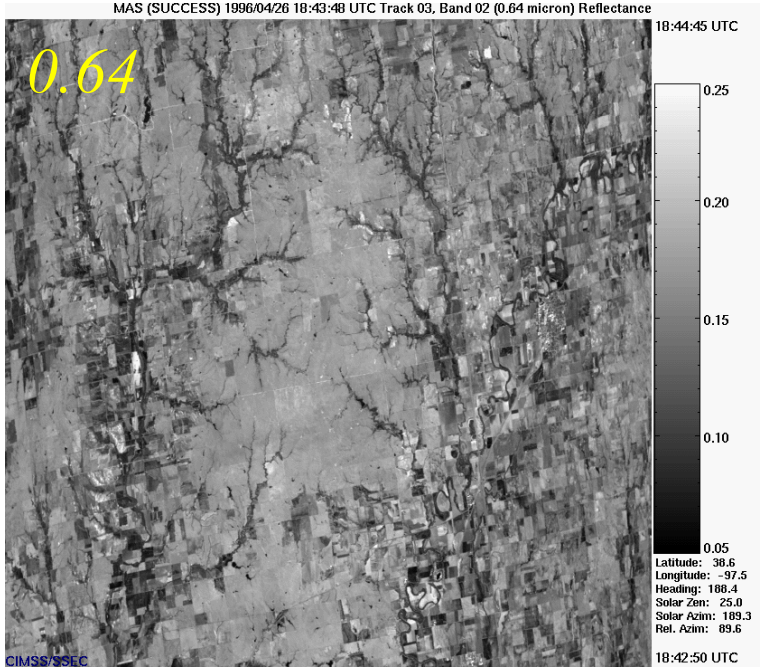
MAS (SUCCESS) 1996/04/26 18:43:48 UTC Track 03, Band 02 (0.64 micron) Reflectance
0.64
18:44:45 UTC
0.25
0.20
0.15
0.10
0.05
Latitude: 38.6
Longitude: -97.5
Heading: 188.4
Solar Zen: 25.0
Solar Azim: 189.3
Rel. Azim: 89.6
CIMSS/SSEC
18:42:50 UTC

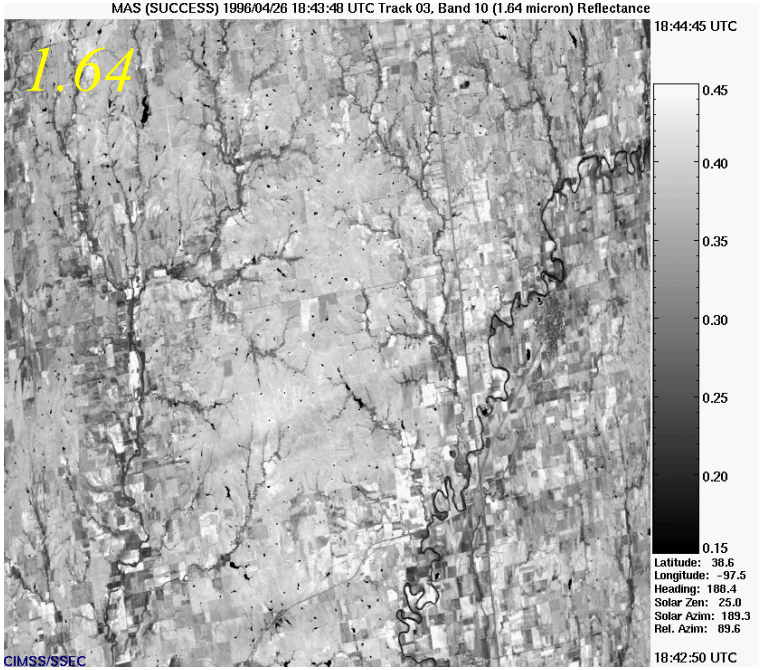
MAS (SUCCESS) 1996/04/26 18:43:48 UTC Track 03, Band 10 (1.64 micron) Reflectance
1.64
18:44:45 UTC
0.45
0.40
0.35
0.30
0.25
0.20
0.15
Latitude: 38.6
Longitude: -97.5
Heading: 188.4
Solar Zen: 25.0
Solar Azim: 189.3
Rel. Azim: 89.6
CIMSS/SSEC
18:42:50 UTC

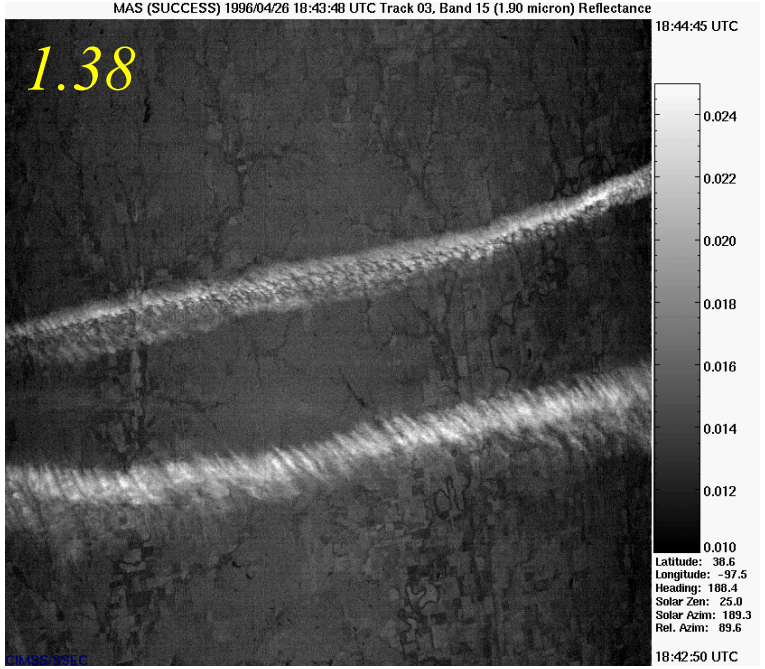
MAS (SUCCESS) 1996/04/26 18:43:48 UTC Track 03, Band 15 (1.90 micron) Reflectance
1.38
18:44:45 UTC
0.024
0.022
0.020
0.018
0.016
0.014
0.012
0.010
Latitude: 38.6
Longitude: -97.5
Heading: 188.4
Solar Zen: 25.0
Solar Azim: 189.3
Rel. Azim: 89.6
CIMSS/SSEC
18:42:50 UTC

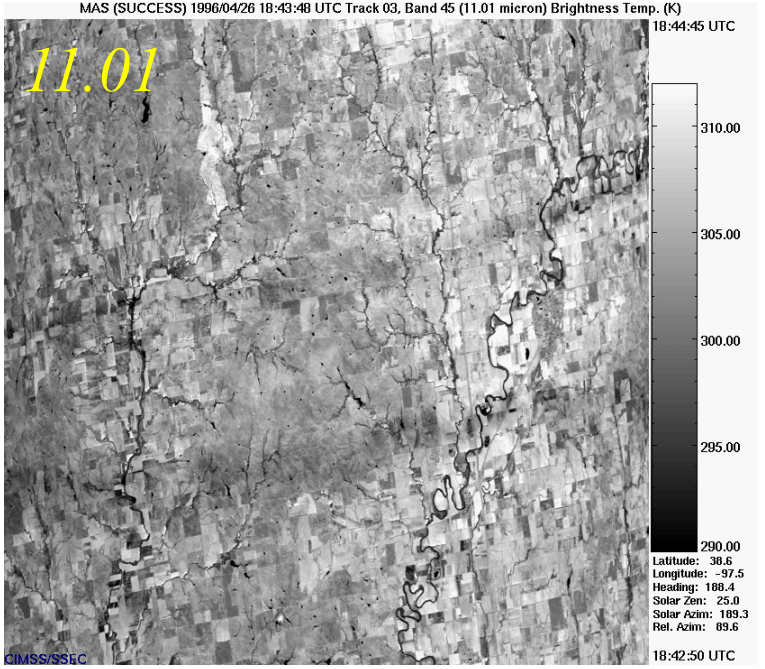
MAS (SUCCESS) 1996/04/26 18:43:48 UTC Track 03, Band 45 (11.01 micron) Brightness Temp. (K)
11.01
18:44:45 UTC
310.00
305.00
300.00
295.00
290.00
Latitude: 38.6
Longitude: -97.5
Heading: 188.4
Solar Zen: 25.0
Solar Azim: 189.3
Rel. Azim: 89.6
CIMSS/SSEC
18:42:50 UTC

Is cirrus related to air traffic?

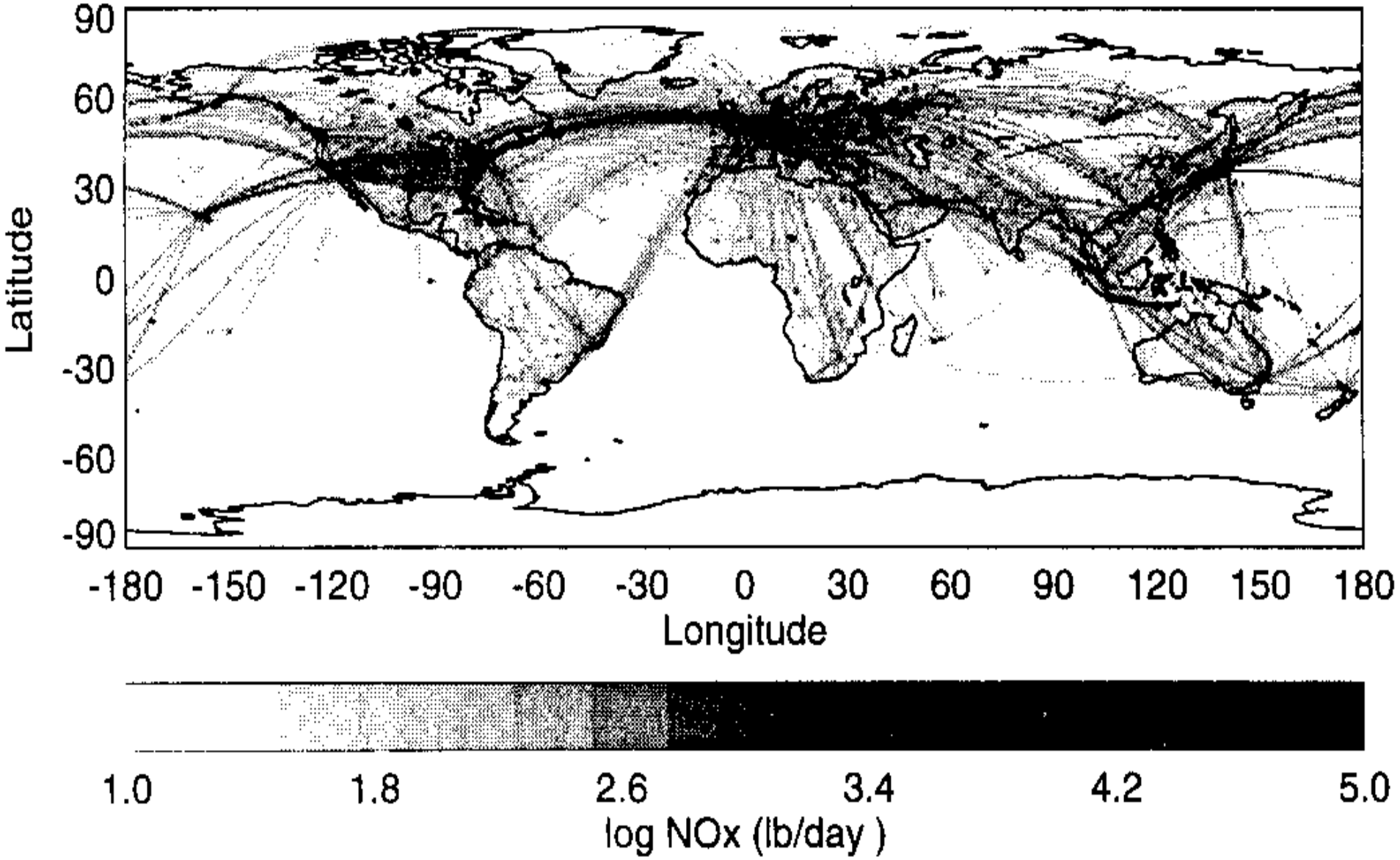

MOPITT CO Column 1-3 June 2002 (Phase 2 Data)

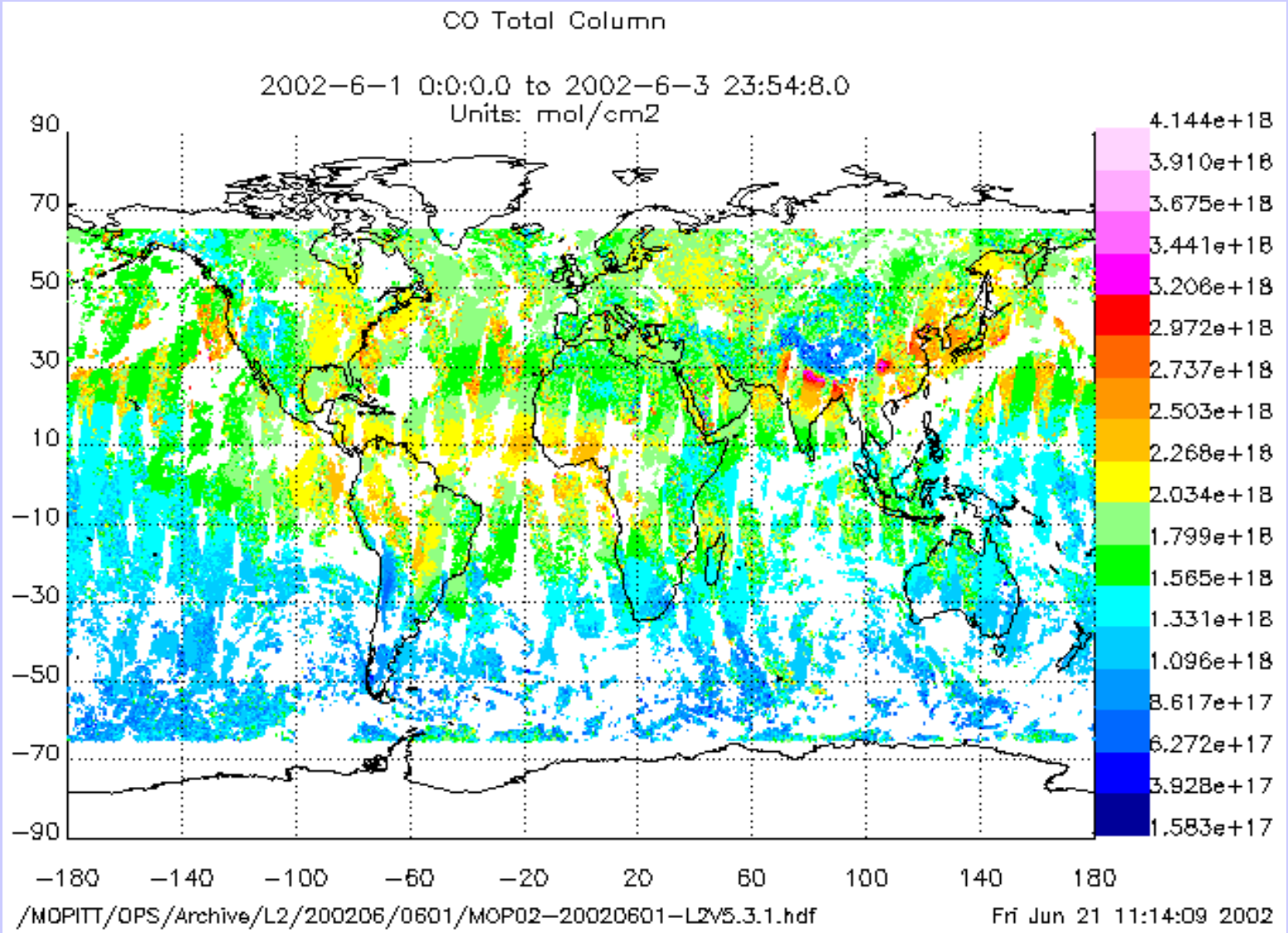

8.6 - 10.5 um observations of sea ice through low cloud cover

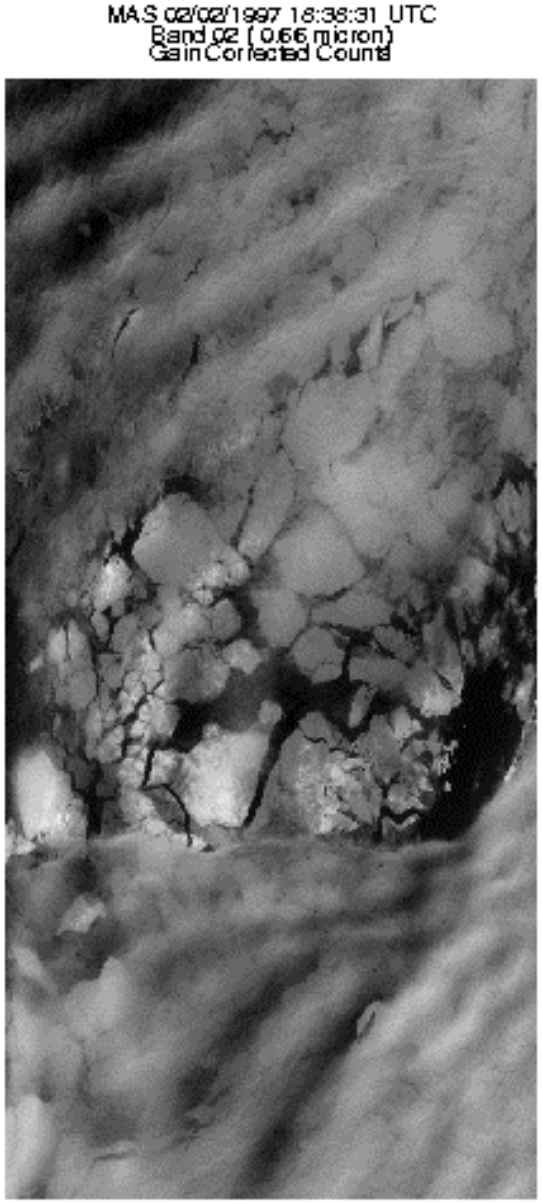

.66 um

10.5 – 11 um

8.6 - 10.5 um

Cloud particle size is revealed in high resolution infrared spectra

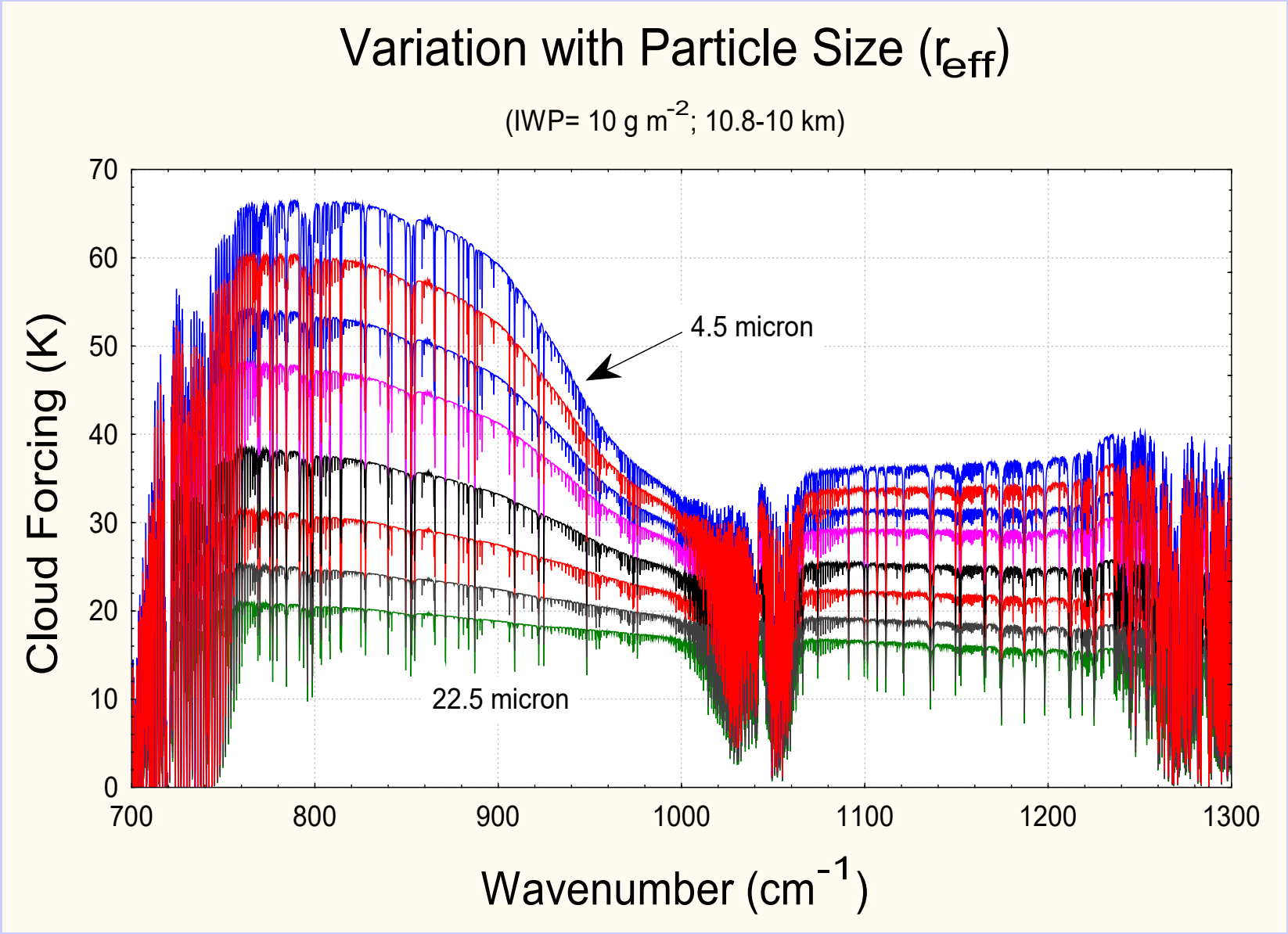

8.6 um sees more reflection than 10.5 um image over snow

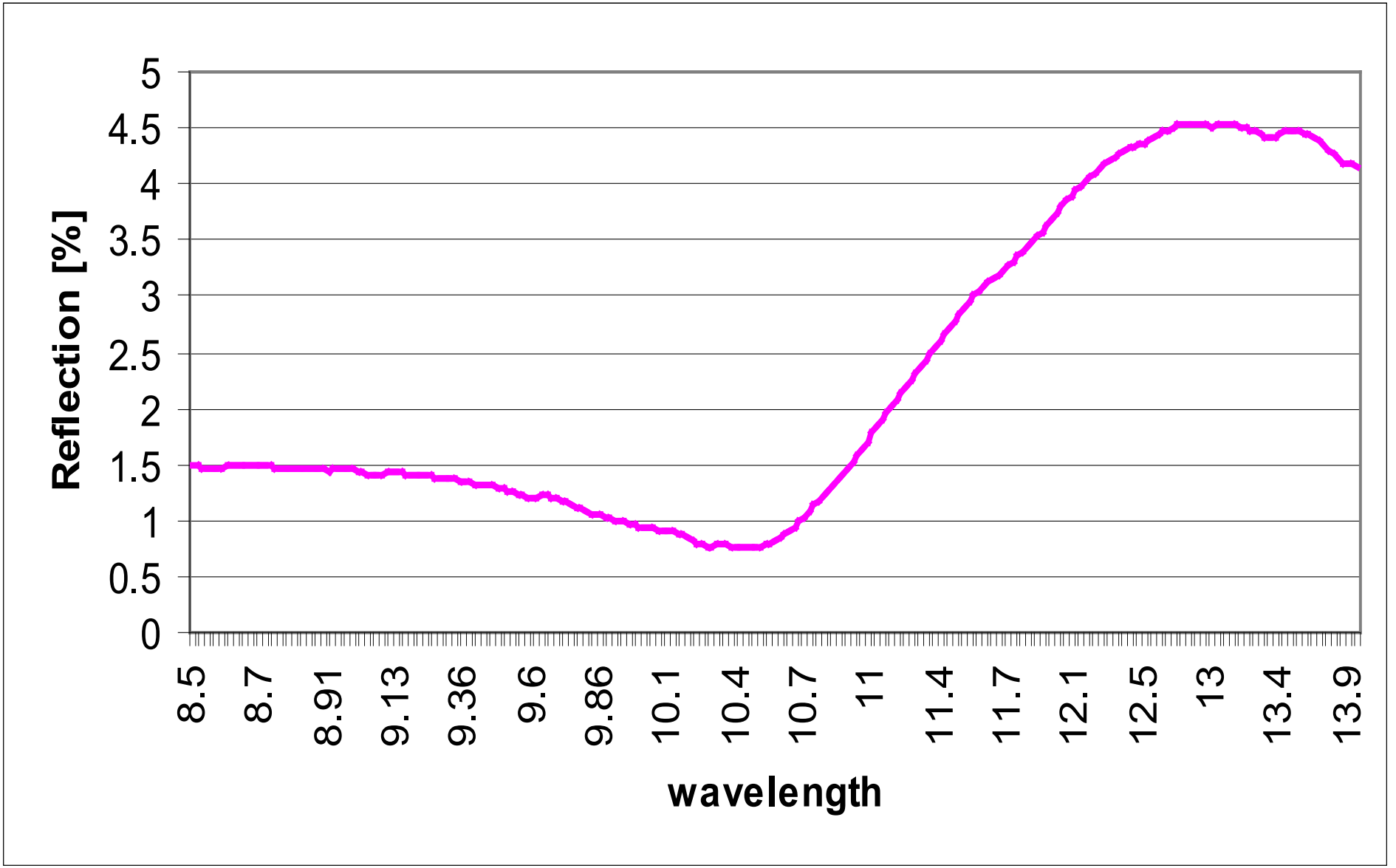

T(p)

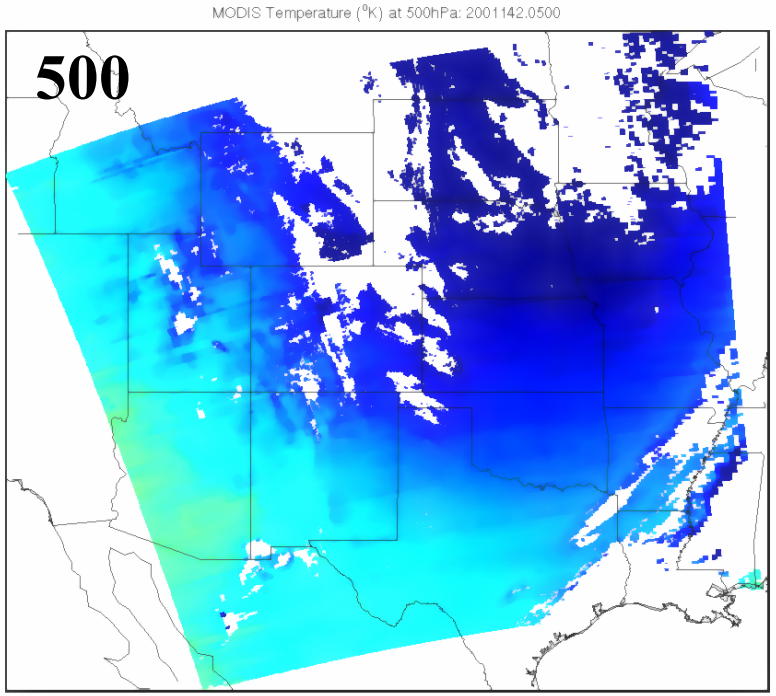
MODIS Temperature (°K) at 500hPa: 2001142.0500
500

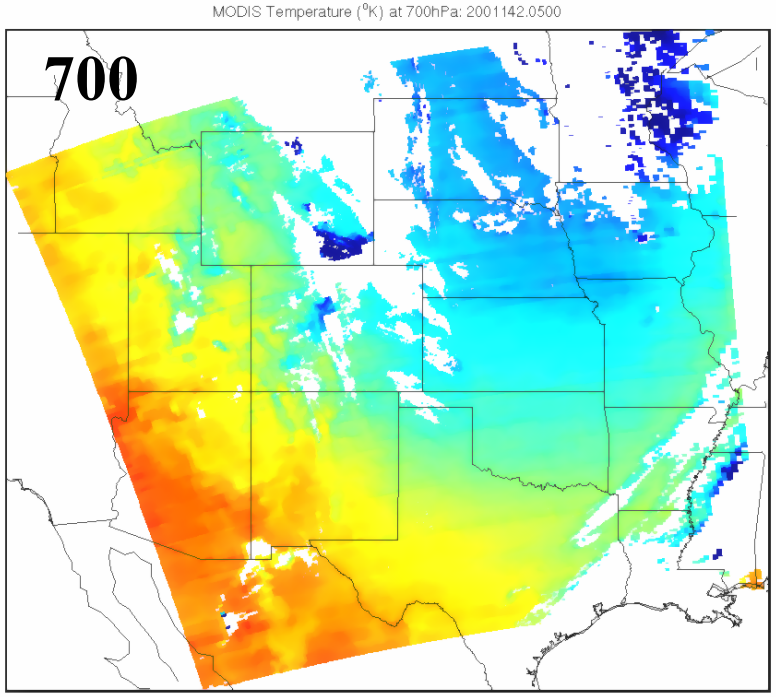
MODIS Temperature (°K) at 700hPa: 2001142.0500
700

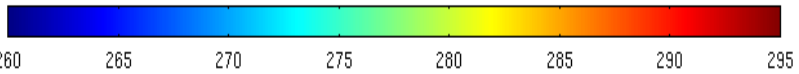
260
265
270
275
280
285
290
295

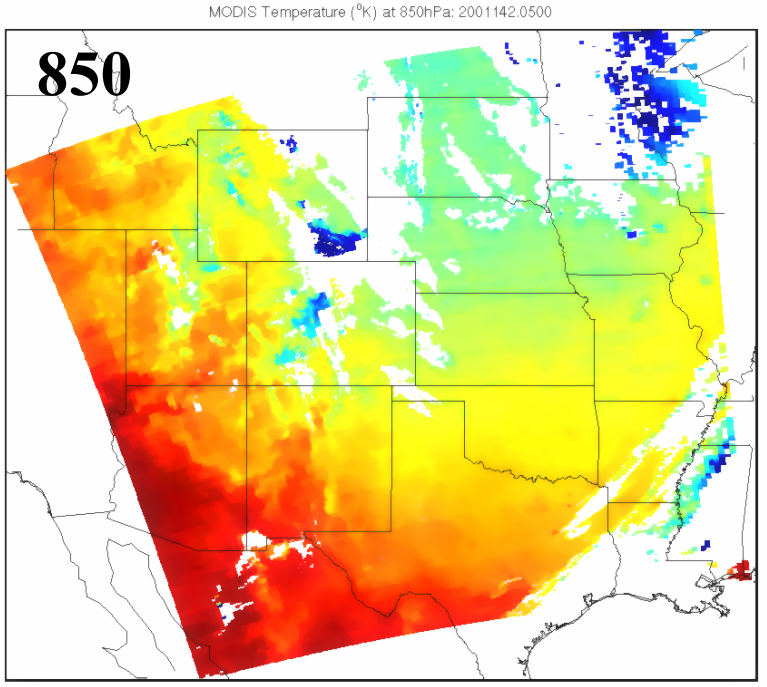
MODIS Temperature (°K) at 850hPa: 2001142.0500
850

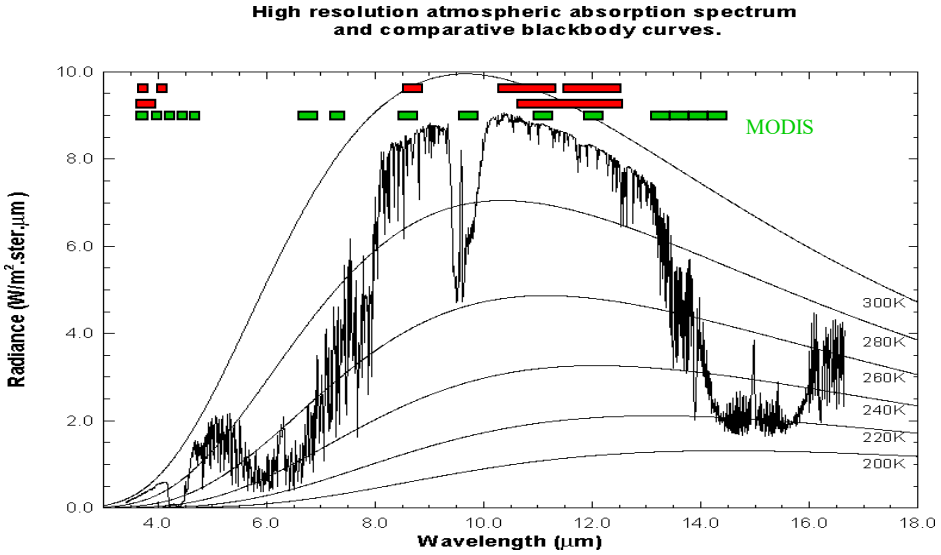
High resolution atmospheric absorption spectrum
and comparative blackbody curves.
MODIS
300K
280K
260K
240K
220K
200K
Radiance (W/m².ster.μm)
Wavelength (μm)
0.0
2.0
4.0
6.0
8.0
10.0
4.0
6.0
8.0
10.0
12.0
14.0
16.0
18.0

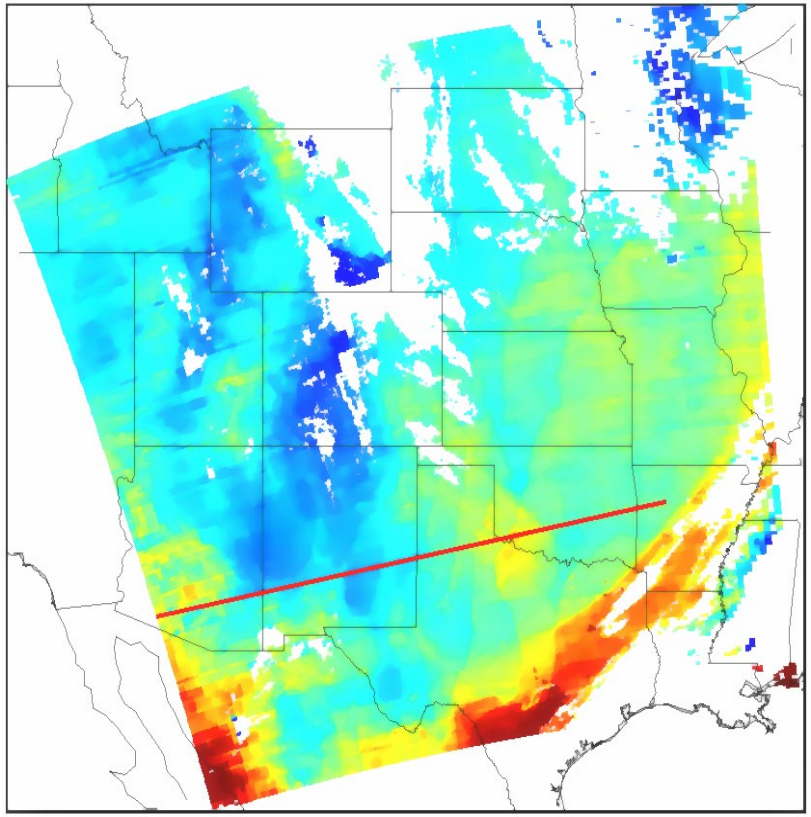

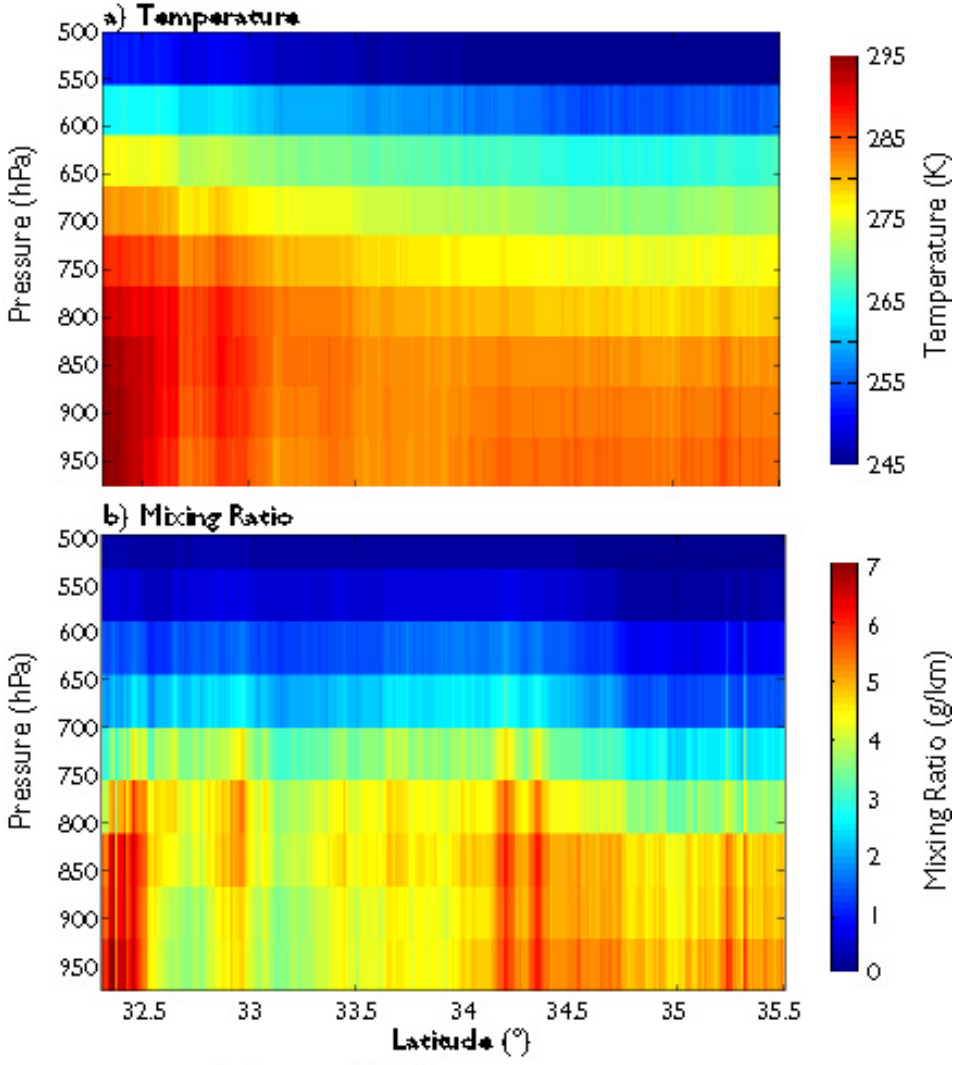

Clear sky layers of temperature and moisture

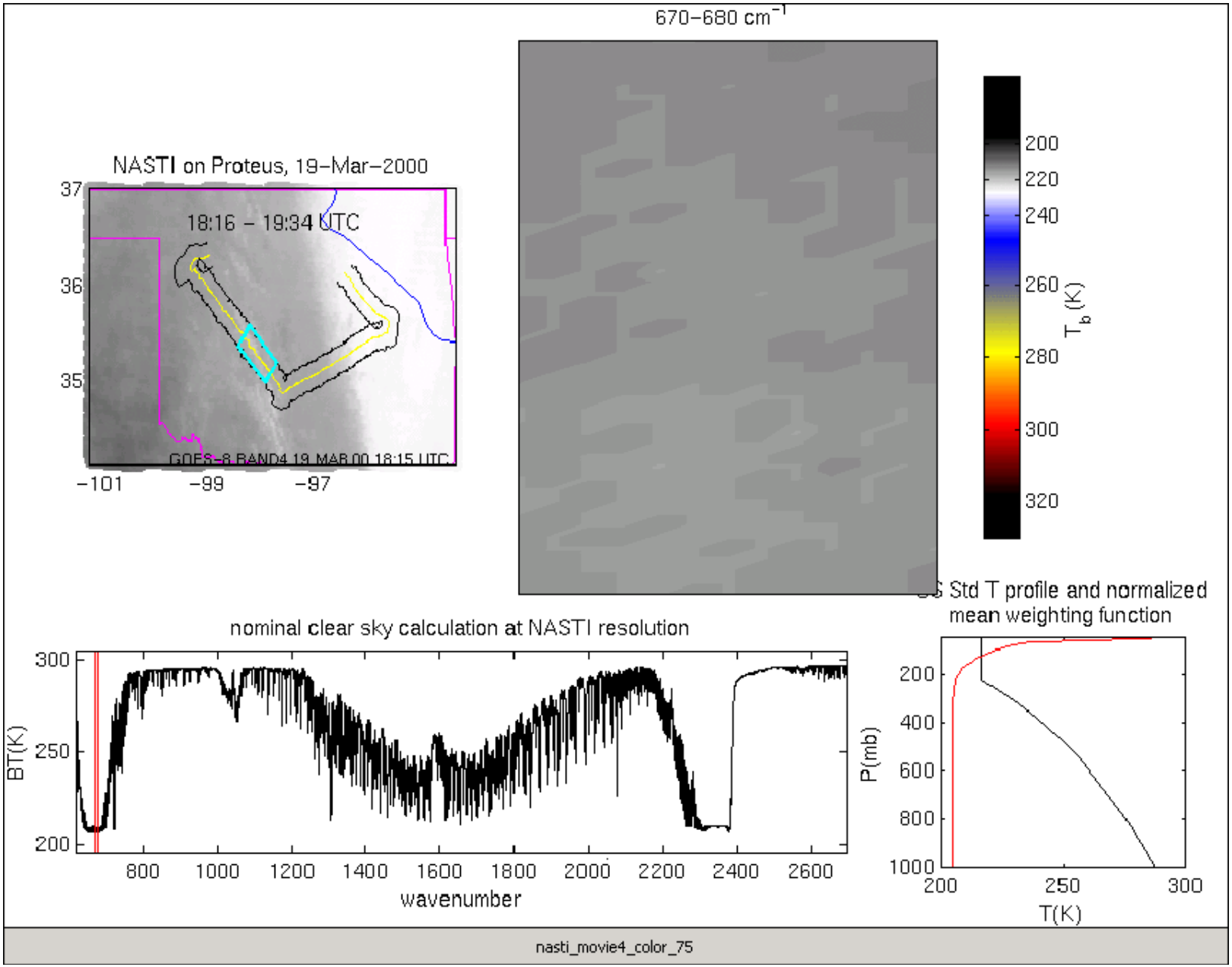
NASTI on Proteus, 19-Mar-2000
18:16 - 19:34 UTC
GOES-8 BAND4 19 MAR 00 18:15 UTC
37
36
35
-101
-99
-97
670-680 cm^{-1}
200
220
240
260
280
300
320
T_b (K)
Std T profile and normalized
mean weighting function
nominal clear sky calculation at NASTI resolution
BT(K)
300
250
200
800
1000
1200
1400
1600
1800
2000
2200
2400
2600
wavenumber
P(mb)
200
400
600
800
1000
200
250
300
T(K)
nasti_movie4_color_75

These water vapor weighting functions reflect the radiance sensitivity of the specific channels to a water vapor % change at a specific level (equivalent to dR/dlnq scaled by dlnp).

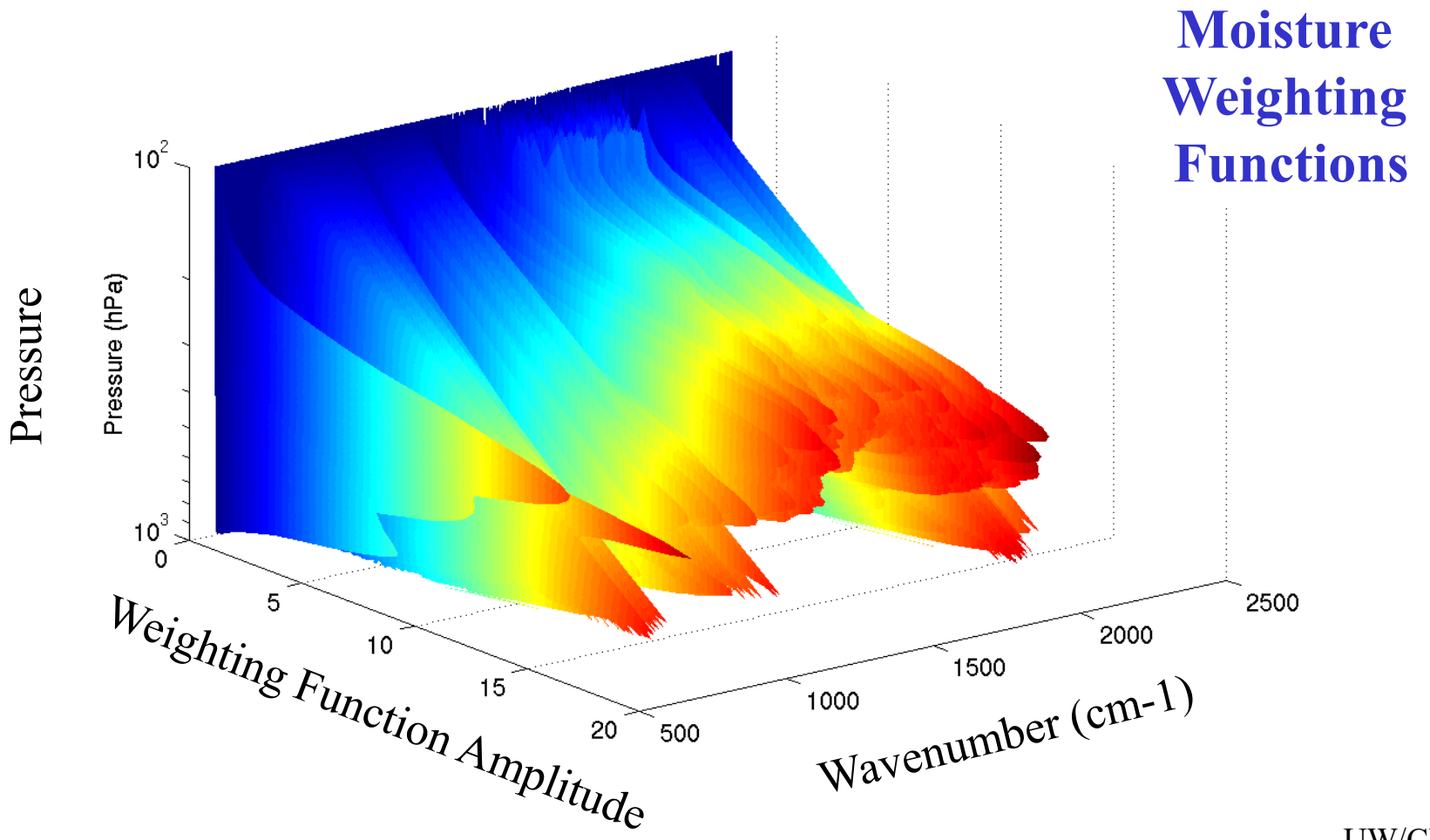

UW/CIMSS

The advanced sounder has more and sharper weighting functions

Climate System Energy Balance

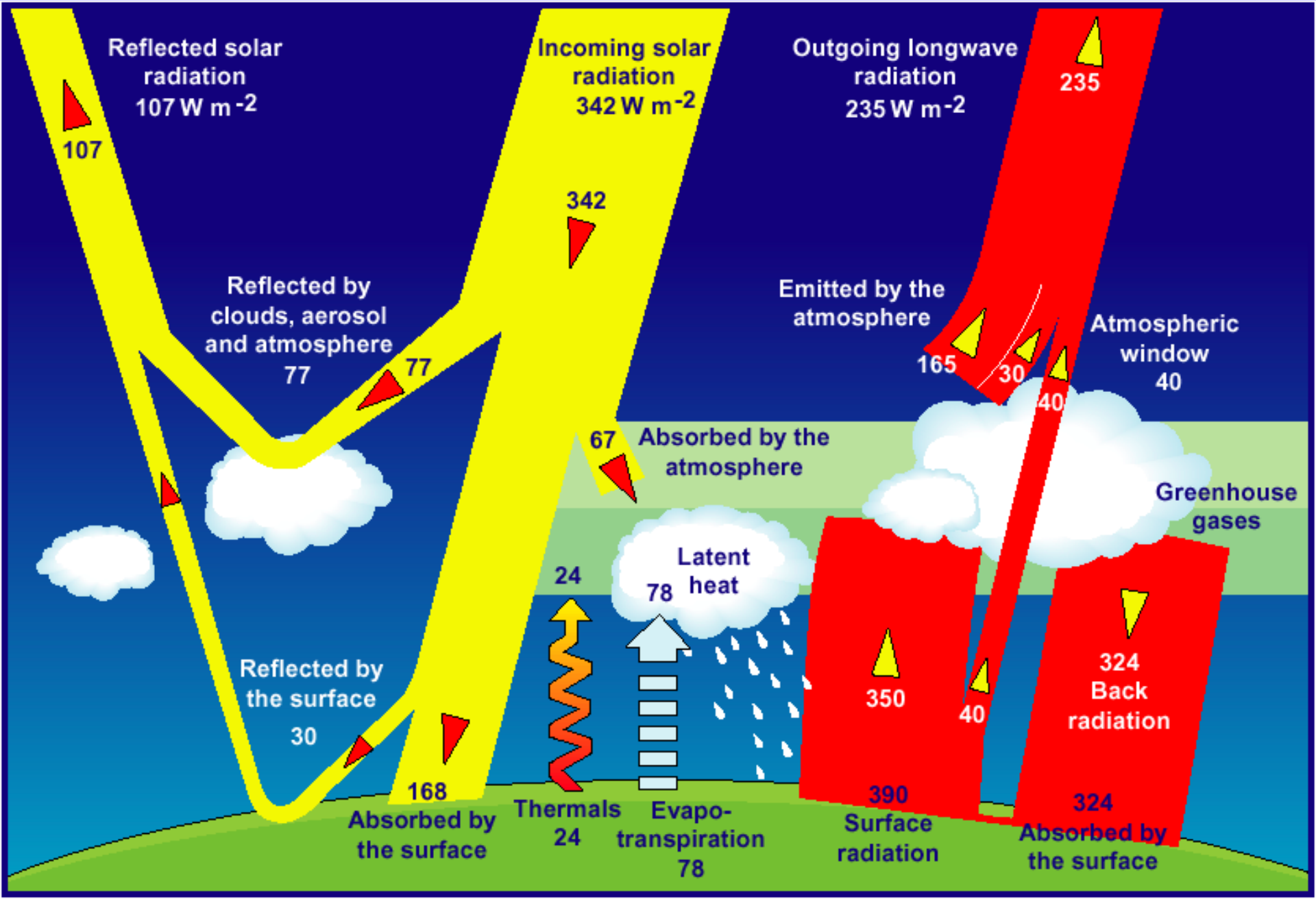

Major Climate System Elements

Carbon Cycle

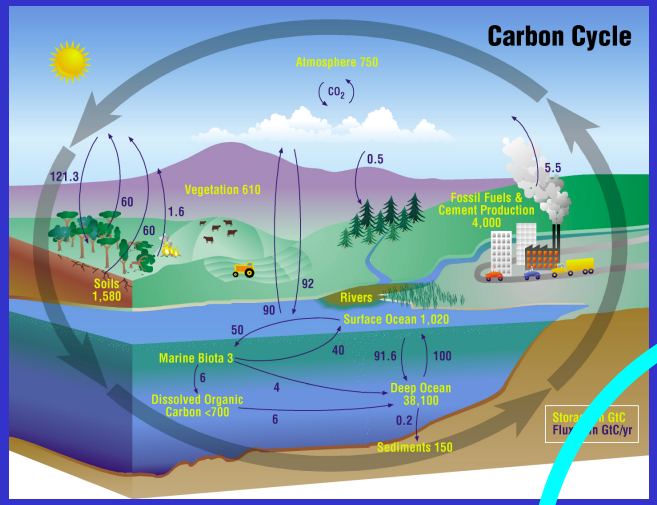

Water & Energy Cycle

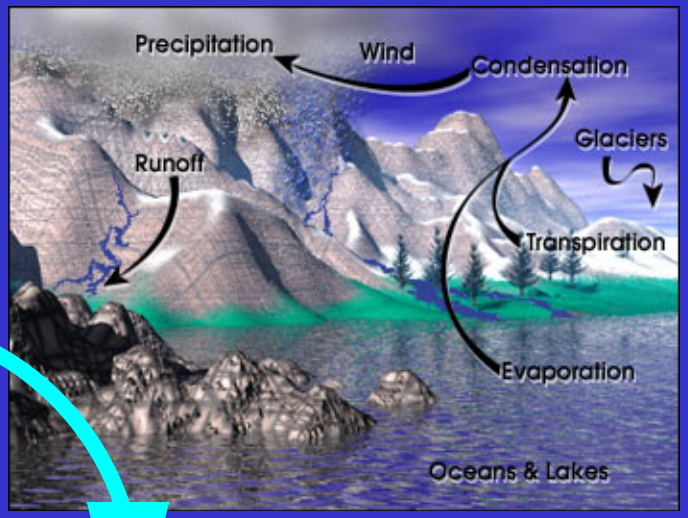

Coupled Chaotic Nonlinear

Atmospheric Chemistry

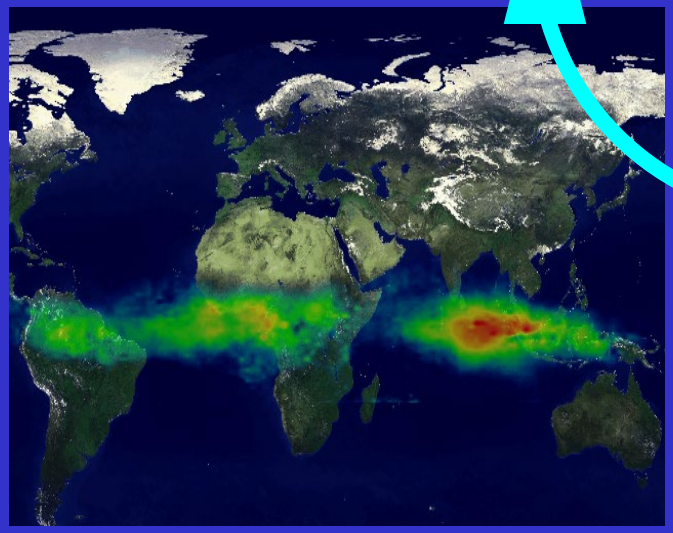

Atmosphere and Ocean Dynamics

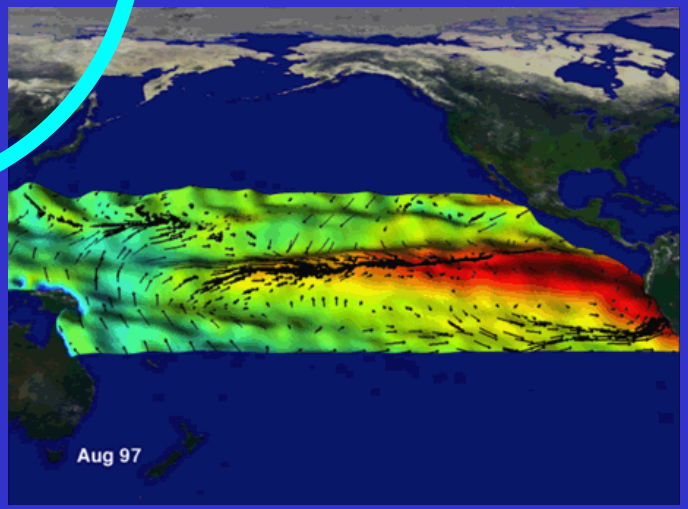

What global surface temperature change has occurred so far?

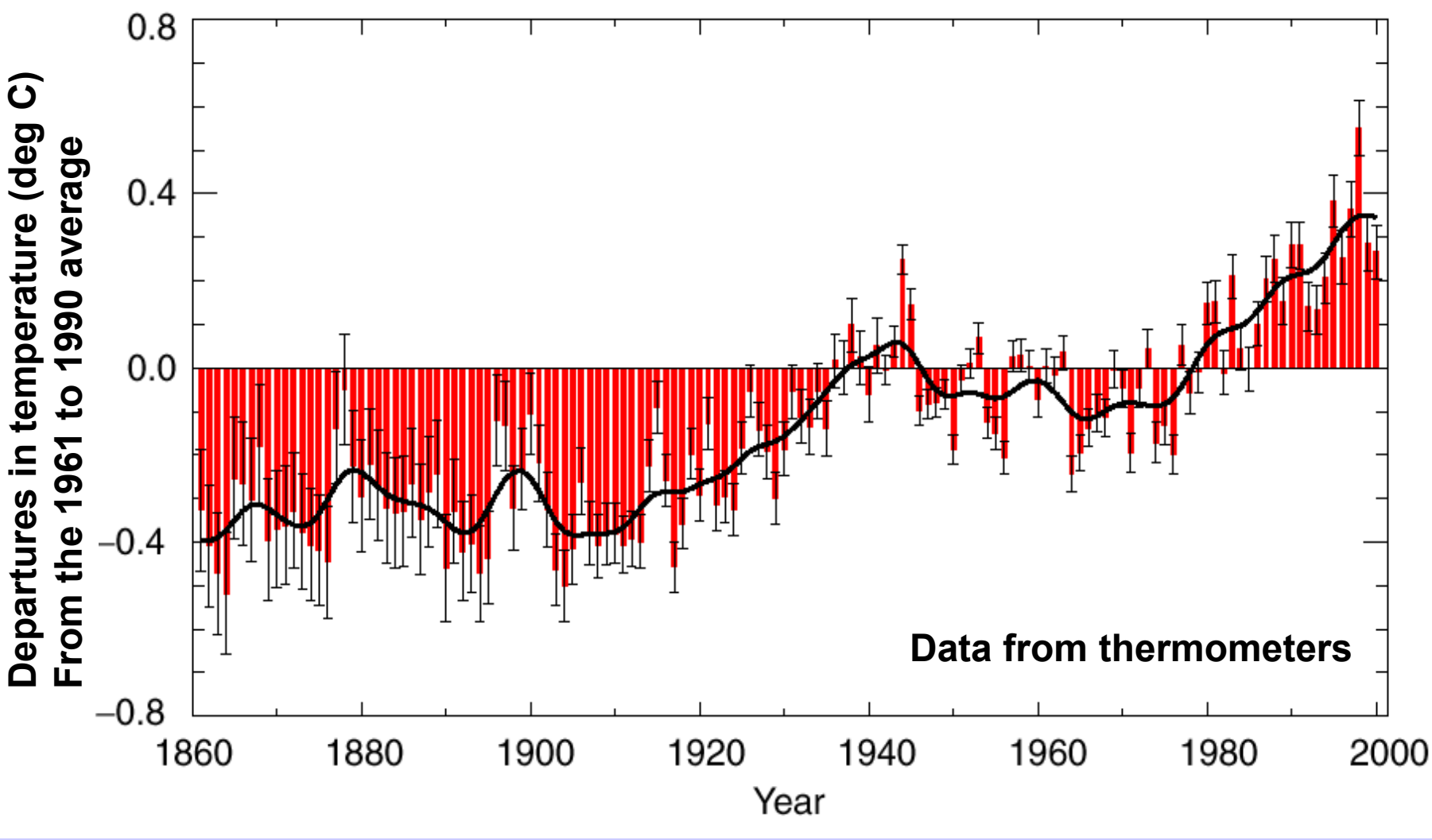

IPCC 2001

Human Influence on Climate

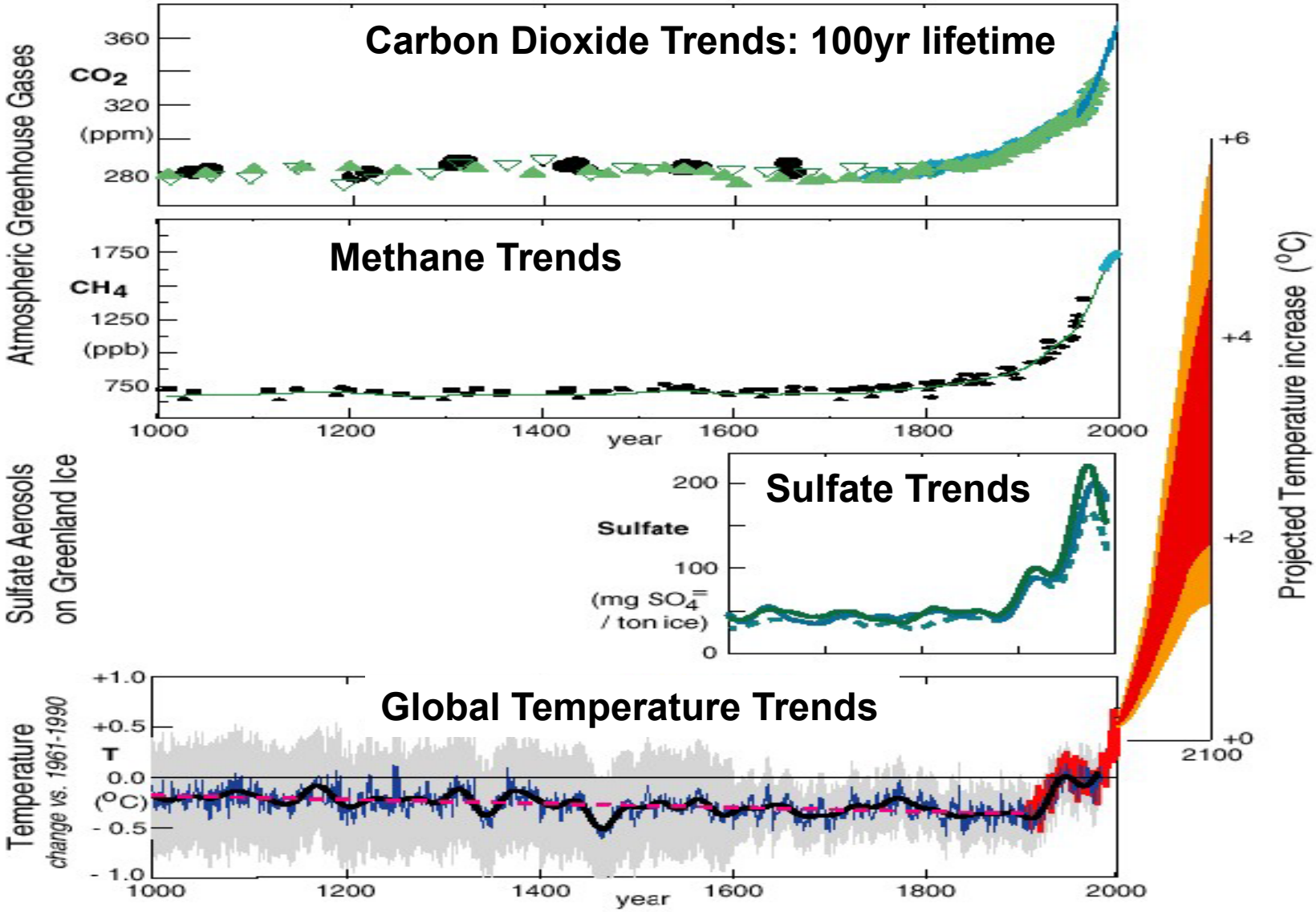

From M. Prather University of California at Irvine

Radiative Forcing from 1750 to 2000

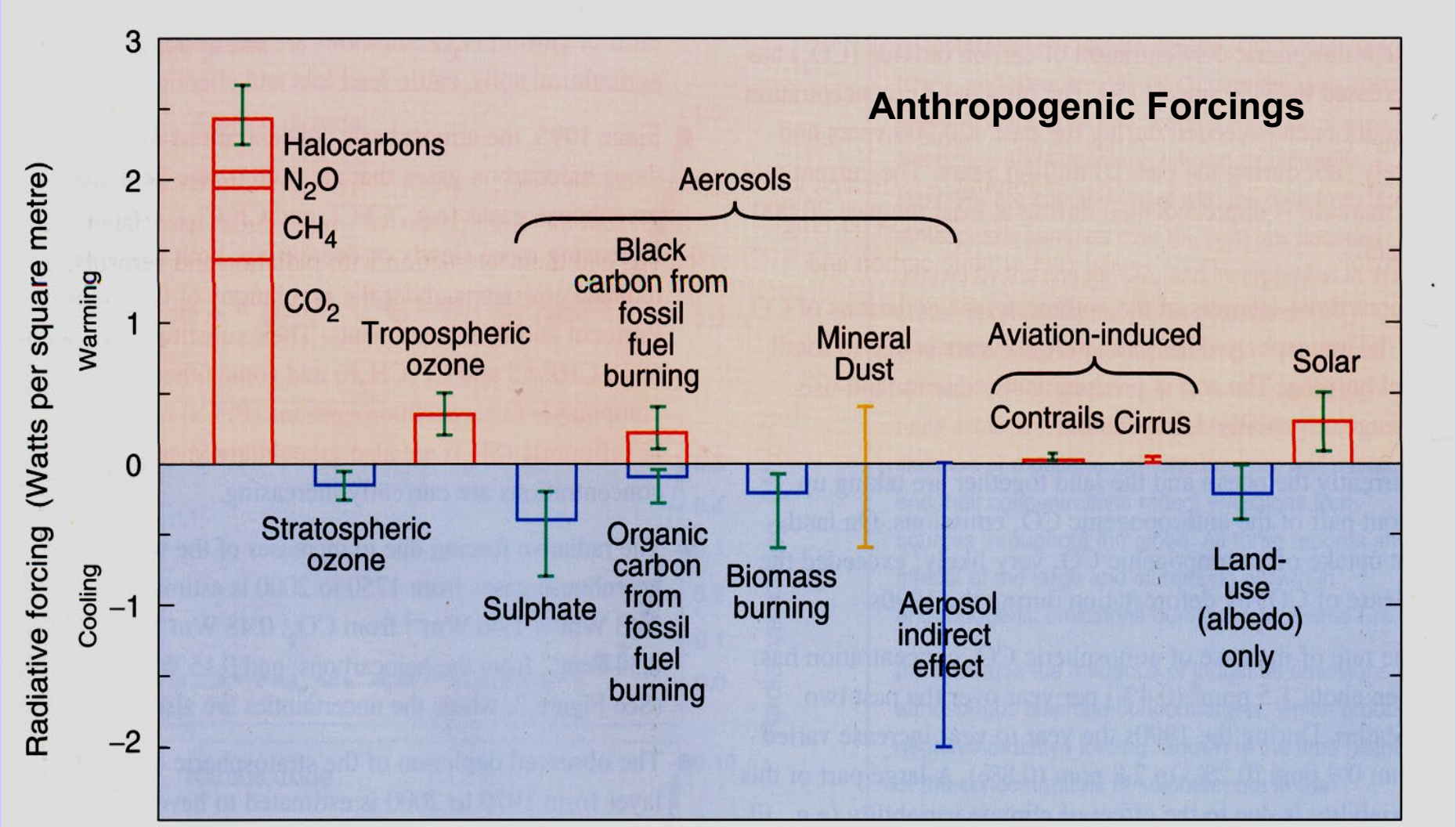

IPCC, 2001

Global Temperature Predictions

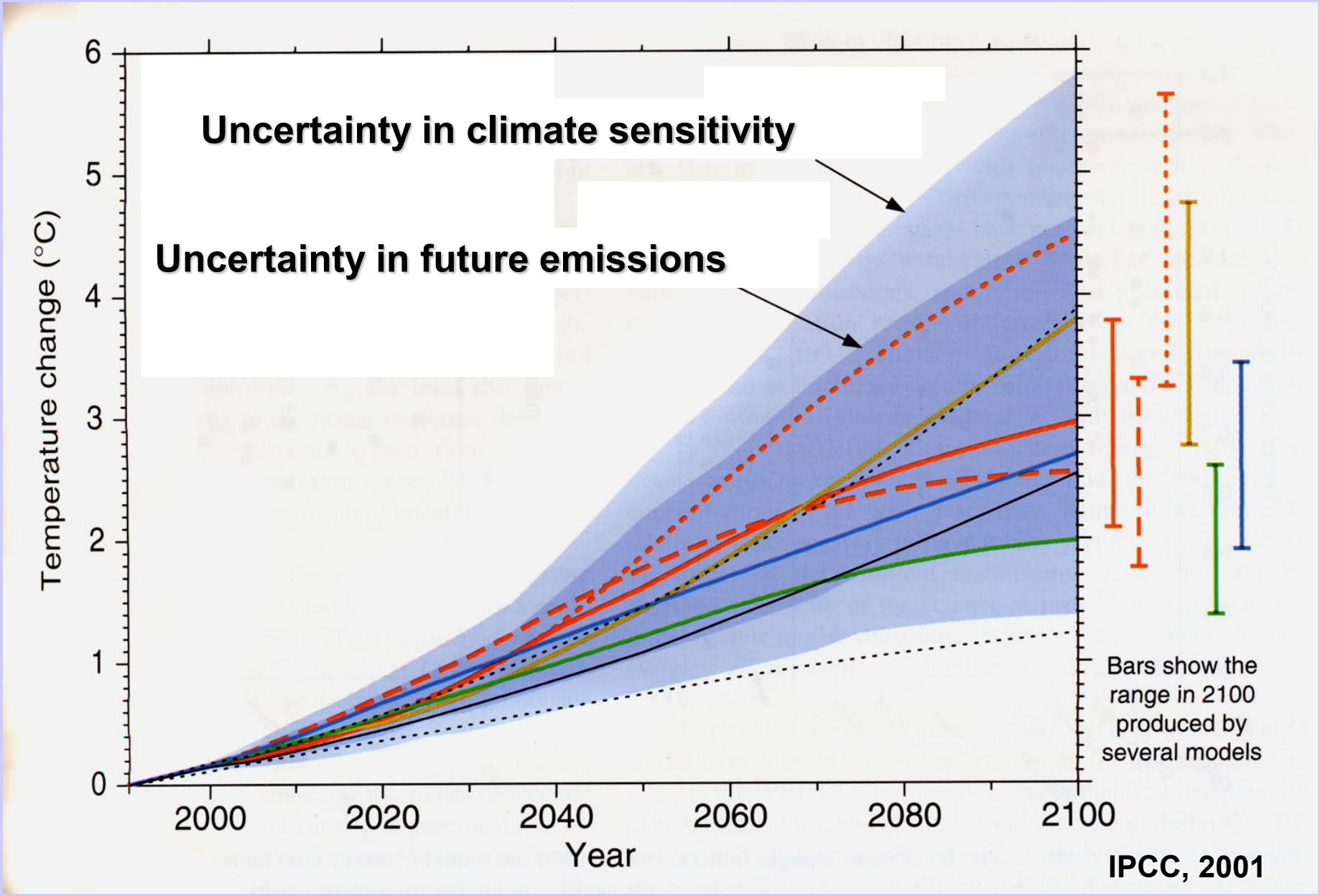

IPCC, 2001

Predicted Sea Level rise from 1990 to 2100

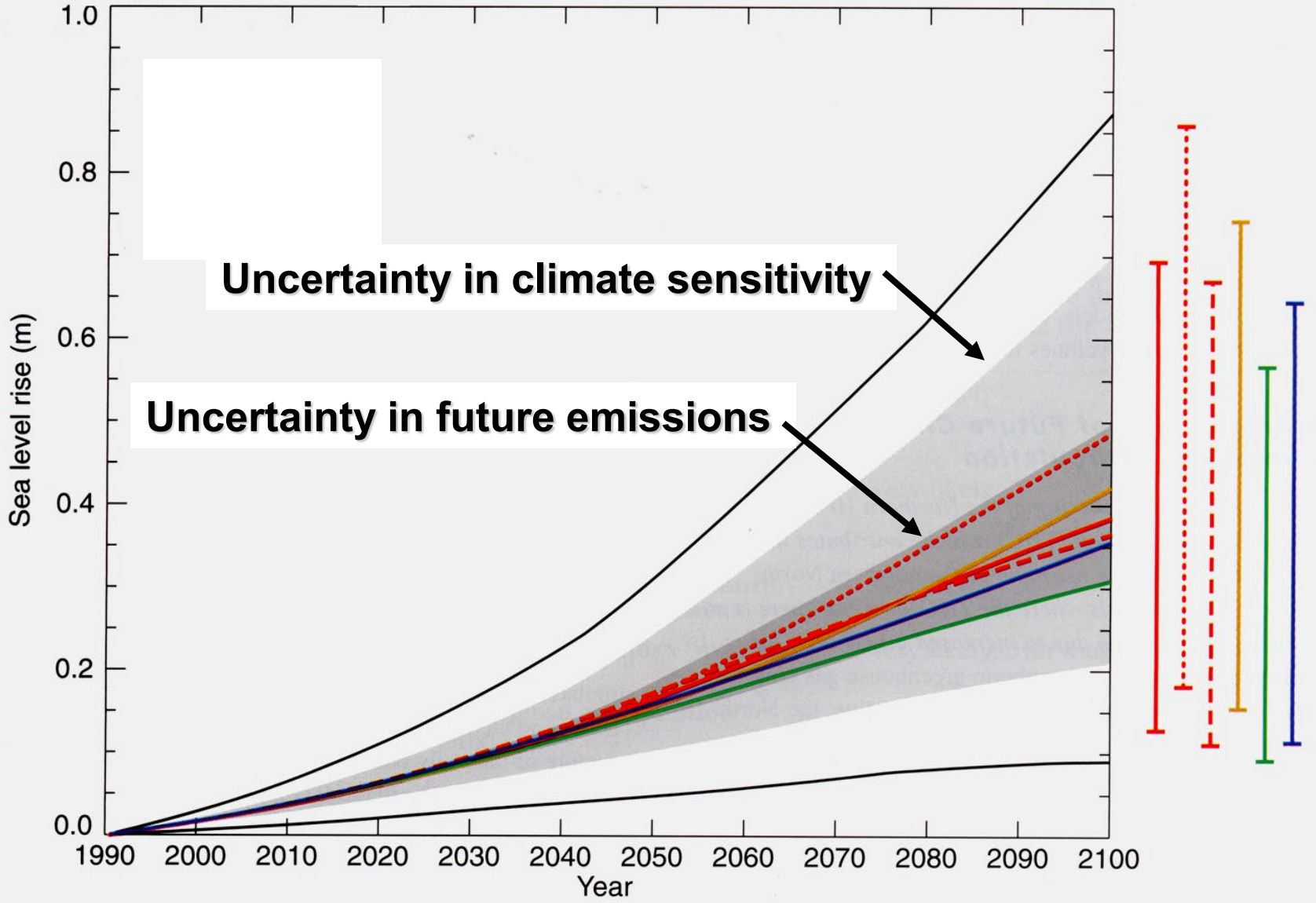

IPCC, 2001

Remote Sensing Products

★ Atmospheric Vertical Moisture Profile
★ Atmospheric Vertical Temp Profile
★ Imagery
★ Sea Surface Temperature
★ Sea Surface Winds
★ Soil Moisture
Aerosol Optical Thickness
Aerosol Particle Size
Albedo (Surface)
Auroral Boundary
Auroral Imagery
Cloud Base Height
Cloud Cover/Layers
Cloud Effective Particle Size
Cloud Ice Water Path
Cloud Liquid Water
Cloud Optical Depth/Transmittance
Cloud Top Height
Cloud Top Pressure
Cloud Top Temperature
Currents (Ocean)

Downward Longwave Radiance (Sfc)
Electric Fields
Electron Density Profile
Fresh Water Ice
Geomagnetic Field
Ice Surface Temperature
Energetic Ions
In-situ Plasma Fluctuations
In-situ Plasma Temperature
Insolation
Medium Energy Charged Particles
Ionospheric Scintillation
Land Surface Temperature
Littoral Sediment Transport
Net Heat Flux
Net Short Wave Radiance (TOA)
Neutral Density Profile
Neutral Winds
Normalized Difference Vegetation Index
Ocean Color/Chlorophyll
Ocean Wave Characteristics

Ozone - Total Column/Profile
Precipitable Water
Precipitation Type/Rate
Pressure (Surface/Profile)
Sea Ice Age and Edge Motion
Sea Surface Height/Topography
Snow Cover/Depth
Solar Irradiance
Supra-Thermal - Auroral Particles
Surface Wind Stress
Suspended Matter
Total Auroral Energy Deposition
Total Longwave Radiance (TOA)
Total Water Content
Turbidity
Vegetation Index/Surface Type

Atmospheric | Oceanic | Terrestrial | Space | Climate

Sensors, Communications, and Computers

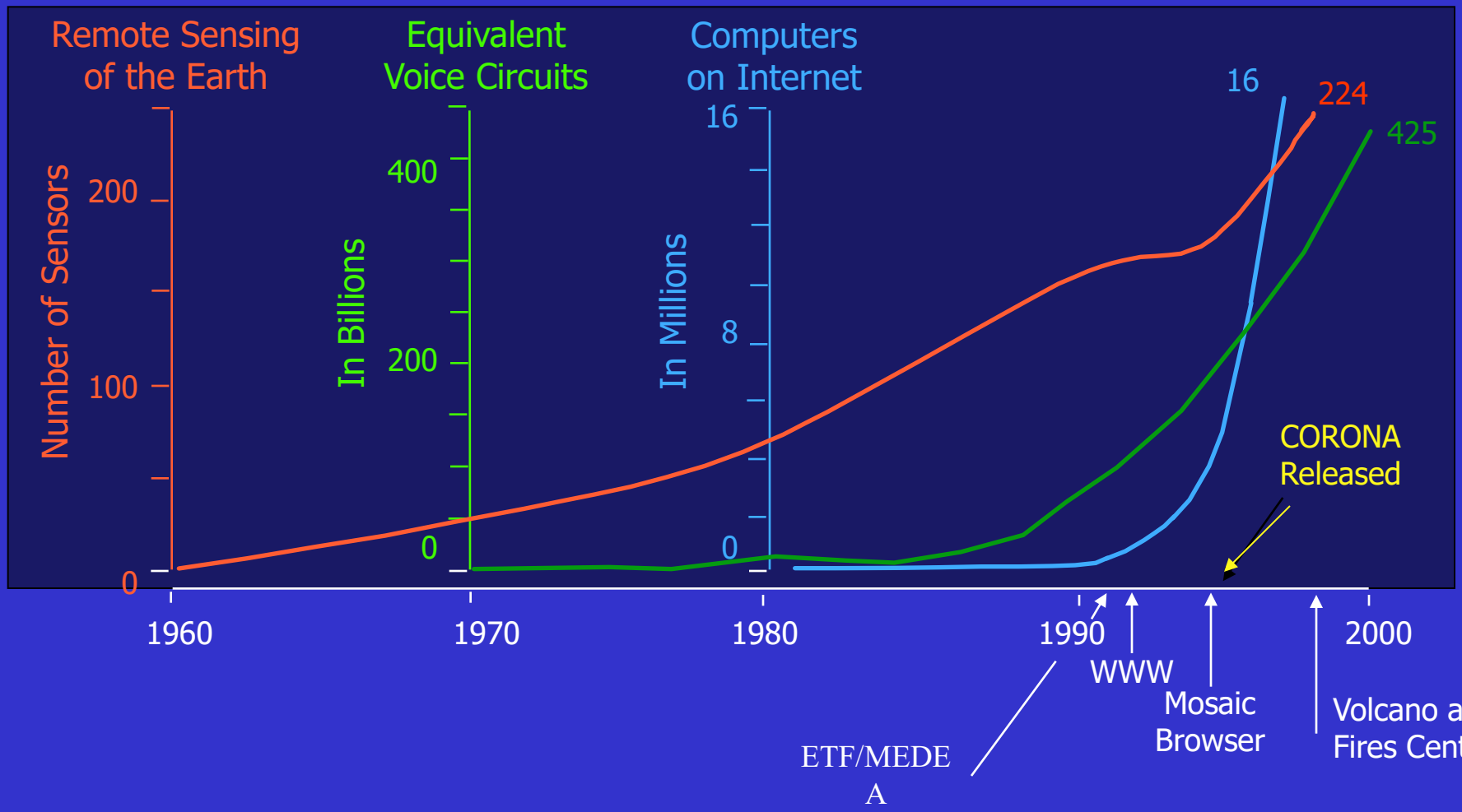

Remote Sensing of the Earth's Environment from Terra
August 25-30, 2002
L'Aquila, ItalyScuola Superiore Guglielmo Reiss Romoli

are now available in a 2 CD set, one containing the PowerPoint lectures and the other the many QuickTime and mpeg movies that were shown during the course (plus one IDL script for bidirectional reflection distribution function). You can find a description of the course and an order form for requesting the CDs at:
http://eospso.gsfc.nasa.gov/eos_homepage/course/
The course material provides a wealth of teaching material that may be of interest to a much broader research community, and those interested in learning more about this extraordinary space-based observing mission.

Dr. Michael D. King
EOS Senior Project Scientist
Code 900
Goddard Space Flight Center
Greenbelt, MD 20771

 # michael.d.king@nasa.gov
 # voice: (301) 614-5636
 # FAX: (301) 614-5620
 # http://eospso.gsfc.nasa.gov